

MESTRADO EM ONCOLOGIA
ESPECIALIZAÇÃO EM ONCOLOGIA LABORATORIAL

LiKidMiRS: unveiling the diagnostic potential of liquid biopsy-based circulating microRNAs in renal tumors

José Pedro Sequeira

M
2021



José Pedro Leite Sequeira

LiKidMiRS: unveiling the diagnostic potential of liquid biopsy-based circulating microRNAs in renal cell tumors

Dissertação de Candidatura ao grau de Mestre em Oncologia – Especialização em Oncologia Laboratorial submetida ao Instituto de Ciências Biomédicas de Abel Salazar da Universidade do Porto.

Orientadora: **Professora Doutora Carmen de Lurdes Fonseca Jerónimo**

Professora Catedrática Convidada

Departamento de Patologia e Imunologia Molecular

Instituto de Ciências Biomédicas Abel Salazar, Universidade do Porto

Investigadora Auxiliar e Coordenadora do Grupo de Epigenética e Biologia do Cancro

Centro de Investigação

Instituto Português de Oncologia do Porto Francisco Gentil, E.P.E

Coorientador: **Professor Doutor Rui Manuel Ferreira Henrique**

Professor Catedrático Convidado, Departamento de Patologia e Imunologia Molecular

Instituto de Ciências Biomédicas Abel Salazar, Universidade do Porto

Investigador Sénior do Grupo de Epigenética e Biologia do Cancro,

Centro de Investigação

Instituto Português de Oncologia do Porto Francisco Gentil, E.P.E

“Nothing in life is to be feared, it is only to be understood. Now is the time to understand more, so that we may fear less”.

Marie Curie



This study was funded by a grant of the Research Centre of Portuguese Oncology Institute of Porto (CI-IPOP-74-2016)

AGRADECIMENTOS

Gostaria de agradecer a todas as pessoas que diretamente e indiretamente contribuíram para a realização desta dissertação.

Em primeiro lugar gostaria de agradecer à Professora Doutora Carmen Jerónimo por ser orientadora deste trabalho e por me ter dado a oportunidade de realizar não só o projeto de licenciatura como também esta dissertação de mestrado no Grupo de Epigenética e Biologia do Cancro. Foi aqui que aprendi como fazer ciência e que pude crescer enquanto pessoa, por tudo o que me transmitiu. Obrigado pela oportunidade!

Em segundo lugar, ao Professor Doutor Rui Henrique, coorientador desta dissertação, agradeço a contribuição e a disponibilidade no esclarecimento de dúvidas nestes últimos 2 anos e meio, assim como, as sugestões para melhorar este trabalho.

Ainda, agradecer ao Professor Doutor Manuel Teixeira, Diretor do Centro de Investigação do IPO do Porto, por ter possibilitado e permitido a realização deste trabalho nestas instalações.

Um agradecimento especial à minha “chefinha”, Vera Constâncio aka Verita, uma pessoa sem a qual nada disto era possível. Obrigado por todos os ensinamentos, reuniões, risadas, receitas e troca de ideias sustentáveis. Obrigado pelos “dias do Zé”, aquelas quartas-feiras com extrações de 60 casos a terminar às 19 horas depois de 11 horas de trabalho. #desculpaPedro! As palavras são poucas para agradecer tudo o que aprendi e cresci contigo.

Ao João Lobo, o outro Digimon macho, um enorme agradecimento pela grande disponibilidade e paciência e ensinamentos. Foi incrível trabalhar contigo e o DigiMiR é a prova disso. Obrigado!

À Cláudia Lima aka Claudita aka Laurinda, muito obrigado por estares sempre aqui, pelas palhaçadas, conversas sérias, pelos calamares, pelas bolachas partidas e pelo estojo vazio/casaco ao contrário. Sem dúvida, uma das melhores com quem podia ter dividido esta experiência.

À Diana Fernandes aka Dianita, muito obrigado por tudo. Pelas conversas, risos e abraços quando tudo parecia correr mal, foste uma parte importante desta dissertação.

À Mariana aka Manhã Paqueco, por todas as conversas sérias e momentos divertidos que tivemos nestes últimos anos.

À minha Ana Rita Marques aka Anita, foi tão bom conhecer-te. Os teus bons dias faziam qualquer um enervar-se por ver tanta felicidade logo pela manhã. Espero que as aventuras no NTA tenham sido o início de um projeto incrível. Obrigado por todas as brincadeiras.

À Catarina Macedo, muito obrigado por tudo. Foram 3 anos incríveis. Continua a defender o galo de Barcelos como defendes e a odiar os galos de Portugal.

À Catarina Teixeira, a minha Teixolas, muito obrigado por todos os bons momentos, por todas as risadas e por dares a conhecer ao mundo imensas palavras e por seres tu pópia (desculpa, tu própria). Genética on fire!

À Vera aka Vera Grande, obrigado por estes últimos anos e por todos os ensinamentos que me deste. Obrigado por relembrares a importância da alimentação (#snickers) e por te ofereceres para abrir falcons na sala de extrações.

Gostaria, também de agradecer, à Ana Lameirinhas, à Beatriz, à Bianca, à Carina, à Catarina Lourenço, à Daniela, à Dona Marta (Martinha), à Filipa aka Pipa, à Filipa aka Pipinha, ao Gonçalo, ao Guilherme, à Helena, à Margareta, à Nair, à Nicole, ao Nuno, à Oriana, à Sandra, à Sara, ao Tiago e à Vânia por todos os conselhos, risadas e pela imensa partilha de conhecimento.

Também, à Bela, quero agradecer pelos dias de processamento, por todas as brincadeiras e por toda a ajuda quando mais precisava.

Ao Diogo, parceiro de Mestrado, por tudo o que foi estes dois anos. Foi um percurso incrível e deu um gozo enorme fazer isto ao teu lado. Era sempre para o “Binte”.

À JC (há quem a chame de Joana Carolina) e ao Mica, por aquilo que têm representado nos últimos meses. Aqueles serões de Monopoly com trocos mal feitos, passadiços do paiva debaixo de chuva e jantares incríveis ajudaram a tornar tudo isto mais fácil.

Ao meu primo Rui, por tudo o que é e o que representa em tudo isto! Por desde cedo despertar este gosto da ciência e por estar sempre presente a acompanhar os pequenos passos que vou dando na ciência.

À minha família, e em especial, aos meus pais, irmã e avós, que são os melhores do Mundo, por me apoiarem em todos os desafios e ajudarem a ultrapassar todos as barreiras. São o meu pilar. Obrigado por todo o vosso amor, carinho e por acreditarem em mim, mesmo quando eu não acredito.

E por fim, à Sofia, pela paciência infinita que tens para me aturar. Tanto a agradecer! Obrigado por acreditares em mim mesmo quando eu só via que tudo podia e que “estava” a correr mal. Obrigado por teres estado ao meu lado quando mais precisava. Obrigado por todas as risadas, todas as conversas sérias, por seres tu. Obrigado por caminhares comigo nesta etapa. As palavras são fúteis para agradecer tudo o que és e foste para mim! Obrigado por tudo!

Obrigado a todos que contribuíram para que isto fosse possível! Let's make science!

RESUMO

Introdução: A redução da mortalidade por cancro continua a ser um importante objetivo da sociedade, sendo materializada nos esforços para desenvolver biomarcadores eficazes para a deteção precoce de tumores. Essa deteção precoce permitiria uma diminuição do número de casos de cancro identificados em estadios avançados associados a um pior prognóstico da doença. Assim, a deteção precoce do carcinoma de células renais (CCR) aumenta significativamente a probabilidade de tratamento curativo, evitando a necessidade de terapias subsequentes com efeitos colaterais e que acarretam mais comorbidades. Assim, o nosso objetivo foi analisar microRNAs que podem auxiliar na deteção/diagnóstico precoce e minimamente invasivo de CCRs.

Métodos: Foram selecionadas amostras de plasma de 142 doentes com CCRs [103 CCR de células claras (ccCCR), 16 CCR papilares, 23 CCR cromóforos], 18 oncocitomas e 78 dadores saudáveis. Foi adicionado, a todas as amostras, o microRNA ath-miR-159a como controlo interno. Os níveis de hsa-miR-21-5p, hsa-miR-126-3p, hsa-miR-141-3p, hsa-miR-155-5p e hsa-miR-200b-3p foram avaliados através de droplet digital PCR. Curvas de características do operador recetor foram construídas e as áreas sob a curva foram calculadas para avaliar o desempenho diagnóstico.

Resultados: Os doentes com CCR apresentaram níveis circulantes de hsa-miR-155-5p significativamente mais elevados do que as amostras de plasma de dadores saudáveis. Contrariamente, os níveis de hsa-miR-21-5p e hsa-miR-141-3p observados foram significativamente mais baixos do que no grupo controlo. Além disso, doentes com tumores confinados ao rim, correspondendo a estadios iniciais (estadios I e II), revelaram níveis circulantes de hsa-miR-141-3p significativamente mais elevados em comparação com os doentes cujo tumor invadia para além da cápsula renal (estadios avançados).

O painel constituído por dois hsa-miRs (hsa-miR-126-3p e hsa-miR-200b-3p) apresentou o maior desempenho na identificação de pacientes com tumores das células do rim, tendo uma sensibilidade de 81,55% e uma acuidade de 76,47%, mas especificidade de, apenas, 52,63%.

Para além disso, o melhor painel para deteção de CCRs é constituído por hsa-miR-21-5p e hsa-miR-155-5p, apresentando uma sensibilidade de 87,32%, especificidade de 47,92% e uma acuidade de 71,43%.

Conclusão: Os nossos resultados demonstram que o painel miR-21/miR-155 avaliado em biópsias líquidas é capaz de identificar doentes com CCR. A inclusão da avaliação do hsa-

miR-126, hsa-miR-141, hsa-miR-155 e hsa-miR-200b permitiu uma identificação específica de ccCCRs. Apesar da necessidade de mais estudos nesta área, os hsa-miRs em circulação, avaliados por droplet digital PCR, podem coadjuvar na detecção precoce de CCR.

ABSTRACT

Background: Cancer mortality reduction remains a major societal goal, in part materialized in the many efforts to develop effective biomarkers for early detection. This would allow for decreasing the proportion of cancers identified at late stages, which carry very poor prognosis. Early detection of renal cell carcinoma (RCC) significantly increases the likelihood of curative treatment, avoiding the need for subsequent therapies, which have side effect and entail more comorbidities. Thus, we aimed to unveil microRNAs that might aid in early, non-invasive, RCCs detection/diagnosis.

Methods: Plasma samples from 142 RCC patients [103 clear cell RCC (ccRCC), 16 papillary RCC, 23 chromophobe RCC], 18 oncocytomas and 78 healthy donors were selected. All samples were spiked with ath-miR-159a. Levels of hsa-miR-21-5p, hsa-miR-126-3p, hsa-miR-141-3p, hsa-miR-155-5p and hsa-miR-200b-3p were assessed using droplet digital PCR. Receiver operator characteristic curves were constructed and the areas under the curve were calculated to assess diagnostic performance.

Results: RCC patients displayed significantly higher hsa-miR-155-5p circulating levels than healthy donors, whereas lower hsa-miR-21-5p and hsa-miR-141-3p were found in the same patients. Also, patients with organ confined tumors (Stages I and II) disclosed significantly higher hsa-miR-141-3p circulating levels than to those invading beyond the renal capsule (advanced stages).

The two-hsa-miRs panel (hsa-miR-126-3p and hsa-miR-200b-3p) presented the highest performance in identifying RCTs patients, with 81.55% sensitivity and 76.47% accuracy but limited specificity.

Regarding malignant tumors, the best panel of circulating miRs for the three major RCC subtypes identification included hsa-miR-21-5p and hsa-miR-155-5p, depicting 87.32% sensitivity, 47.92% specificity and 71.43% accuracy. Remarkably, hsa-miR-141-3p levels decreased in advanced stage RCC patients.

Conclusion: Our results demonstrate that miR-21/miR-155 panel is able to discriminate patients with malignant tumors from controls, and that circulating miR-126, miR-141, miR-155 and miR-200b might allow for specific identification of ccRCCs. Although further studies are need, circulating hsa-miRs assessed by droplet digital PCR might aid in early detection of RCC.

TABLE OF CONTENTS

I.	INTRODUCTION	1
II.	PRELIMINARY DATA	19
1.	Comparison of PCR techniques and validation of ddPCR	21
2.	Identification of some microRNAs that might aid in the diagnostic and prognostic workup of RCTs	24
III.	AIM	27
IV.	MATERIAL AND METHODS	31
1.	Plasma samples.....	33
1.1.	Patients and Samples Collection	33
2.	RNA extraction.....	33
3.	TaqMan miRNA reverse transcription.....	34
4.	Droplet digital PCR.....	35
5.	Quality control steps.....	35
6.	Statistical analysis.....	36
V.	RESULTS	37
1.	Patients cohortS characterization	39
2.	Optimization phase and comparison of pipelines.....	40
2.1.	Input and temperature settings	40
2.2.	Positive Control	42
2.3.	Further optimization of ddPCR protocol.....	43
3.	Evaluation of biomarker detection performance – validation cohort	45
3.1.	Distribution of circulating miRNAs levels and biomarkers’ performance to detect Malignant Tumors	45
4.	MiRNAs Levels and clinicopathological features	48
VI.	DISCUSSION.....	51
VII.	CONCLUSIONS AND	57
	FUTURE PERSPECTIVES	57
VIII.	REFERENCES.....	61
IX.	APPENDIX.....	I
I.	Article I – Under Revision.....	III
II.	Detection of Renal Cell Carcinoma.....	XXXI

III.	Distribution of circulating miRNAs levels in Renal Cell Tumors and Biomarkers performance.....	XXXII
IV.	Detection of Early Stages Renal Cell Carcinomas.....	XXXV
V.	Detection of Clear Cell Renal Cell Carcinomas	XXXVI
VI.	Comparison between early stages RCC and Advanced Stages RCC.....	XXXVII

FIGURES INDEX

Figure 1 – Comparison of pipelines. A-C: TaqMan Advanced (global) microRNA pipeline; D-F: TaqMan (target-specific) microRNA pipeline; G-H: DigiMir pipeline. X-axis: #1 and #2 – stage I seminomas; #3 – stage II embryonal carcinoma; #4 – stage III embryonal carcinoma; #5 – age-matched healthy blood donor. Color code: setting #1 – different extraction; setting #2 – different cDNA synthesis; setting #3 – different operator; setting #4 – same operator; and reference for comparison.....	22
Figure 2 – Correlation between hsa-miR-371a-3p quantifications. A-D: TaqMan Advanced (global) microRNA pipeline; E-H: TaqMan (target-specific) microRNA pipeline; I-L: DigiMir pipeline; M – correlation between the DigiMir pipeline and the TaqMan (target-specific) microRNA pipeline quantifications.	23
Figure 3 – Distribution of miRNA levels in kidney tissues. (A) Normal vs tumour tissues. (B) Benign vs malignant tumour tissues. Statistically significant differences are represented as ***P<0.001, **P<0.01 and *P<0.02. Figure from Silva-Santos et al. [1].	24
Figure 4 – Disease specific-survival according with hsa-miR-21-5p, hsa-miR-141-3p and hsa-miR-155-5p levels. Figure from Silva-Santos et al. [1].	25
Figure 5 – Pipeline of LiKidMiRs. Created with BioRender.com.	34
Figure 6 – Optimization of LiKidMiRs pipeline. Hsa-miR-21-5p (A), hsa-miR-126-3p (B), hsa-miR-141-3p (C), hsa-miR-155-5p (D) and hsa-miR-200b-3p (E) input optimization. Validation of ath-miR-159a input (F). Blue squares indicate the optimal input.	41
Figure 7 – Temperature gradient for optimization of hsa-miR-21-5p (A), hsa-miR-126-3p (B), hsa-miR-141-3p (C), hsa-miR-155-5p (D) and hsa-miR-200b-3p (E). Validation of temperature optimized for ath-miR-159a (F). The best separation was optimized around 56°C for ath-miR-159a and around 55°C for the other assays. Blue rectangles indicate the optimal temperature.	42
Figure 8 – Optimization of LiKidMiRs pipeline. Best separation of positive and negative droplets in the hsa-miR-141-3p positive control without dilution (C) and 1:50 for the other miRNAs (A,B,D,E). Importantly, for hsa-miR-21-3p, hsa-miR-155-5p and hsa-200b-3p (A,D,E) there is no separation of droplets in the undiluted sample.	43
Figure 9 – Limit of quantification of for hsa-miR-21-5p (A), hsa-miR-126-3p (B), hsa-miR-141-3p (C), hsa-miR-155-5p (D) and hsa-miR-200b-3p (E). The red arrow points to the number of copies that the assay can still reliably quantify.....	44

Figure 10 – Violin plots of miRNAs levels in oncocytomas and Healthy Donors (HD) samples of hsa-miR-21-5p (p-value=0.154), hsa-miR-126-3p (p-value=0.851), hsa-miR-141-3p (p-value=0.376), hsa-miR-155-5p (p-value=0.066) and hsa-miR-200b-3p (p-value=0.535). Abbreviations: HD – Healthy Donors, n.s. – not significant....45

Figure 11 – Violin plots with all points of miRNAs levels in Benign tumors (Oncocytomas) with Healthy Donors (HD) and Renal Cell Carcinomas (RCC) samples of hsa-miR-21-5p (A), hsa-miR141-3p (B) and hsa-miR-155-5p (C) and respective Receiver Operating Characteristic Curve (D-F). Abbreviations: AUC – Area Under the Curve; CI – Confidence Interval, HD – Healthy Donors, RCC – Renal Cell Carcinoma.....46

Figure 12 – Violin plots of miRNAs levels in Healthy Donors (HD) and early stages of Renal Cell Carcinomas (Stage I and II) samples of hsa-miR-21-5p (A) and hsa-miR-155-5p (B) and respective Receiver Operating Characteristic Curve (C-D). Abbreviations: AUC – Area Under the Curve; CI – Confidence Interval; HD – Healthy Donors.....47

Figure 13 – Violin plots of hsa-miR-21-5p (A), hsa-miR-126-3p (B), hsa-miR-141-3p (C), hsa-miR-155-5p (D) and hsa-miR-200b-3p (E) levels in the malignant subtypes (ccRCC, pRCC and chRCC). Dashed lines indicate the interquartile range and horizontal line the median of miRs levels. Abbreviations: ccRCC – Clear Cell Renal Cell Carcinoma; chRCC – Chromophobe Renal Cell Carcinoma; pRCC – Papillary Renal Cell Carcinoma; n.s. – not significant.....48

Figure 14 – Violin plots of hsa-miR-21-5p (A), hsa-miR-126-3p (B), hsa-miR-141-3p (C), hsa-miR-155-5p (D) and hsa-miR-200b-3p (E) levels in ccRCC and other RCCs (pRCC and chRCC). Abbreviations: ccRCC – Clear Cell Renal Cell Carcinoma; RCC – Renal Cell Carcinomas; n.s. – not significant.....49

Figure 15 – Receiver Operating Characteristic Curves of hsa-miR-126-3p (A), hsa-miR-141-3p (B), hsa-miR-155-5p (C) and hsa-miR-200b-3p (D) in ccRCC and other RCC (pRCC and chRCC). Abbreviations: AUC – Area Under the Curve; CI – Confidence Interval.....50

Figure 16 – Violin plot of hsa-miR-141-3p levels in early stages and advanced stages.....50

Figure 17 – Algorithm for LiKidMiRs' clinical application. Created with BioRender.com.....56

TABLES INDEX

Table 1 – Validity estimates for each miRNA and for the best combination of miRNAs in different diagnostic settings, in fresh-frozen tissues. Table from Silva-Santos et al. [1].	25
Table 2 – Description of time and temperature of TaqMan microRNA Reverse Transcription kit.	34
Table 3 – Components and volumes required for TaqMan microRNA Reverse Transcription per sample.	35
Table 4 – Formulas for biomarker parameters calculation.	36
Table 5 – Clinicopathological data of Optimization cohort (5 samples) and Validation cohort (compound by 160 Renal Cell Tumors and 78 Healthy donors samples) used in this study.	39
Table 6 – Optimization of LiKidMiRs pipeline. Determination of Limit of Blank (LOB) and Limit of Detection (LOD). LOB and LOD are presented as number of positive droplets.	43
Table 7 – Performance of miRNAs as biomarkers for detection of Renal Cell Carcinoma.	46
Table 8 – Performance of miRNAs as biomarkers for identification of early stages Renal Cell Carcinomas.	47
Table 9 – Performance of miRNAs as biomarkers for identification of Clear Cell Renal Cell Carcinoma.	50

List of Abbreviations

μL – Microliters

μm – Micrometers

AFP – Alpha Fetoprotein

AJCC – American Joint Committee on Cancer

AUC – Area Under the Curve

BRT – Benign Renal Tumor

ccRCC – Clear Cell RCC

cDNA – Complementary DNA

chRCC – Chromophobe RCC

CI – Confidence Interval

CTC – Circulating Tumor Cell

ctDNA – Circulating DNA

ddPCR – Droplet Digital PCR

DFS – Disease-Free Survival

DNA – Deoxyribonucleic Acid

dNTP – Deoxyribonucleotide Triphosphate

DSS – Disease-Specific Survival

dTTP – Deoxythymidine Triphosphate

EDTA – Ethylenediamine tetraacetic acid

EV – Extracellular Vesicle

FN – False Negative

FP – False Positive

HCG – Human Chorionic Gonadotropin

HD – Healthy Donor

IPO – Portuguese Institute of Oncology

IQR – Interquartile Range

ISEV – International Society of Extracellular Vesicles

LDH – Lactate dehydrogenase

lncRNA – Long Non-Coding RNA

LOB – Limit of Blank

LOD – Limit of Detection

LOQ – Limit of Quantification
miR – microRNA
miRNA – microRNA
miRNA – microRNA
N.A. – Not Applicable
N.S. – Not Significant
NK – Natural Killer
Nm – Nanometers
nM – Nanomolar
NPV – Negative Predictive Value
NTA – Nanoparticle Tracking Analysis
NTC – No-Template Control
OS – Overall Survival
PFS – Progression-Free Survival
PK – Proteinase K
PPV – Positive Predictive Value
pRCC – Papillary RCC
qRT-PCR – Quantitative Real-Time Polymerase Chain Reaction
RC – Renal Cancer
RCC – Renal Cell Carcinoma
RCT – Renal Cell Tumor
REF – Reference
RNA – Ribonucleic Acid
ROC – Receiver Operating Characteristic
RPM – Revolutions per Minute
rRNA – Ribosomal RNA
RT – Reverse Transcription
SE – Sensitivity
SP - Specificity
sRCC – Sarcomatoid RCC
SSIGN – Stage, Size, Grade and Necrosis
TEM – Transmission Electron Microscopy

TEP – Tumor-educated Platelet
TGCT – Testicular Germ Cell Tumor
TN – True Negative
TP – True Positive
U – Unit
WB – Western Blot

I.INTRODUCTION

(Review Article:






Unveiling the world of circulating and exosomal microRNAs in renal cell carcinoma

José Pedro Sequeira, Vera Constâncio, João Lobo Rui Henrique, Carmen Jerónimo

Published on Cancers [<https://doi.org/10.3390/cancers13215252>]

Review

Unveiling the World of Circulating and Exosomal microRNAs in Renal Cell Carcinoma

José Pedro Sequeira ^{1,2} , Vera Constâncio ^{1,3} , João Lobo ^{1,4,5} , Rui Henrique ^{1,4,5,*} ,
and Carmen Jerónimo ^{1,5,*} 

- ¹ Cancer Biology & Epigenetics Group, IPO Porto Research Center (GEBC CI-IPOP), Portuguese Oncology Institute of Porto (IPO Porto), Porto Comprehensive Cancer Center (P.CCC), RISE@CI-IPOP (Health Research Network), Portuguese Oncology Institute of Porto (IPO Porto), R. Dr. António Bernardino de Almeida, 4200-072 Porto, Portugal jose.leite.sequeira@ipporto.min-saude.pt (J.P.S.); vera.salvado.constancio@ipporto.min-saude.pt (V.C.); jpedro.lobo@ipporto.min-saude.pt (J.L.)
 - ² Master Programme in Oncology, School of Medicine & Biomedical Sciences, University of Porto (ICBAS-UP), Rua Jorge Viterbo Ferreira 228, 4050-513 Porto, Portugal
 - ³ Doctoral Programme in Biomedical Sciences, School of Medicine & Biomedical Sciences, University of Porto (ICBAS-UP), Rua Jorge Viterbo Ferreira 228, 4050-513 Porto, Portugal
 - ⁴ Department of Pathology, Portuguese Oncology Institute of Porto (IPOP), R. Dr. António Bernardino de Almeida, 4200-072 Porto, Portugal
 - ⁵ Department of Pathology and Molecular Immunology, School of Medicine & Biomedical Sciences, University of Porto (ICBAS-UP), Rua Jorge Viterbo Ferreira 228, 4050-513 Porto, Portugal
- * Correspondence: henrique@ipporto.min-saude.pt (R.H.); carmenjeronimo@ipporto.min-saude.pt (C.J.); Tel.: +351-225-084-000 (ext. 7264) (C.J.); Fax: +351-225-084-199 (C.J.)
- † Joint senior authors.



Citation: Sequeira, J.P.; Constâncio, V.; Lobo, J.; Henrique, R.; Jerónimo, C. Unveiling the World of Circulating and Exosomal microRNAs in Renal Cell Carcinoma. *Cancers* **2021**, *13*, 5252. <https://doi.org/10.3390/cancers13215252>

Academic Editor: Jean-Yves Blay

Received: 23 September 2021
Accepted: 18 October 2021
Published: 20 October 2021

Publisher's Note: MDPI stays neutral with regard to jurisdictional claims in published maps and institutional affiliations.



Copyright: © 2021 by the authors. Licensee MDPI, Basel, Switzerland. This article is an open access article distributed under the terms and conditions of the Creative Commons Attribution (CC BY) license (<https://creativecommons.org/licenses/by/4.0/>).

Simple Summary: Liquid biopsies have emerged as a new tool for early diagnosis. In renal cell carcinoma, this need is also evident and may represent an improvement in disease management. Hence, in this review we discuss the most updated advances in the assessment of miRNAs in liquid biopsies. Moreover, we explore the potential of circulating or exosome miRNAs in renal cell carcinoma to overcome the tissue biopsies limitations.

Abstract: Renal cell carcinoma is the third most common urological cancer. Despite recent advances, late diagnosis and poor prognosis of advanced-stage disease remain a major problem, entailing the need for novel early diagnosis tools. Liquid biopsies represent a promising minimally invasive clinical tool, providing real-time feedback of tumor behavior and biological potential, addressing its clonal evolution and representing its heterogeneity. In particular, the study of circulating microRNAs and exosomal microRNAs in liquid biopsies experienced an exponential increase in recent years, considering the potential clinical utility and available technology that facilitates implementation. Herein, we provide a systematic review on the applicability of these biomarkers in the context of renal cell carcinoma. Issues such as additional benefit from extracting microRNAs transported in extracellular vesicles, use for subtyping and representation of different histological types, correlation with tumor burden, and prediction of patient outcome are also addressed. Despite the need for more conclusive research, available data indicate that exosomal microRNAs represent a robust minimally invasive biomarker for renal cell carcinoma. Thus, innovative research on microRNAs and novel detection techniques are likely to provide clinically relevant biomarkers, overcome current clinical challenges, and improve patient management.

Keywords: renal cell carcinoma; biomarkers; liquid biopsies; microRNA; extracellular vesicles; exosomes

1. Introduction

Reducing cancer mortality remains a main goal of the scientific community, in part materialized by the many efforts to develop effective biomarkers for early detection to

decrease the proportion of cancers identified at late stages, which carry poor prognosis. Concerning renal cell carcinoma (RCC), early detection increases the likelihood of performing partial nephrectomy and, possibly, avoiding the need for adjuvant therapies, which have associated toxicities [1–4]. Moreover, in cases where such early detection is not possible, there are predictive biomarkers for response to therapy that may allow the use of second-line treatments in a timely manner. Moreover, prognostic biomarkers may provide information for selecting the best therapeutic strategy [5,6].

Overall, a cancer biomarker refers to any biological observation that can ideally replace and predict a clinically relevant outcome or an intermediate result that is more difficult to observe, and that might correspond to a protein, metabolite, RNA or DNA molecule, or an epigenetic alteration [7,8]. In addition, the pre-analytics, measurability and variability of a biomarker must be considered for its clinical application [7].

Over time, tumor tissue samples have always been the gold standard for diagnosis and prognostication. Nevertheless, this strategy faces relevant challenges. For instance, histological specimens only reflect the tumor composition at the time of sample taking. In addition, the limited quality and quantity of biomaterials derived from tissues may hamper accurate and reliable assessment of disease, and a biopsy may not provide a complete picture of the entire tumor landscape, which is particularly problematic in heterogeneous cancers such as RCC [9,10]. In addition, tissue biopsy sampling is an invasive and technically challenging tool, again particularly relevant in the kidney, considering its retroperitoneal topography [8,9]. To overcome these challenges of tissue biopsy sampling, liquid biopsies have emerged as alternative sources of clinically relevant information.

2. Liquid Biopsies

Unlike tissue biopsy sampling, liquid biopsies provide real-time feedback on the patient's condition, in a minimally invasive and repeatable manner, increasing early diagnoses rate [11,12]. They often reflect tumor burden and the shifting molecular landscape of cancers, being optimal tools that favor the applicability of cellular and molecular therapies that depend on systematic and routine measurements of critical biomarkers [13].

Liquid biopsies involve the collection of body fluids, for example, blood, urine, spills or saliva using a minimally invasive method. They allow for the study of circulating tumor cells and DNA, tumor-educated platelets, extracellular vesicles (EVs) and cell-free RNA or microRNA (miRNA) (Figure 1) [8,9].

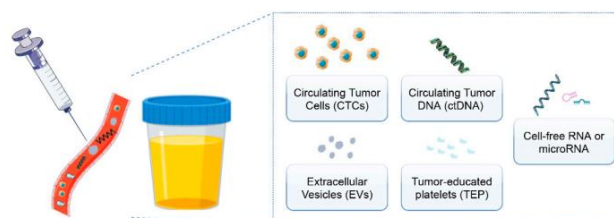


Figure 1. Clinical potential of liquid biopsies: what can we analyze using this promising non-invasive technique? Circulating tumor cells/DNA, extracellular vesicles, tumor-educated platelets and cell-free RNA or miRNA can be detected in the context of a liquid biopsy.

Each of them offers an immense potential, either together or as independent biomarkers for cancer, and importantly, each has its own advantages and limitations, many times related to sample type and preanalytical variables.

This emerging technique represents an ideal tool for early detection, subtyping, risk stratification and follow-up of cancer because it better represents tumor heterogeneity than tissue biopsies. In addition, they may aid in monitoring patients throughout specific targeted therapies, and pinpoint emergence of resistance that might entail the need for

changing treatment schedule. Moreover, they might allow for circulating biomarkers assessment at various time points in a timely, cost-effective, specific and sensitive minimally invasive manner [8,10,14]. Thus, it is imperative to unveil and develop minimally invasive markers that may not only detect cancer, but also prognosticate and predict response to therapy [15,16].

3. Renal Cell Tumors

According to the World Health Organization, renal cancer (RC) was, in 2020, the 16th most incident and the 17th most deadly cancer, worldwide [17].

Among RC, RCC accounts for approximately 90% of all cases, and originates from epithelial cells of the nephron [18,19]. RCC is highly heterogeneous, as depicted by the multiple entities and molecular subtypes. Each histological entity has specific molecular backgrounds, stressing the need for subtype-specific biomarkers and, likewise, subtype-specific therapies [20].

In addition, discriminating RCC from oncocytoma (the most common benign tumor originating from the renal cortex) is a relevant clinical challenge, especially the distinction between oncocytoma and chromophobe RCC (chRCC), which may be particularly difficult in the case of the eosinophilic variant of the latter [21].

3.1. Diagnosis

In recent years, and despite the drop of mortality rate, RCC incidence has increased, which can be attributed mainly to incidental detection owing to the easier access to medical imaging performed for other reasons [22].

Early diagnosis of RCC is a challenge mainly because 70% of patients with localized disease remain asymptomatic or with mild symptoms, which is also related to retroperitoneal location of the kidney [3,4]. Hence, patients often develop symptoms only at later stages, and these may include acute or chronic flank pain, hypertension, anemia and cachexia [3].

RCC diagnosis is often a presumptive one, until histological confirmation. The role of physical examination is limited, although when a palpable abdominal mass, new-onset varicocele, or lower extremity edema are found, the patient should be evaluated by imaging for the presence of retroperitoneal neoplasia. Imaging may comprise computed tomography, abdominal ultrasound, magnetic resonance imaging (diffusion-weighted and perfusion-weighted imaging) and positron emission tomography [3,23]. Furthermore, a renal biopsy may be performed for diagnosis, although this technique remains underused [3]. Yet, the confirmation of malignancy may require specialized assessment of the nephrectomy specimen [24]. In this context, liquid biopsies may have the potential to become a central tool in RCC diagnosis, eventually sparing the need for nephrectomy in non-malignant conditions, although studies in this direction are still evolving [25–27].

3.2. Prognosis

The prognosis of RCC patients is highly dependent on histological subtype and TNM stage, among other factors. Some studies found that patients with advanced stage disease that undergo partial nephrectomy endure a better outcome and better post-surgical renal function than patients that undergo radical nephrectomy. Therefore, partial nephrectomy has become the first-choice therapeutic strategy, as it offers approximately the same survival time and superior renal function than radical nephrectomy [1,2].

Early diagnosis and treatment of RCC are important to increase global five-year survival, as inferred by the 90% survival rate for early-stage RCC compared to 13% of locally advanced or metastatic disease. However, patients with stage III that undergo nephrectomy have a survival rate above 70%. In addition, metastatic disease, advanced stage and invasion into the renal vein are predictors of poor prognosis in RCC [28,29]. According to a population-based study (2005–2009), 1 in 3 RCC patients was diagnosed

with metastatic disease [6,30]. In addition, local recurrence or distant metastasis may be found in 20–40% of patients undergoing surgery [30,31].

In view of this, the prognosis of recurrence is variable, with the detection of early relapse being the main factor for patient prognosis [5,6]. Thus, early RCC detection, which may be provided by liquid biopsy techniques, will result in improved outcome.

4. MicroRNAs

MiRNAs are small non-coding RNAs, which can suppress gene expression at the translational level by directly targeting mRNA molecules. Moreover, they are involved in cell differentiation, growth, apoptosis, and proliferation [32,33]. MiRNA deregulation in cancer was first described in 2002 (chronic lymphocytic leukemia), and since then, it has been increasingly implicated in tumorigenesis [32–35].

MiRNAs have the ability to act as tumor suppressors or as oncogenic miRNAs, which are usually found down- or upregulated in cancer, respectively [34]. Moreover, miRNAs signatures seem to differ between cancer and normal tissues, as well as among cancer subtypes, thus representing a promising tumor biomarker in liquid biopsies [32,33].

Although several miRNA quantification techniques have been developed over the years, quantitative real-time polymerase chain reaction (qRT-PCR) has been the most widely used technology, especially due to the more disseminated know-how [36,37]. However, the emergence and progress of digital PCR may lead to improved miRNA analysis. With this technique, it is advocated that the steps of normalization to housekeeping miRNAs and preamplification can be obviated. In addition, it does not require triplicates and is easier to set cutoffs of positivity, compared with qRT-PCR [36–39].

Circulating miRNAs have been reported in many clinical contexts. In cancer, they have been described as biomarkers in several cancer models, including prostate and breast cancers, disclosing a diagnostic and predictive role [40–42].

Circulating microRNAs in Renal Cell Carcinoma

In RCC, miRNAs have been assessed in serum, plasma and urine. A detailed description of miRNAs thus far reported for RCC diagnosis is presented in Table 1. The upregulated miR-21 and miR-106a, isolated from serum, is a potential diagnostic biomarker for ccRCC, disclosing 86.7% sensitivity and 70% specificity, with lower levels found in healthy donors and in ccRCC patients post-operatively, compared with ccRCC patients before surgery [43]. Thus, further studies are required to determine whether miR-106a levels may predict recurrence after surgery. Although the results were normalized to U6, recent studies indicate that some RNA species (i.e., U6, RNU6b, RNU48) are susceptible to degradation by serum RNAses; thus, normalization by these reference miRNAs is not reasonable [44]. Furthermore, a panel combining miR-141 and miR-1233 was reported as ccRCC diagnostic biomarker, with high sensitivity and specificity (100% and 73.3%, respectively), although no association was found between miRNAs levels and TNM stage, Furrman's grade and SSIGN (Stage, Size, Grade and Necrosis) score [45].

MiR-210 has been reported as a diagnostic biomarker in several studies [46–48]. The most recent meta-analysis by Chen et al. reported 74% sensitivity and 76% specificity for this miRNA in detection of RCC [49]. Remarkably, in association with miR-378, sensitivity and specificity reached 80% and 78%, respectively [46]. When the two miRNAs levels were analyzed one week and three months after surgery, lower values were found compared to before the nephrectomy [46], which may signify that these miRNAs may be useful for clinical-decision making and evaluation of disease burden after nephrectomy. However, there was no correlation with Furrman's grade, overall survival or histological RCC subtypes.

A minority of circulating miRNAs was reported in urine and plasma. Specifically, in urine, miR-15a was found to be upregulated in ccRCC patients and could detect ccRCC with a 98.1% sensitivity and 100% specificity, associating with tumor size [50]. However, no differences of miR-15a levels were found among RCC subtypes [50]. Notwithstanding the high sensitivity and specificity of urinary biomarkers, doubts about circulating miRNAs have emerged, since the aggressive urinary environment may lead to miRNAs instability and hamper detection [51].

All circulating and exosomal miRNA studies reported in this review are based on qRT-PCR. The greatest difficulty of qRT-PCR in the analysis of results is the normalization of data, as there is no consensus on which reference miRNA is most appropriate since some studies report that RNU6B/U6, 5s rRNA, RNU44/RNU48, for example, are not stable in body fluids and are hence not reliable means of normalization [44,47].

Recent studies describe that in kidney cancer studies, results' normalization should be performed using miR-16a [47,52–54], however, a normalization with the above described RNAs has still being executed [43–45,48,50,55–59]. Furthermore, some authors do not normalize their results, performing absolute quantification instead. Nonetheless, no details are provided by them concerning the samples used as standards for the quantification [46,60].

Additionally, miRNAs have been reported as prognostic biomarkers (Table 2). In plasma samples, detection of lower miR-150 levels was significantly associated with both shorter overall and ccRCC-specific survival, and detection of higher miR-221 levels was also associated with poor overall survival in RCC [58,61]. Of note, however, downregulation of miR-150 may reflect an effect of blood cells, related to treatment or to impaired immune response, since this miRNA is highly expressed in mature B and T cells [61].

Table 1. Promising diagnostic circulating miRNA in renal cell carcinoma (RCC).

Biomarker	Clinical Application	Source	Number of Cases/Controls	Quantification Technique	Normalizer	Sensitivity %	Specificity %	AUC ^a	REF ^b
miR-21 ↑ miR-106a ↑	Diagnostic of ccRCC	Serum	30 ccRCC ^c patients/30 cancer-free blood donor volunteers	qRT-PCR	U6	77.3 86.7	96.4 70.0	0.865 0.819	[43]
miR-34a ↓ miR-141 ↓ miR-1233 ↑ miR-141 + miR-1233	Diagnostic of ccRCC	Serum	30 ccRCC patients (without metastatic disease)/15 non-renal benign diseases patients	qRT-PCR	Cel-miR-39	80.76 93.33 73.33 100.0	75.0 80.0 100.0	0.920 0.780 0.970 n.a. d	[45]
miR-210 ↑	Diagnostic of ccRCC	Serum	68 ccRCC patients before surgery/42 healthy controls	qRT-PCR	5s rRNA	81.0	79.4	0.874	[48]
miR-210 ↑	Diagnostic of ccRCC	Serum	34 ccRCC patients/23 healthy controls	qRT-PCR	miR-16-5p	65.0	83.0	0.770	[47]
miR-210 ↑ + miR-378 ↑	Diagnostic of RCC ^e	Serum	195 RCC patients (157 ccRCC, 26 pRCC ^f , 12 chrRCC ^g)/100 healthy controls	qRT-PCR	Data not normalized	80.0	78.0	0.850	[46]
miR-378 ↑ + miR-451 ↓	Diagnostic of RCC	Serum	Screening Phase: 15 ccRCC patients/12 matched healthy controls Validation Phase: 90 RCC patients (73 ccRCC, 8 pRCC, 9 chrRCC)/35 matched healthy controls	qRT-PCR	miR-16-5p	81.0	83.0	0.860	[52]
miR-1233-3p ↑	Diagnostic of RCC (No differences between RCC patients and Benign renal masses)	Serum	84 RCC patients (69 ccRCC, 10 pRCC, 3 chrRCC, 2 sRCC ^h)/93 healthy controls/13 benign renal masses	qRT-PCR	Cel-miR-39	77.4	37.6	0.588	[44]
miR-193a-3p ↑ + miR-362 ↑ + miR-572 ↑ + miR-28-5p ↓ + miR-378 ↓	Diagnostic of early-stage ccRCC	Serum	107 ccRCC patients/107 healthy controls	qRT-PCR	Let-7d/g/i	80.0	71.0	0.807	[56]
miR-210 ↑	Diagnostic of ccRCC	Serum	45 ccRCC patients/30 healthy controls	qRT-PCR	miR-16-5p	67.5	70.0	0.789	[53]

Table 1. Cont.

Biomarker	Clinical Application	Source	Number of Cases/Controls	Quantification Technique	Normalizer	Sensitivity %	Specificity %	AUC ^a	REF ^b
let-7a-5p ↑	Diagnostic of ccRCC	Urine	69 non-metastatic ccRCC patients/36 healthy controls	qRT-PCR	Data not normalized	71.0	81.0	0.831	[60]
miR-15a ↑	Diagnostic of RCC	Urine	67 renal tumor patients (22 ccRCC, 16 pRCC, 14 chRCC, 8 oncocytoma, 2 papillary adenoma, 5 angiomyolipoma)/15 healthy controls without kidney pathology	qRT-PCR	U6	98.1	100.0	0.955	[50]
miR-15a ↑	Diagnostic of RCC	Urine	7 ccRCC/5 chRCC/6 pRCC & 5 Oncocytoma/5 Healthy Controls	qRT-PCR	5s rRNA	n.a.	n.a.	n.a.	[55]
miR-508-3p ↓	Diagnostic of RCC	Plasma	10 RCC patients/10 Healthy Controls	qRT-PCR	U6	n.a.	n.a.	n.a.	[57]

^a AUC—area under the curve; ^b REF—reference; ^c ccRCC—clear cell renal cell carcinoma; ^d n.a.—not applicable; ^e RCC—renal cell carcinoma; ^f pRCC—papillary renal cell carcinoma; ^g chRCC—chromophobe renal cell carcinoma; ^h sRCC—sarcomatoid renal cell carcinoma not otherwise specified. ↑ means upregulated and ↓ means downregulated.

Table 2. Promising predictive and prognostic circulating miRNA in renal cell carcinoma (RCC).

Biomarker	Clinical Application	Source	Number of Cases/Controls	Quantification Technique	Normalizer	Consequences	REF ^a
miR-183 (high levels)	Predictive	Serum	82 RCC ^b patients/19 healthy controls	qRT-PCR	U6	↑ resistance to NK ^c cells cytotoxicity	[59]
miR-378 (high levels)	Prognostic	Serum	195 RCC patients (157 ccRCC ^d , 26 pRCC ^e , 12 chRCC ^f)/100 healthy controls	qRT-PCR	Data not normalized	↓ DFS ^g	[46]
miR-122-5p (high levels)	Prognostic	Serum	68 ccRCC/47 BRT ^h /28 healthy controls	qRT-PCR	miR-16-5p + miR-191-5p + miR-320a	↓ OS ⁱ , CSS ^j , PFS ^k	[54]
miR-206 (high levels)	Prognostic	Plasma	94 ccRCC patients/100 healthy controls	qRT-PCR	Quantile	↑ OS, DSS ^l	[61]
miR-150-5p (low levels)	Prognostic	Plasma	43 RCC patients/34 healthy controls	qRT-PCR	RNU44	↓ OS	[58]

^a REF—reference; ^b RCC—renal cell carcinoma; ^c NK—natural killer; ^d ccRCC—clear cell renal cell carcinoma; ^e pRCC—papillary renal cell carcinoma; ^f chRCC—chromophobe renal cell carcinoma; ^g DFS—disease-free survival; ^h BRT—benign renal tumors; ⁱ OS—overall survival; ^j CSS—cancer-specific survival; ^k PFS—progression-free survival; ^l DSS—disease-specific survival. ↑ means longer survival and ↓ means shorter survival.

5. Extracellular Vesicles

Although circulating miRNAs seem promising as non-invasive or minimally invasive means to obtain diagnostic and/or prognostic information and to evaluate disease evolution, extracellular vesicles (EVs) have recently surfaced as an auspicious source of biomarkers for several diseases, including cancer. The vast majority of cells release EVs [23], which may resemble the alterations of tumor cells. Importantly, EVs can protect their cargo, such as miRNAs, thus representing a valuable resource for potential cancer biomarkers.

EVs have a membrane of variable size and diverse content, possibly containing lipids, peptides, enzymes, functional/structural proteins, mitochondrial DNA and a wide variety of RNAs (small RNAs, lncRNAs and messenger RNAs) capable of regulating virtually all cellular functions (Figure 2) [23,62,63]. EVs can be found in body fluids, such as plasma, serum and urine, since their bilipid membrane serves as protection against urine and blood circulation [23].

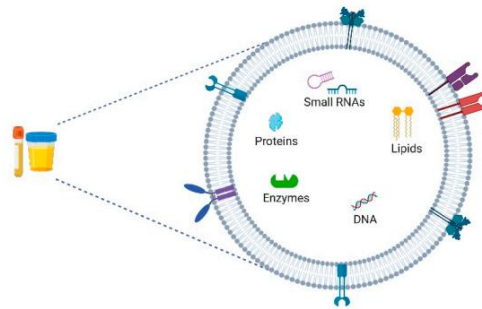


Figure 2. Content and cargo of extracellular vesicles: small RNAs, lipids, proteins, enzymes and DNA. Created with BioRender.com.

The most studied subpopulation of EVs are the exosomes. Yet, no consensus has been reached thus far concerning the definition and size of exosomes, representing the first difficulty when comparing/assessing studies related to miRNAs carried in EVs. Specifically, for the purposes of this review, we will follow the International Society of Extracellular Vesicles (ISEV) consensus, which recommends the use of the generic term “extracellular vesicles”. Nonetheless, several authors sustain that exosomes are EVs with a size between 50 and 150 nm [23]. Notwithstanding, exosome size has been a matter of debate across literature and scientific community [23,62,63], since the classification may lead to misinterpretation, because the size of microvesicles and apoptotic bodies lies between 100 nm–1 μ m and 50 nm–5 μ m, respectively [64].

EVs can be isolated by two major isolation techniques: density-based and size-based. Isolation by density can be performed by differential ultracentrifugation or density gradient ultracentrifugation [65]. Ultrafiltration, size exclusion chromatography, polymer precipitation and microfluidic based-strategies are techniques of EVs isolation by size [65].

The potential of EVs as RCC biomarkers, especially EV-containing miRNAs, has been addressed in several publications (summarized in Table 3) [66–71]. Isolated from serum EVs, miR-210 and miR-1233 have been shown as ccRCC diagnostic biomarkers with 70% and 81% sensitivity, and 62.2% and 76.0% specificity, respectively, and notably decreasing after nephrectomy [71]. However, no differences were found among TNM stages, raising the question as to whether they might reflect tumor burden. Wang and colleagues reported that miR-210 identified RCC with 82.5% sensitivity and 80.0% specificity. In this case, higher miR-210 levels were found in more advanced stages and higher Fuhrman grades, with no associations found with gender or age [53].

Table 3. Promising diagnostic exosomal miRNA in Renal Cell Carcinoma (RCC).

Biomarker	Clinical Application	Source	Number of Cases/Controls	Sensitivity %	Specificity %	AUC ^a	Isolation	Characterization	Quantification Technique	Normalizer	REF ^b
miR-210 ↑ miR-1233 ↑	Diagnostic of ccRCC ^c	Serum	82 ccRCC patients/ 80 healthy controls	70.0 81.0	62.2 76.0	n.a. ^d n.a.	Total exosome isolation reagent (Invitrogen, Carlsbad, CA, USA)	Flow cytometry analysis and immunofluorescence	qRT-PCR	U6	[71]
miR-210 ↑	Diagnostic of ccRCC	Serum	45 ccRCC patients/ 30 healthy controls	82.5	80.0	n.a.	Total Exosome Isolation Reagent (from serum; Invitrogen, Carlsbad, CA, USA)	TEM ^e ; WB ^f	qRT-PCR	miR-16-5p	[53]
Combination of miR-126-3p-miR-449a	Diagnostic of ccRCC	Urine	81 ccRCC patients/ 24 patients with benign lesions/ 33 healthy controls	60.6	100.0	0.820	Urine Exosome RNA Isolation Kit (Cat. 47200)	TEM	qRT-PCR	miR-16-5p + miR-106a-5p	[66]
Combination of miR-126-3p-miR-34b-5p				67.3	82.8	0.800					
Combination of miR-126-3p-miR-486-5p				52.9	95.8	0.790					
Combination of miR-25-3p-miR-34b-5p				73.1	79.3	0.760					
Combination of miR-21-5p-miR-34b-5p				74.0	72.4	0.760					
Combination of miR-150-3p-miR-126-3p	61.5	82.8	0.760								
miR-30c-5p ↓	Diagnostic biomarker of early-stage ccRCC	Urine	70 early-stage (T1aN0M0) ccRCC patients/ 30 early-stage prostate cancer (T1N0M0) patients/ 30 early-stage bladder cancer (T1N0M0) patients/ 30 healthy controls	68.57	100.0	0.819	Ultracentrifugation	NTA ^g ; TEM	qRT-PCR	Not Specified	[70]

^a AUC—area under the curve; ^b REF—reference; ^c ccRCC—clear cell renal cell carcinoma; ^d n.a.—not applicable; ^e TEM—transmission electron microscopy; ^f WB—Western blot; ^g NTA—nanoparticle tracking analysis. ↑ means upregulated and ↓ means downregulated.

Regarding urine, different combinations of miRNAs, comprising miR-126-3p + miR-449a, miR-126-3p + miR-34b-5p, miR-126-3p + miR-486-5p, miR-25-3p + miR-34b-5p, miR-21-5p + miR-34b-5p and miR-150-5p + miR-126-3p, have been reported as diagnostic biomarkers for ccRCC, with 60.6%, 67.3%, 52.9%, 73.1%, 74% and 61.5% sensitivity, respectively, as well as 100%, 82.8%, 95.8%, 79.3%, 72.4% and 82.8% specificity, respectively [66]. The putative targets of these miRNAs were implicated in cell cycle regulation, tumorigenesis and angiogenesis [66]. Furthermore, downregulated miR-30c-5p has been reported as a potential diagnostic biomarker for early-stage ccRCC, with 68.57% sensitivity and 100% specificity [70].

Additionally, mRNA, proteins, lipids and lncRNA were also assessed in EVs released by RCC. Lower levels of mRNAs GSTA1, CEBPA and PCBD1 were found in EVs of ccRCC patients compared to healthy donors [67]. Expression of these biomarkers was higher in papillary and chromophobe RCC than in clear cell RCC [67]. Moreover, a panel composed by proteins CD10, MMP9, EMMPRIN, CAIX, DPEP1, DKK4, Syntenin 1 and AQP1 was shown to significantly differ between RCC and healthy subjects [69].

When EVs are isolated from plasma, a decrease of miR-26a-1-3p, miR-let-7-I, miRNA-615-3p was found, disclosing a significant association with highly aggressive metastatic disease in clear cell RCC [72] (Table 4). miR-let-7i-5p is a tumor suppressor in RCC cell lines, downregulating C-myc and its target genes. Dysregulation of this miRNA leads to 5-fluoro-uracil resistance of RCC cells [72].

Additionally, lncARSR might represent a predictive biomarker and potential alternative target against sunitinib resistance, since this long non-coding RNA can be secreted by resistant cells, making sensitive cells resistant and fostering drug resistance. Inhibition of lncARSR in both orthotopic xenografts and PDX models suggests that this strategy may be used for overcoming sunitinib-resistant RCC [73] (Table 4).

Finally, the first association between lipid composition of urinary exosomes and RCC was first described by Del Boccio et al., disclosing a panel of 22 lipids which may allow for accurate diagnosis of clear cell RCC [68].

Table 4. Promising prognostic exosomal miRNA in renal cell carcinoma (RCC).

Biomarker	Clinical Application	Source	Number of Cases/Controls	Consequences	Isolation	Characterization	Quantification Technique	Normalizer	REF ^a
miR-224 (high levels)	Prognostic	Serum	108 ccRCC ^b patients	↓ OS ^c , CSS ^d , PFS ^e	Total Exosome Isolation kit (from serum) (Invitrogen, Waltham, MA, USA)	TEM ^f , WB ^g	qRT-PCR	miR-16-5p	[74]
miR-26a-1-3p, miR-let-7f-5p, miRN-615-3p (high levels)	Prognostic	Plasma	Screening Phase: 40 ccRCC, 2 pRCC ^h , 2 unspecified Validation Phase: 52 ccRCC, 2 chRCC ⁱ , 6 pRCC, 5 unspecified	↑ OS	ExoQuick (System Biosciences, Mountain View, CA, USA)	n.a. ^j	qRT-PCR	miR-127-3p	[72]

^a REF—reference; ^b ccRCC—clear cell renal cell carcinoma; ^c OS—overall survival; ^d CSS—cancer-specific survival; ^e PFS—progression-free survival; ^f TEM—transmission electron microscopy; ^g WB—Western blot; ^h pRCC—papillary renal cell carcinoma; ⁱ chRCC—chromophobe renal cell carcinoma; ^j n.a.—not applicable. † means longer survival and ‡ means shorter survival.

6. Circulating miRNAs versus Exosomal miRNAs

In recent years, circulating miRNAs and exosomal miRNAs (exomiRNAs) in liquid biopsies have been intensively studied. However, only few studies aimed to compare these two sources of miRNAs. Most authors argue that exosomal miRNAs represent a better way to analyze miRNAs since these seem to have more quantity and better quality and stability than circulating miRNAs [75]. Moreover, for urinary miRNAs, significant differences between circulating miRNAs and exomiRNAs have been reported [76,77].

Hence, the method that reaches the best accuracy and maximizes the detection of biomarkers should be established. For instance, Tian et al. explored the differences between the two sources of miRNAs obtained from plasma samples. In healthy donors, no differences between circulating miRNAs and exomiRNAs were apparent. However, in lung cancer patients, miRNAs (miR-181b-5p and miR-21-5p) were more enriched in exosomes than free in circulation [76].

Comparative studies have been performed in several cancer models. In lung adenocarcinoma, from a panel of six plasma miRNAs, only two were found upregulated in plasma exosomes [78]. In gastric cancer, miR-132-3p and miR-185-5p disclosed normal expression in serum exosomes, although these miRNAs were found upregulated in serum [79]. Notwithstanding the lack of comparative studies in RCC, considering the data collected and analyzed for this review, it seems that exomiRNAs disclose higher sensitivity and specificity than circulating miRNAs [44,45,48,49,53,71]. miR-1233 depicted an increase in sensitivity and specificity when detected in exosomes (of 4.4% and 50.5%, respectively [44,71]). In addition, for miR-210, Wang and colleagues found that the increase in sensitivity and specificity in exosomes was of 18.2% and 12.5%, respectively [53]. However, validation studies providing direct comparisons are required to draw more definitive conclusions [44,45,48,49,53,71]. Depending on the specific miRNA, its expression in circulation or exosomes is variable, and it may be better detected in one source or the other [80]. We thus recommend that the choice of method for studying miRNAs should be dependent on the specific miRNA and its biological context.

7. Conclusions

Overall, the reviewed supports the importance that EVs and miRNAs have as promising biomarkers for RCC, using liquid biopsies. This minimally invasive technique is likely to overcome the limitations of tissue biopsies and provide a more accurate and timely picture of the evolution of RCC. Nonetheless, future studies on EVs and miRNAs should focus more directly on clinical application, exploring the development of a more cost-effective and accurate tool for diagnosis and prognosis of RCC.

Author Contributions: Conceptualization, J.P.S., V.C. and C.J.; manuscript writing, J.P.S.; critical revision of manuscript, V.C., J.L., R.H. and C.J.; images were conceptualized and performed by J.P.S.; supervision, R.H. and C.J. All authors have read and agreed to the published version of the manuscript.

Funding: C.J.'s work is funded by Research Center-Portuguese Oncology Institute of Porto (Grant PI 74-CI-IPOP-19-2015 and PI-27-CI-IPOP). V.C. received the support of a fellowship from "la Caixa" Foundation (ID 100010434). The fellowship code is LCF/BQ/DR20/11790013. J.L. is recipient of a fellowship from FCT—Fundação para a Ciência e Tecnologia—(SFRH/BD/132751/2017).

Conflicts of Interest: The authors declare no conflict of interest.

References

1. Alvim, R.; Tin, A.; Nogueira, L.; Lebdai, S.; Wong, N.; Takeda, T.; Assel, M.; Hakimi, A.A.; Touijer, K.; Russo, P.; et al. A comparison of oncologic and functional outcomes in patients with pT3a renal cell carcinoma treated with partial and radical nephrectomy. *Int. Braz. J. Urol.* **2021**, *47*, 777–783. [\[CrossRef\]](#)
2. Deng, H.; Fan, Y.; Yuan, F.; Wang, L.; Hong, Z.; Zhan, J.; Zhang, W. Partial nephrectomy provides equivalent oncologic outcomes and better renal function preservation than radical nephrectomy for pathological T3a renal cell carcinoma: A meta-analysis. *Int. Braz. J. Urol.* **2021**, *47*, 46–60. [\[CrossRef\]](#)

3. Capitanio, U.; Montorsi, F. Renal cancer. *Lancet* **2016**, *387*, 894–906. [[CrossRef](#)]
4. Huang, J.J.; Hsieh, J.J. The Therapeutic Landscape of Renal Cell Carcinoma: From the Dark Age to the Golden Age. *Semin. Nephrol* **2020**, *40*, 28–41. [[CrossRef](#)] [[PubMed](#)]
5. Dabestani, S.; Beisland, C.; Stewart, G.D.; Bensalah, K.; Gudmundsson, E.; Lam, T.B.; Gietzmann, W.; Zakikhani, P.; Marconi, L.; Fernández-Pello, S.; et al. Long-term Outcomes of Follow-up for Initially Localised Clear Cell Renal Cell Carcinoma: RECUR Database Analysis. *Eur. Urol. Focus* **2019**, *5*, 857–866. [[CrossRef](#)] [[PubMed](#)]
6. Dias, F.; Teixeira, A.L.; Nogueira, I.; Morais, M.; Maia, J.; Bodo, C.; Ferreira, M.; Silva, A.; Vilhena, M.; Lobo, J.; et al. Extracellular Vesicles Enriched in hsa-miR-301a-3p and hsa-miR-1293 Dynamics in Clear Cell Renal Cell Carcinoma Patients: Potential Biomarkers of Metastatic Disease. *Cancers* **2020**, *12*, 1450. [[CrossRef](#)] [[PubMed](#)]
7. Aronson, J.K.; Ferner, R.E. Biomarkers—A General Review. *Curr. Protoc. Pharmacol.* **2017**, *76*, 9–23. [[CrossRef](#)] [[PubMed](#)]
8. Constâncio, V.; Nunes, S.P.; Henrique, R.; Jerónimo, C. DNA Methylation-Based Testing in Liquid Biopsies as Detection and Prognostic Biomarkers for the Four Major Cancer Types. *Cells* **2020**, *9*, 624. [[CrossRef](#)]
9. Cui, S.; Cheng, Z.; Qin, W.; Jiang, L. Exosomes as a liquid biopsy for lung cancer. *Lung Cancer* **2018**, *116*, 46–54. [[CrossRef](#)] [[PubMed](#)]
10. Mader, S.; Pantel, K. Liquid Biopsy: Current Status and Future Perspectives. *Oncol. Res. Treat.* **2017**, *40*, 404–408. [[CrossRef](#)]
11. Alix-Panabieres, C. The future of liquid biopsy. *Nature* **2020**, *579*, S9. [[CrossRef](#)] [[PubMed](#)]
12. Lianidou, E.; Pantel, K. Liquid biopsies. *Genes Chromosomes Cancer* **2019**, *58*, 219–232. [[CrossRef](#)] [[PubMed](#)]
13. Vaidyanathan, R.; Soon, R.H.; Zhang, P.; Jiang, K.; Lim, C.T. Cancer diagnosis: From tumor to liquid biopsy and beyond. *Lab. Chip* **2018**, *19*, 11–34. [[CrossRef](#)] [[PubMed](#)]
14. Heitzer, E.; Ulz, P.; Geigl, J.B. Circulating tumor DNA as a liquid biopsy for cancer. *Clin. Chem.* **2015**, *61*, 112–123. [[CrossRef](#)]
15. Campi, R.; Stewart, G.D.; Staehler, M.; Dabestani, S.; Kuczyk, M.A.; Shuch, B.M.; Finelli, A.; Bex, A.; Ljungberg, B.; Capitanio, U. Novel Liquid Biomarkers and Innovative Imaging for Kidney Cancer Diagnosis: What Can Be Implemented in Our Practice Today? A Systematic Review of the Literature. *Eur. Urol. Oncol.* **2021**, *4*, 22–41. [[CrossRef](#)] [[PubMed](#)]
16. Di Meo, A.; Saleeb, R.; Wala, S.J.; Khella, H.W.; Ding, Q.; Zhai, H.; Krishan, K.; Krizova, A.; Gabril, M.; Evans, A.; et al. A miRNA-based classification of renal cell carcinoma subtypes by PCR and in situ hybridization. *Oncotarget* **2017**, *9*, 2092–2104. [[CrossRef](#)]
17. Sung, H.; Ferlay, J.; Siegel, R.L.; Laversanne, M.; Soerjomataram, I.; Jemal, A.; Bray, F. Global Cancer Statistics 2020: GLOBOCAN Estimates of Incidence and Mortality Worldwide for 36 Cancers in 185 Countries. *CA Cancer J. Clin.* **2021**, *71*, 209–249. [[CrossRef](#)]
18. Pandey, J.; Syed, W. Renal Cancer. In *StatPearls*; StatPearls Publishing LLC: Treasure Island, FL, USA, 2021.
19. Arora, R.D.; Limaem, F. Renal Clear Cell Cancer. In *StatPearls*; StatPearls Publishing LLC: Treasure Island, FL, USA, 2021.
20. Ricketts, C.J.; De Cubas, A.A.; Fan, H.; Smith, C.C.; Lang, M.; Reznik, E.; Bowlby, R.; Gibb, E.A.; Akbani, R.; Beroukhi, R.; et al. The Cancer Genome Atlas Comprehensive Molecular Characterization of Renal Cell Carcinoma. *Cell Rep.* **2018**, *23*, 313–326.e5. [[CrossRef](#)]
21. Shuch, B.; Amin, A.; Armstrong, A.J.; Eble, J.N.; Ficarra, V.; Lopez-Beltran, A.; Martignoni, G.; Rini, B.I.; Kutikov, A. Understanding pathologic variants of renal cell carcinoma: Distilling therapeutic opportunities from biologic complexity. *Eur. Urol.* **2015**, *67*, 85–97. [[CrossRef](#)]
22. Capitanio, U.; Bensalah, K.; Bex, A.; Boorjian, S.A.; Bray, F.; Coleman, J.; Gore, J.L.; Sun, M.; Wood, C.; Russo, P. Epidemiology of Renal Cell Carcinoma. *Eur. Urol.* **2019**, *75*, 74–84. [[CrossRef](#)]
23. Zieren, R.C.; Dong, L.; Pierorazio, P.M.; Pienta, K.J.; de Reijke, T.M.; Amend, S.R. Extracellular vesicle isolation from human renal cancer tissue. *Med. Oncol.* **2020**, *37*, 28. [[CrossRef](#)]
24. Ljungberg, B.; Albiges, L.; Abu-Ghanem, Y.; Bensalah, K.; Dabestani, S.; Fernández-Pello, S.; Giles, R.H.; Hofmann, F.; Hora, M.; Kuczyk, M.A.; et al. European Association of Urology Guidelines on Renal Cell Carcinoma: The 2019 Update. *Eur. Urol.* **2019**, *75*, 799–810. [[CrossRef](#)]
25. Drula, R.; Ott, L.F.; Berindan-Neagoe, I.; Pantel, K.; Calin, G.A. MicroRNAs from Liquid Biopsy Derived Extracellular Vesicles: Recent Advances in Detection and Characterization Methods. *Cancers* **2020**, *12*, 2009. [[CrossRef](#)]
26. Lakshminarayanan, H.; Rutishauser, D.; Schraml, P.; Moch, H.; Bolck, H.A. Liquid Biopsies in Renal Cell Carcinoma—Recent Advances and Promising New Technologies for the Early Detection of Metastatic Disease. *Front. Oncol.* **2020**, *10*, 2302. [[CrossRef](#)]
27. Smith, C.G.; Moser, T.; Moulriere, F.; Field-Rayner, J.; Eldridge, M.; Riediger, A.L.; Chandrananda, D.; Heider, K.; Wan, J.C.M.; Warren, A.Y.; et al. Comprehensive characterization of cell-free tumor DNA in plasma and urine of patients with renal tumors. *Genome Med.* **2020**, *12*, 23. [[CrossRef](#)]
28. Anderson, C.B.; Clark, P.E.; Morgan, T.M.; Stratton, K.L.; Herrell, S.D.; Davis, R.; Cookson, M.S.; Smith, J.A., Jr.; Chang, S.S. Urinary collecting system invasion is a predictor for overall and disease-specific survival in locally invasive renal cell carcinoma. *Urology* **2011**, *78*, 99–104. [[CrossRef](#)]
29. Ballard, B.D.; Guzman, N. Renal Mass. In *StatPearls*; StatPearls Publishing LLC: Treasure Island, FL, USA, 2021.
30. Dabestani, S.; Thorstenson, A.; Lindblad, P.; Harmenberg, U.; Ljungberg, B.; Lundstam, S. Renal cell carcinoma recurrences and metastases in primary non-metastatic patients: A population-based study. *World J. Urol.* **2016**, *34*, 1081–1086. [[CrossRef](#)] [[PubMed](#)]

31. Dias, F.; Teixeira, A.L.; Nogueira, I.; Morais, M.; Maia, J.; Bodo, C.; Ferreira, M.; Vieira, I.; Silva, J.; Lobo, J.; et al. Plasma Extracellular Vesicle-Derived TIMP-1 mRNA as a Prognostic Biomarker in Clear Cell Renal Cell Carcinoma: A Pilot Study. *Int. J. Mol. Sci.* **2020**, *21*, 4624. [[CrossRef](#)]
32. Filella, X.; Foj, L. miRNAs as novel biomarkers in the management of prostate cancer. *Clin. Chem. Lab. Med.* **2017**, *55*, 715–736. [[CrossRef](#)] [[PubMed](#)]
33. Lu, J.; Getz, G.; Miska, E.A.; Alvarez-Saavedra, E.; Lamb, J.; Peck, D.; Sweet-Cordero, A.; Ebert, B.L.; Mak, R.H.; Ferrando, A.A.; et al. MicroRNA expression profiles classify human cancers. *Nature* **2005**, *435*, 834–838. [[CrossRef](#)] [[PubMed](#)]
34. Guil, S.; Esteller, M. DNA methylomes, histone codes and miRNAs: Tying it all together. *Int. J. Biochem. Cell Biol.* **2009**, *41*, 87–95. [[CrossRef](#)] [[PubMed](#)]
35. Outeiro-Pinho, G.; Barros-Silva, D.; Correia, M.P.; Henrique, R.; Jerónimo, C. Renal Cell Tumors: Uncovering the Biomarker Potential of ncRNAs. *Cancers* **2020**, *12*, 2214. [[CrossRef](#)] [[PubMed](#)]
36. Campomenosi, P.; Gini, E.; Noonan, D.M.; Poli, A.; D'Antona, P.; Rotolo, N.; Dominioni, L.; Imperatori, A. A comparison between quantitative PCR and droplet digital PCR technologies for circulating microRNA quantification in human lung cancer. *BMC Biotechnol.* **2016**, *16*, 60. [[CrossRef](#)]
37. Lobo, J.; Leão, R.; Gillis, A.J.M.; van den Berg, A.; Anson-Cartwright, L.; Atenafu, E.G.; Kuhathaas, K.; Chung, P.; Hansen, A.; Bedard, P.L.; et al. Utility of Serum miR-371a-3p in Predicting Relapse on Surveillance in Patients with Clinical Stage I Testicular Germ Cell Cancer. *Eur. Urol. Oncol.* **2020**, *4*, 483–491. [[CrossRef](#)]
38. Cirillo, P.D.R.; Margiotti, K.; Mesoraca, A.; Giorlandino, C. Quantification of circulating microRNAs by droplet digital PCR for cancer detection. *BMC Res. Notes* **2020**, *13*, 351. [[CrossRef](#)]
39. Ferracin, M.; Negrini, M. Quantification of Circulating MicroRNAs by Droplet Digital PCR. *Methods Mol. Biol.* **2018**, *1768*, 445–457. [[CrossRef](#)]
40. Bidarra, D.; Constancio, V.; Barros-Silva, D.; Ramalho-Carvalho, J.; Moreira-Barbosa, C.; Antunes, L.; Mauricio, J.; Oliveira, J.; Henrique, R.; Jerónimo, C. Circulating MicroRNAs as Biomarkers for Prostate Cancer Detection and Metastasis Development Prediction. *Front. Oncol.* **2019**, *9*, 900. [[CrossRef](#)]
41. Amorim, M.; Salta, S.; Henrique, R.; Jerónimo, C. Decoding the usefulness of non-coding RNAs as breast cancer markers. *J. Transl. Med.* **2016**, *14*, 265. [[CrossRef](#)]
42. Torres-Ferreira, J.; Ramalho-Carvalho, J.; Gomez, A.; Menezes, F.D.; Freitas, R.; Oliveira, J.; Antunes, L.; Bento, M.J.; Esteller, M.; Henrique, R.; et al. MiR-193b promoter methylation accurately detects prostate cancer in urine sediments and miR-34b/c or miR-129-2 promoter methylation define subsets of clinically aggressive tumors. *Mol. Cancer* **2017**, *16*, 26. [[CrossRef](#)]
43. Tusong, H.; Maolakuerban, N.; Guan, J.; Rexiati, M.; Wang, W.G.; Azhati, B.; Nuerrula, Y.; Wang, Y.J. Functional analysis of serum microRNAs miR-21 and miR-106a in renal cell carcinoma. *Cancer Biomark.* **2017**, *18*, 79–85. [[CrossRef](#)] [[PubMed](#)]
44. Wulfken, L.M.; Moritz, R.; Ohlmann, C.; Holdenrieder, S.; Jung, V.; Becker, F.; Herrmann, E.; Walgenbach-Brünagel, G.; von Ruecker, A.; Müller, S.C.; et al. MicroRNAs in Renal Cell Carcinoma: Diagnostic Implications of Serum miR-1233 Levels. *PLoS ONE* **2011**, *6*, e25787. [[CrossRef](#)]
45. Yadav, S.; Khandelwal, M.; Seth, A.; Saini, A.K.; Dogra, P.N.; Sharma, A. Serum microRNA Expression Profiling: Potential Diagnostic Implications of a Panel of Serum microRNAs for Clear Cell Renal Cell Cancer. *Urology* **2017**, *104*, 64–69. [[CrossRef](#)]
46. Fedorko, M.; Stanik, M.; Iliev, R.; Redova-Lojova, M.; Machackova, T.; Svoboda, M.; Pacik, D.; Dolezel, J.; Slaby, O. Combination of MiR-378 and MiR-210 Serum Levels Enables Sensitive Detection of Renal Cell Carcinoma. *Int. J. Mol. Sci.* **2015**, *16*, 23382–23389. [[CrossRef](#)]
47. Iwamoto, H.; Kanda, Y.; Sejima, T.; Osaki, M.; Okada, F.; Takenaka, A. Serum miR-210 as a potential biomarker of early clear cell renal cell carcinoma. *Int. J. Oncol.* **2014**, *44*, 53–58. [[CrossRef](#)]
48. Zhao, A.; Li, G.; Péoc'h, M.; Genin, C.; Gigante, M. Serum miR-210 as a novel biomarker for molecular diagnosis of clear cell renal cell carcinoma. *Exp. Mol. Pathol.* **2013**, *94*, 115–120. [[CrossRef](#)]
49. Chen, Y.; Wang, X.; Zhu, X.; Shao, S. Detection Performance of Circulating MicroRNA-210 for Renal Cell Carcinoma: A Meta-Analysis. *Clin. Lab.* **2018**, *64*, 569–576. [[CrossRef](#)]
50. Mytsyk, Y.; Dosenko, V.; Borys, Y.; Kucher, A.; Gazdikova, K.; Busselberg, D.; Caprnda, M.; Kruzliak, P.; Farooqi, A.A.; Lubov, M. MicroRNA-15a expression measured in urine samples as a potential biomarker of renal cell carcinoma. *Int. Urol. Nephrol.* **2018**, *50*, 851–859. [[CrossRef](#)]
51. Mall, C.; Rocke, D.M.; Durbin-Johnson, B.; Weiss, R.H. Stability of miRNA in human urine supports its biomarker potential. *Biomark Med.* **2013**, *7*, 623–631. [[CrossRef](#)] [[PubMed](#)]
52. Redova, M.; Poprach, A.; Někřindova, J.; Iliev, R.; Radova, L.; Lakomy, R.; Svoboda, M.; Vyzula, R.; Slaby, O. Circulating miR-378 and miR-451 in serum are potential biomarkers for renal cell carcinoma. *J. Transl. Med.* **2012**, *10*, 55. [[CrossRef](#)] [[PubMed](#)]
53. Wang, X.; Wang, T.; Chen, C.; Wu, Z.; Bai, P.; Li, S.; Chen, B.; Liu, R.; Zhang, K.; Li, W.; et al. Serum exosomal miR-210 as a potential biomarker for clear cell renal cell carcinoma. *J. Cell Biochem.* **2018**, *120*, 1492–1502. [[CrossRef](#)] [[PubMed](#)]
54. Heinemann, F.G.; Tolkach, Y.; Deng, M.; Schmidt, D.; Perner, S.; Kristiansen, G.; Müller, S.C.; Ellinger, J. Serum miR-122-5p and miR-206 expression: Non-invasive prognostic biomarkers for renal cell carcinoma. *Clin. Epigenetics* **2018**, *10*, 11. [[CrossRef](#)]
55. von Brandenstein, M.; Pandarakalam, J.J.; Kroon, L.; Loeser, H.; Herden, J.; Braun, G.; Wendland, K.; Dienes, H.P.; Engelmann, U.; Fries, J.W. MicroRNA 15a, inversely correlated to PKC α , is a potential marker to differentiate between benign and malignant renal tumors in biopsy and urine samples. *Am. J. Pathol.* **2012**, *180*, 1787–1797. [[CrossRef](#)]

56. Wang, C.; Hu, J.; Lu, M.; Gu, H.; Zhou, X.; Chen, X.; Zen, K.; Zhang, C.-Y.; Zhang, T.; Ge, J.; et al. A panel of five serum miRNAs as a potential diagnostic tool for early-stage renal cell carcinoma. *Sci. Rep.* **2015**, *5*, 7610. [\[CrossRef\]](#)
57. Zhai, Q.; Zhou, L.; Zhao, C.; Wan, J.; Yu, Z.; Guo, X.; Qin, J.; Chen, J.; Lu, R. Identification of miR-508-3p and miR-509-3p that are associated with cell invasion and migration and involved in the apoptosis of renal cell carcinoma. *Biochem. Biophys. Res. Commun.* **2012**, *419*, 621–626. [\[CrossRef\]](#)
58. Teixeira, A.L.; Ferreira, M.; Silva, J.; Gomes, M.; Dias, F.; Santos, J.L.; Mauricio, J.; Lobo, F.; Medeiros, R. Higher circulating expression levels of miR-221 associated with poor overall survival in renal cell carcinoma patients. *Tumour Biol.* **2014**, *35*, 4057–4066. [\[CrossRef\]](#)
59. Zhang, Q.; Di, W.; Dong, Y.; Lu, G.; Yu, J.; Li, J.; Li, P. High serum miR-183 level is associated with poor responsiveness of renal cancer to natural killer cells. *Tumour Biol.* **2015**, *36*, 9245–9249. [\[CrossRef\]](#)
60. Fedorko, M.; Juracek, J.; Stanik, M.; Svoboda, M.; Poprach, A.; Buchler, T.; Pacik, D.; Dolezel, J.; Slaby, O. Detection of let-7 miRNAs in urine supernatant as potential diagnostic approach in non-metastatic clear-cell renal cell carcinoma. *Biochem. Med.* **2017**, *27*, 411–417. [\[CrossRef\]](#) [\[PubMed\]](#)
61. Chanudet, E.; Wozniak, M.B.; Bouaoun, L.; Byrnes, G.; Mukeriy, A.; Zaridze, D.; Brennan, P.; Muller, D.C.; Scelo, G. Large-scale genome-wide screening of circulating microRNAs in clear cell renal cell carcinoma reveals specific signatures in late-stage disease. *Int. J. Cancer* **2017**, *141*, 1730–1740. [\[CrossRef\]](#) [\[PubMed\]](#)
62. Barreiro, K.; Holthofer, H. Urinary extracellular vesicles. A promising shortcut to novel biomarker discoveries. *Cell Tissue Res.* **2017**, *369*, 217–227. [\[CrossRef\]](#) [\[PubMed\]](#)
63. Jella, K.K.; Nasti, T.H.; Li, Z.; Malla, S.R.; Buchwald, Z.S.; Khan, M.K. Exosomes, Their Biogenesis and Role in Inter-Cellular Communication, Tumor Microenvironment and Cancer Immunotherapy. *Vaccines* **2018**, *6*, 69. [\[CrossRef\]](#) [\[PubMed\]](#)
64. Lourenço, C.; Constância, V.; Henrique, R.; Carvalho, A.; Jerónimo, C. Urinary Extracellular Vesicles as Potential Biomarkers for Urologic Cancers: An Overview of Current Methods and Advances. *Cancers* **2021**, *13*, 1529. [\[CrossRef\]](#) [\[PubMed\]](#)
65. Zhou, M.; Weber, S.R.; Zhao, Y.; Chen, H.; Sundstrom, J.M. Chapter 2—Methods for exosome isolation and characterization. In *Exosomes*; Edelstein, L., Smythies, J., Quesenberry, P., Noble, D., Eds.; Academic Press: Cambridge, MA, USA, 2020; pp. 23–38.
66. Butz, H.; Nofech-Mozes, R.; Ding, Q.; Khella, H.W.Z.; Szabó, P.M.; Jewett, M.; Finelli, A.; Lee, J.; Ordon, M.; Stewart, R.; et al. Exosomal MicroRNAs Are Diagnostic Biomarkers and Can Mediate Cell-Cell Communication in Renal Cell Carcinoma. *Eur. Urol. Focus* **2016**, *2*, 210–218. [\[CrossRef\]](#) [\[PubMed\]](#)
67. De Palma, G.; Sallustio, F.; Curci, C.; Galleggiante, V.; Rutigliano, M.; Serino, G.; Dittono, P.; Battaglia, M.; Schena, F.P. The Three-Gene Signature in Urinary Extracellular Vesicles from Patients with Clear Cell Renal Cell Carcinoma. *J. Cancer* **2016**, *7*, 1960–1967. [\[CrossRef\]](#)
68. Del Boccio, P.; Raimondo, F.; Pieragostino, D.; Morosi, L.; Cozzi, G.; Sacchetta, P.; Magni, F.; Pitto, M.; Urbani, A. A hyphenated microLC-Q-TOF-MS platform for exosomal lipidomics investigations: Application to RCC urinary exosomes. *Electrophoresis* **2012**, *33*, 689–696. [\[CrossRef\]](#)
69. Raimondo, F.; Morosi, L.; Corbetta, S.; Chinello, C.; Brambilla, P.; Della Mina, P.; Villa, A.; Albo, G.; Battaglia, C.; Bosari, S.; et al. Differential protein profiling of renal cell carcinoma urinary exosomes. *Mol. Biosyst.* **2013**, *9*, 1220–1233. [\[CrossRef\]](#)
70. Song, S.; Long, M.; Yu, G.; Cheng, Y.; Yang, Q.; Liu, J.; Wang, Y.; Sheng, J.; Wang, L.; Wang, Z.; et al. Urinary exosome miR-30c-5p as a biomarker of clear cell renal cell carcinoma that inhibits progression by targeting HSPA5. *J. Cell Mol. Med.* **2019**, *23*, 6755–6765. [\[CrossRef\]](#)
71. Zhang, W.; Ni, M.; Su, Y.; Wang, H.; Zhu, S.; Zhao, A.; Li, G. MicroRNAs in Serum Exosomes as Potential Biomarkers in Clear-cell Renal Cell Carcinoma. *Eur. Urol. Focus* **2018**, *4*, 412–419. [\[CrossRef\]](#) [\[PubMed\]](#)
72. Du, M.; Giridhar, K.V.; Tian, Y.; Tschannen, M.R.; Zhu, J.; Huang, C.-C.; Kilar, D.; Kohli, M.; Wang, L. Plasma exosomal miRNAs-based prognosis in metastatic kidney cancer. *Oncotarget* **2017**, *8*, 63703–63714. [\[CrossRef\]](#)
73. Qu, L.; Ding, J.; Chen, C.; Wu, Z.J.; Liu, B.; Gao, Y.; Chen, W.; Liu, F.; Sun, W.; Li, X.F.; et al. Exosome-Transmitted lncARSR Promotes Sunitinib Resistance in Renal Cancer by Acting as a Competing Endogenous RNA. *Cancer Cell* **2016**, *29*, 653–668. [\[CrossRef\]](#) [\[PubMed\]](#)
74. Fujii, N.; Hirata, H.; Ueno, K.; Mori, J.; Oka, S.; Shimizu, K.; Kawai, Y.; Inoue, R.; Yamamoto, Y.; Matsumoto, H.; et al. Extracellular miR-224 as a prognostic marker for clear cell renal cell carcinoma. *Oncotarget* **2017**, *8*, 109877–109888. [\[CrossRef\]](#) [\[PubMed\]](#)
75. Nik Mohamed Kamal, N.N.S.B.; Shahidan, W.N.S. Non-Exosomal and Exosomal Circulatory MicroRNAs: Which Are More Valid as Biomarkers? *Front. Pharmacol.* **2020**, *10*, 6513–6525. [\[CrossRef\]](#)
76. Tian, F.; Shen, Y.; Chen, Z.; Li, R.; Ge, Q. No Significant Difference between Plasma miRNAs and Plasma-Derived Exosomal miRNAs from Healthy People. *BioMed Res. Int.* **2017**, *2017*, 1304816. [\[CrossRef\]](#) [\[PubMed\]](#)
77. Zavesky, L.; Jandakova, E.; Turyna, R.; Langmeierova, L.; Weinberger, V.; Minar, L. Supernatant versus exosomal urinary microRNAs. Two fractions with different outcomes in gynaecological cancers. *Neoplasma* **2016**, *63*, 121–132. [\[CrossRef\]](#) [\[PubMed\]](#)
78. Zhou, X.; Wen, W.; Shan, X.; Zhu, W.; Xu, J.; Guo, R.; Cheng, W.; Wang, F.; Qi, L.W.; Chen, Y.; et al. A six-microRNA panel in plasma was identified as a potential biomarker for lung adenocarcinoma diagnosis. *Oncotarget* **2017**, *8*, 6513–6525. [\[CrossRef\]](#) [\[PubMed\]](#)

79. Huang, Z.; Zhu, D.; Wu, L.; He, M.; Zhou, X.; Zhang, L.; Zhang, H.; Wang, W.; Zhu, J.; Cheng, W.; et al. Six Serum-Based miRNAs as Potential Diagnostic Biomarkers for Gastric Cancer. *Cancer Epidemiol. Biomark. Prev.* **2017**, *26*, 188. [[CrossRef](#)] [[PubMed](#)]
80. Eicheler, C.; Stückerath, I.; Müller, V.; Milde-Langosch, K.; Wikman, H.; Pantel, K.; Schwarzenbach, H. Increased serum levels of circulating exosomal microRNA-373 in receptor-negative breast cancer patients. *Oncotarget* **2014**, *5*, 9650–9663. [[CrossRef](#)] [[PubMed](#)]

II.PRELIMINARY DATA

This study is based in two larger projects developed in the Cancer Biology & Epigenetics Group (CI-IPO-Porto) and in St. Michael's Hospital (Canada). The first project aimed to compare droplet digital polymerase chain reaction (ddPCR) and quantitative real-time PCR (qRT-PCR) techniques in plasma samples and validate the ddPCR technique for the quantification/detection of a circulating microRNA (miRNA) with higher sensitivity and specificity when compared with other techniques (Supplementary file 1).

1. COMPARISON OF PCR TECHNIQUES AND VALIDATION OF DDPCR

The present study was submitted to an international indexed journal as:

DigiMir test: establishing a novel pipeline for miR-371a quantification using droplet digital PCR in liquid biopsies from testicular germ cell tumor patients

José Pedro Sequeira^{a,*}, João Lobo^{a,c,d*}, Vera Constâncio^{a,e*}, Tiago Brito-Rocha^{a,b}, Carina Carvalho-Maia^a, Isaac Braga^f, Joaquina Maurício^g, Rui Henrique^{a,c,d,§,#}, Carmen Jerónimo^{a,d,§,#}

Herein, we described and compared the performance of two approaches for hsa-miR-371a-3p detection in plasma by qRT-PCR, the TaqMan Advanced (global) microRNA (miRNA) and the TaqMan (target-specific) miRNA qPCR protocols, which were further compared with ddPCR.

For this comparison, four experimental settings were evaluated to assess the variability of the pipelines: "Setting #1", with 5 cases being extracted in two different timings; "Setting #2", where the same extraction was used but with two different cDNA syntheses; "Setting #3", with samples with the same extraction and cDNA synthesis, but with two different operators performing the PCR reaction; and "Setting #4", with samples with the same extraction and cDNA synthesis and by the same operator (Figure 1)

From the three pipelines, the one that showed the poorest results was the TaqMan Advanced (global) miRNA pipeline with high variability between the studied settings (Figure 1A-C). Moreover, when compared with TaqMan (target-specific) miRNA protocol (Figure 1D-F), the quantification of the spike-in ath-miR-159a was rather limited (later Ct range) resulting in higher variability detection between samples.

For the DigiMir pipeline, the ath-miR-159a recover performed well (Figure 1G) with hsa-miR-371a-3p detection in all experimental instances, with tumor burden representation

(higher detection in the advanced stage sample) and miRNA negative for the healthy donor (Figure 1H).

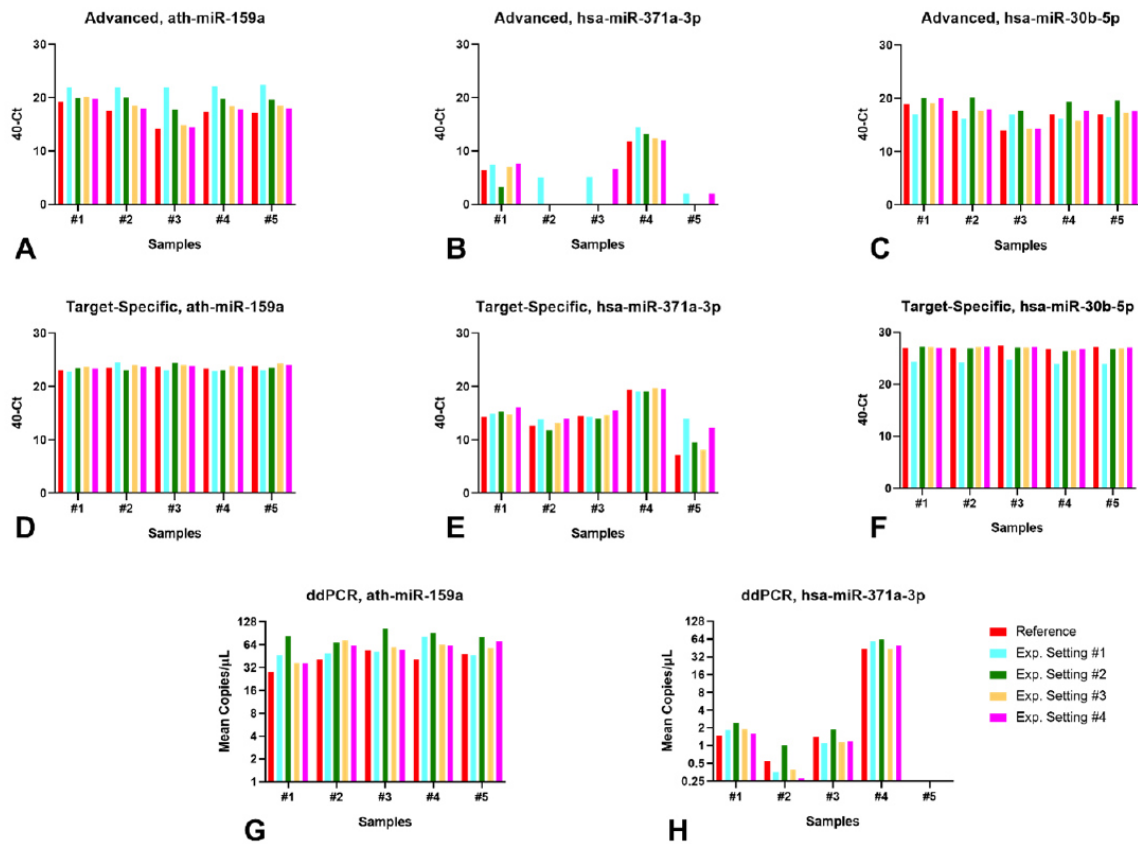


Figure 1 – Comparison of pipelines. A-C: TaqMan Advanced (global) microRNA pipeline; D-F: TaqMan (target-specific) microRNA pipeline; G-H: DigiMir pipeline. X-axis: #1 and #2 – stage I seminomas; #3 – stage II embryonal carcinoma; #4 – stage III embryonal carcinoma; #5 – age-matched healthy blood donor. Color code: setting #1 – different extraction; setting #2 – different cDNA synthesis; setting #3 – different operator; setting #4 – same operator; and reference for comparison.

Furthermore, the comparison of hsa-miR-371a-3p quantification between the experimental settings demonstrated a strong positive correlation for all instances (Figure 2A-L). In addition, the quantification of hsa-miR-371a-3p using the TaqMan (target-specific) miRNA protocol compared with the DigiMir pipeline showed a strong positive correlation between the target miRNA relative levels (normalized to hsa-miR-30b-5p) in qRT-PCR and the absolute copies/μL in ddPCR (Figure 2M).

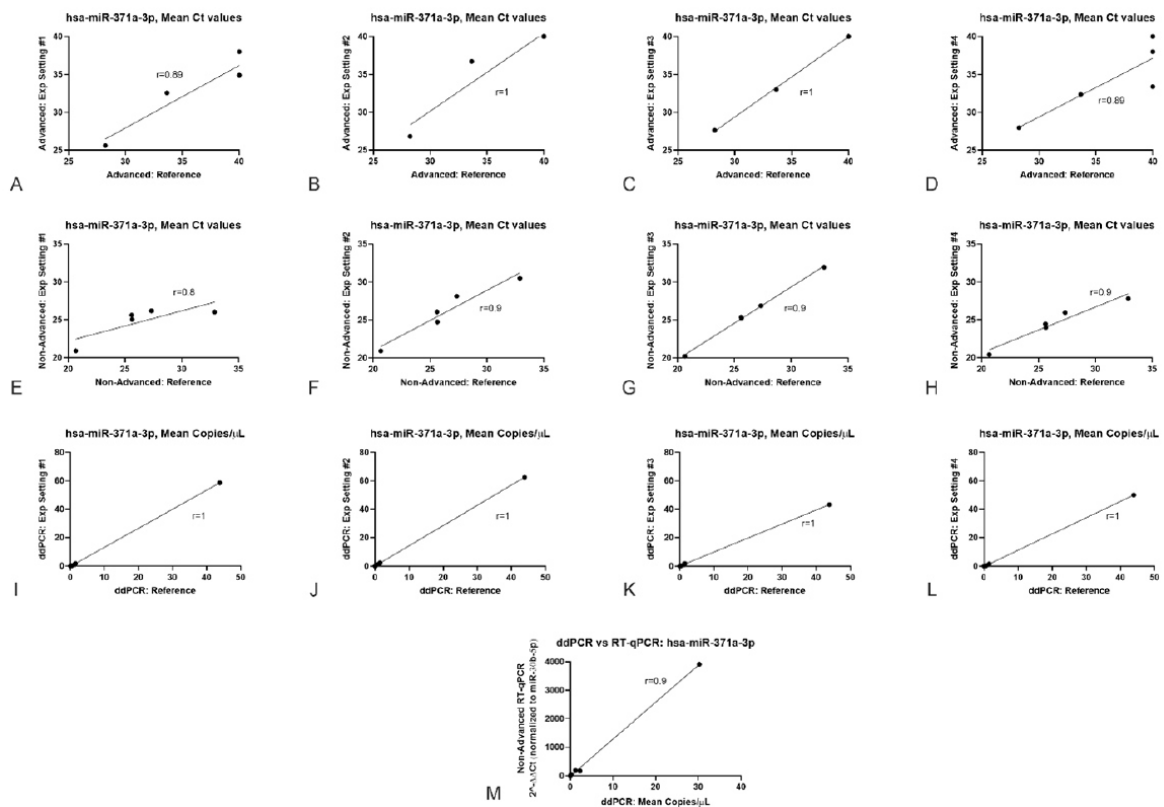


Figure 2 – Correlation between hsa-miR-371a-3p quantifications. A-D: TaqMan Advanced (global) microRNA pipeline; E-H: TaqMan (target-specific) microRNA pipeline; I-L: DigiMir pipeline; M – correlation between the DigiMir pipeline and the TaqMan (target-specific) microRNA pipeline quantifications.

After this comparison and validation, ddPCR pipeline (DigiMir) was fully optimized.

Hsa-miR-371a-3p, assessed by ddPCR, outperformed the classical serum tumor markers, detecting 93.6% Testicular Germ Cell Tumors (TGCT) patients in the pre-orchietomy setting, with 100% specificity and 97.5% accuracy. As observed, no positivity for our target miRNA was found in healthy blood donors, while in tumor patients only two seminomas (remarkably, negative for all three classical markers) did not show detectable hsa-miR-371a-3p.

The analyzed cohort also included three patients with non-TGCT testicular masses and one hepatocarcinoma [elevated Alfa Fetoprotein (AFP)] that were not detected by the target miRNA. Moreover, two classical serum markers [Human Chorionic Gonadotropin (HCG), Lactate dehydrogenase (LDH)] and tumor size were positively correlated with hsa-miR-371a-3p levels ($r=0.57$, $p<0.001$; $r=0.544$, $p=0.002$; and $r=0.475$, $p=0.007$, respectively).

The follow-up samples of TGCT patients were also tested for circulating hsa-miR-371a-3p and one stage III patient with disease progression was positive. The remaining samples were miRNA negative since no signs of disease after the orchietomy were found and the

patients presented classical serum tumor markers normalization and negative imaging scans [Sequeira, Lobo, Constâncio et al. (*submitted*)].

In the second project the major goal was identifying some miRNAs that might aid in the diagnostic and prognostic workup of renal cell tumors (RCT).

2. IDENTIFICATION OF SOME MICRORNAS THAT MIGHT AID IN THE DIAGNOSTIC AND PROGNOSTIC WORKUP OF RCTS

A previous report by Silva-Santos et al. that assessed by qRT-PCR the levels of hsa-miR-21-5p, hsa-miR-141-3p, hsa-miR-155-5p, hsa-miR-183-5p and hsa-miR-200b-3p in fresh-frozen tissues from 120 RCT, 10 normal renal tissues and 60 cases of ex-vivo fine-needle aspiration biopsies from RCTs, demonstrated the significantly lower hsa-miR-21-5p, hsa-miR-141-3p and hsa-miR-200b-3p levels in RCTs comparing with in normal tissues (Figure 3A), being significantly different between oncocytomas and renal cell carcinomas (RCC) (Figure 3B).

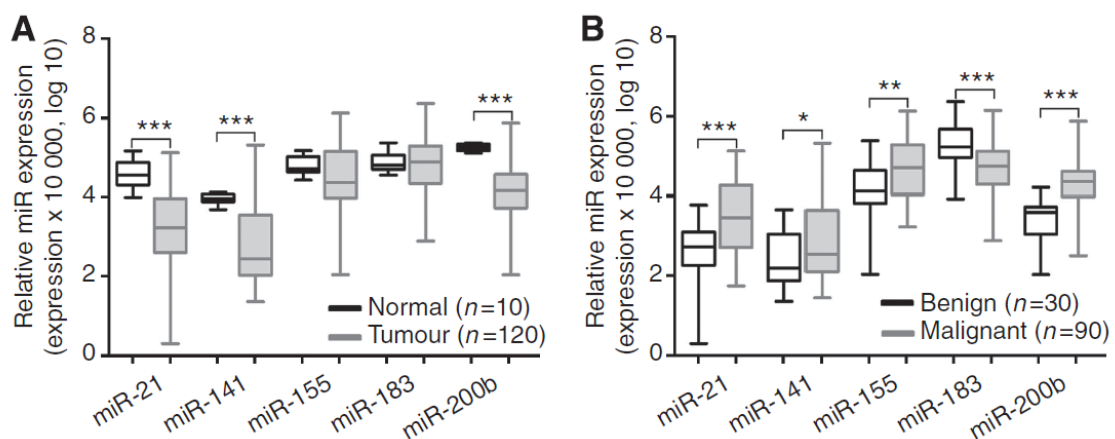


Figure 3 – Distribution of miRNA levels in kidney tissues. (A) Normal vs tumour tissues. (B) Benign vs malignant tumour tissues. Statistically significant differences are represented as *** $P < 0.001$, ** $P < 0.01$ and * $P < 0.02$. Figure from Silva-Santos et al. [1].

Furthermore, hsa-miR-141-3p/hsa-miR-200b-3p were able to distinguish RCTs and normal tissue, benign from malignant and chromophobe RCC (chRCC) from oncocytoma (Table 1).

Table 1 – Validity estimates for each miRNA and for the best combination of miRNAs in different diagnostic settings, in fresh-frozen tissues. Table from Silva-Santos et al. [1].

miRNAs	SE %	SP %	PPV %	NPV %	Accuracy %
RCT vs normal renal tissue					
hsa-miR-21-5p	76.7	100.0	100.0	26.0	78.0
hsa-miR-141-3p	81.7	100.0	100.0	31.0	83.0
hsa-miR-200b-3p	97.5	100.0	100.0	77.0	98.0
hsa-miR-141-3p/hsa-miR-200b-3p	99.2	100.0	100.0	90.9	99.2
RCC vs oncocytoma					
hsa-miR-21-5p	48.9	93.3	95.7	37.8	60.0
hsa-miR-141-3p	25.6	100.0	100.0	13.0	33.0
hsa-miR-155-5p	50.0	83.3	90.0	35.2	58.3
hsa-miR-200b-3p	96.7	90.0	96.7	67.5	95.0
hsa-miR-141-3p/hsa-miR-200b-3p	85.6	100.0	100.0	69.8	89.2
chRCC vs oncocytoma					
hsa-miR-141-3p	76.7	86.7	85.2	78.7	81.6
hsa-miR-200b-3p	83.3	90.0	89.3	84.4	86.7
hsa-miR-141-3p/hsa-miR-200b-3p	90.0	100.0	100.0	90.9	95.0

Abbreviations: SE – Sensitivity; SP – Specificity; PPV – Positive Predictive Value; NPV – Negative Predictive Value; RCT – Renal cell tumor; RCC – Renal cell carcinoma; chRCC – chromophobe RCC

On other hand, hsa-miR-21-5p, hsa-miR-141-3p and hsa-miR-155-5p showed to be useful as prognostic markers in a univariable analysis (Figure 4).

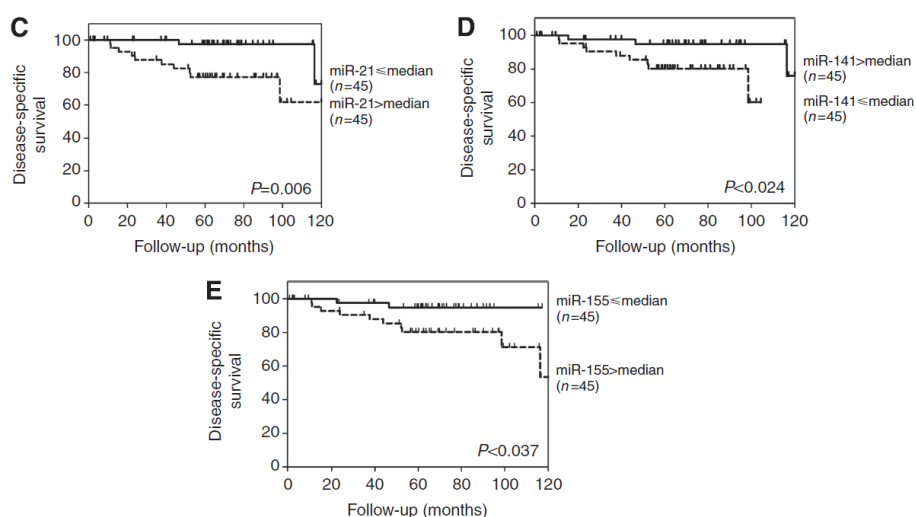


Figure 4 – Disease specific-survival according with hsa-miR-21-5p, hsa-miR-141-3p and hsa-miR-155-5p levels. Figure from Silva-Santos et al. [1].

As before described in serum samples, (Table 1 of Review Article) miR-21 was able to detect clear cell RCC (ccRCC) with 77.3% sensitivity and 96.4% specificity (Table 1 of Review Article). Hence, from the initial five miRNAs, four of them (hsa-miR-21-5p, hsa-miR-141-3p, hsa-miR-155-5p and hsa-miR-200b-3p) showed to be a promise diagnostic and prognostic biomarkers in RCC.

Additionally, Di Meo and colleagues from St. Michael's Hospital (Canada), demonstrated that hsa-miR-126-3p discriminate ccRCC from papillary RCC (pRCC) and that hsa-miR-200b-3p distinguish chRCC from oncocytoma in renal tissue.

III.AIM

Reducing mortality associated with renal cell carcinoma remains an important societal goal and collective efforts have been made to expand the knowledge on effective early detection biomarkers. These would allow for a decrease in the number of RCC cases identified at advanced stage, increasing the likelihood of curative treatment and avoiding the need for subsequent therapies with its adverse effects.

Thus, the aim of our dissertation was to investigate miRNAs' potential as biomarkers for early detection, as well as for renal cell tumor subtyping.

Specifically, we planned to:

- Optimize ddPCR for five miRNAs (hsa-miR-21-5p, hsa-miR-126-3p, hsa-miR-141-3p, hsa-miR-155-5p and hsa-miR-200b-3p) detection and quantification using spiked plasma samples.
- Assess the levels of six miRNAs (ath-miR-159a, hsa-miR-21-5p, hsa-miR-126-3p, hsa-miR-141-3p, hsa-miR-155-5p and hsa-miR-200b-3p) in a plasma samples set from patients with renal cell tumor and healthy donors, using ddPCR.
- Evaluate the association between levels and standard clinicopathological parameters, assessing the diagnostic value of those five miRNAs (hsa-miR-21-5p, hsa-miR-126-3p, hsa-miR-141-3p, hsa-miR-155-5p and hsa-miR-200b-3p).

IV.MATERIAL AND METHODS

1. PLASMA SAMPLES

1.1. Patients and Samples Collection

A total of five plasma samples were included in the optimization phase of the study, where the pipeline was tested: one oncocytoma, one stage I pRCC, one stage I ccRCC, one stage I chRCC and one adult healthy blood donor.

After optimization of the ddPCR pipeline, a cohort of 238 plasma samples was studied, comprising: 160 samples collected from renal cell tumors patients at the time of diagnosis and 78 healthy blood donors. Regarding renal tumor patients, 103 were diagnosed with ccRCC, 23 were chRCC, 16 were pRCC, while 18 patients were diagnosed with a benign tumor: oncocytoma. All patients were treated at IPO Porto by the same multidisciplinary team between 2015 and 2021. After peripheral blood collection into EDTA-containing tubes, plasma was separated by centrifugation at 2,500g for 30 min at 4°C, and subsequently stored at -80°C in the institutional tumor bank until further use. All blood samples were processed within 4h maximum from collection. Relevant clinical and pathological data was analysed from clinical charts and grouped in an anonymized database that was constructed for the analysis.

This study was approved by the institutional review board (Comissão de Ética para a Saúde) of Portuguese Oncology Institute of Porto, Portugal (CES 518/2010).

2. RNA EXTRACTION

Total RNA was extracted from 100µL plasma using the MagMAX miRvana Total RNA Isolation kit (Thermo Fisher, A27828), according to manufacturer's protocol (Figure 5). Briefly, Proteinase K (PK) and PK digestion buffer were added to the plasma in the plate. After 5 minutes of shaking at 950 rpm and 30 minutes of incubation at 65°C to the activation of proteinase K, 100 µL of a solution compound by Lysis Buffer and 2-Mercaptoethanol was added. Also, as a technical control, the non-human synthetic spike-in ath-miR-159a (0.2µL per sample of a stock solution at 0.2nM) was added, in all samples, to the lysis buffer. Then, 20 µL of RNA binding beads were added and the plate were mixed by 7 minutes at 700 rpm using Thermo Scientific™ Compact Digital Microplate Shaker (Thermo Fisher, 88882006). To precipitate RNA, 270 µL of isopropanol was added to the sample and shaking 15 minutes at 400 rpm. After that, the supernatant was discarded and proceed to wash RNA in the RNA binding beads, with shaking of 950 rpm by 1 minute and 1 minute at Magnetic Stand-96 (Thermo Fisher, AM10027) between washes. Then, it was necessary to shake the uncovered plate for 5 minutes at 1150 rpm to dry the RNA Binding beads. The sample was treated with Turbo DNase and the RNA was rebounded to the RNA Binding beads.

Each sample was washed twice with 150 μL of Wash solution 2 and shaken by 950 rpm for 1 minute and 1 minute at Magnetic Stand-96 (Thermo Fisher, AM10027) between washes. Lastly, RNA was eluted in 50 μL of Elution buffer, agitated for 2 minutes at 1050 rpm, heated for 5 minutes at 65°C, then agitated for 2 minutes at 1050 rpm and then the plate was placed at Magnetic Stand-96 by 3 mins. The supernatant was collected to a 1.5 mL RNase-free tube. All steps were performed at room temperature. The extracted RNA was stored at -80°C until further use.

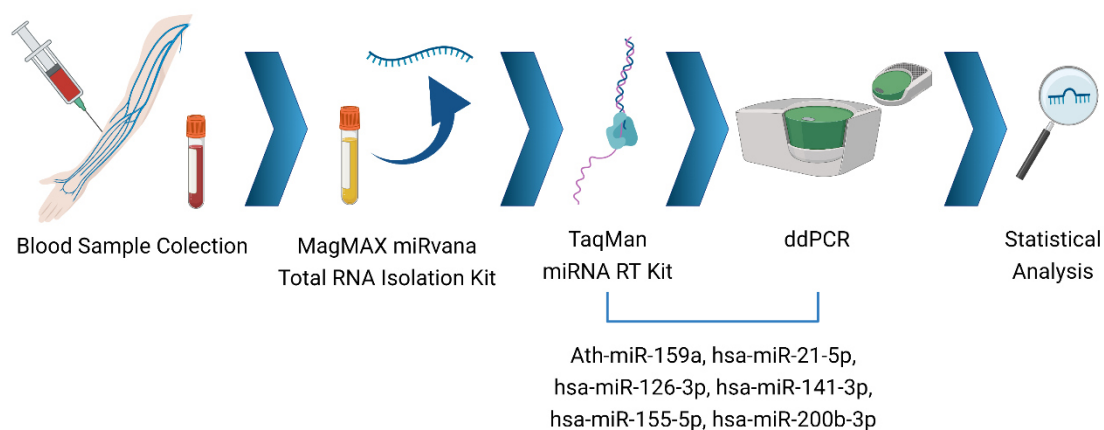


Figure 5 – Pipeline of LiKidMiRs. Created with BioRender.com.

3. TAQMAN MIRNA REVERSE TRANSCRIPTION

Using the TaqMan microRNA reverse transcription kit (Thermo Fisher, 4366596) according to the manufacturer's protocol (Table 2), 5 μL of previously isolated RNA were reverse transcribed in the Veriti™ thermocycler for the miRNAs of interest and for spike-in (ath-miR-159a, hsa-miR-21-5p, hsa-miR-126-3p, hsa-miR-141-3p, hsa-miR-155-5p, hsa-miR-200b-3p). Briefly, 0.15 μL of 100mM dNTPs (with dTTP), 1 μL of MultiScribe™ Reverse Transcriptase (50 U/ μL), 1.5 μL of 10 \times Reverse Transcription Buffer, 0.19 μL of RNase Inhibitor (20U/ μL), 6.41 μL of Nuclease-free water and 0.75 μL of a mix with the four assays with a concentration of 20x (0.1875 μL of each assay) were added to 5 μL of isolated RNA (Table 3).

Table 2 – Description of time and temperature of TaqMan microRNA Reverse Transcription kit.

Time (min)	Temperature (°C)
30	16
30	42
5	85
Hold	4

Table 3 – Components and volumes required for TaqMan microRNA Reverse Transcription per sample.

Components	Master Mix Volume/sample (15μL)
100mM dNTPs (with dTTP)	0.15 μ L
MultiScribe™ Reverse Transcriptase (50 U/ μ L)	1 μ L
10 \times Reverse Transcription Buffer	1.5 μ L
RNase Inhibitor (20U/ μ L)	0.19 μ L
Nuclease-free water	6.41 μ L
Mix Assays	0.75 μ L
Total	10μL
	5 μ L of RNA

4. DROPLET DIGITAL PCR

DdPCR reactions were prepared according with optimizations performed: volume of cDNA input [2 μ L (ath-miR-159a, hsa-miR-21-5p, hsa-miR-126-3p), 5 μ L (hsa-miR-155-5p and hsa-miR-200b-3p) and 6 μ L (hsa-miR-141-3p)], 11 μ L ddPCR Supermix for probes (Bio-Rad, California, USA, #1863010), 1 μ L TaqMan hsa-miRNA Assay (20x) and volume of bidistilled water [8 μ L (ath-miR-159a, hsa-miR-21-5p, hsa-miR-126-3p), 5 μ L (hsa-miR-155-5p and hsa-miR-200b-3p) or 4 μ L (hsa-miR-141-3p)]; assays: ath-miR-159a – 000338, FAM; hsa-miR-21-5p – 000397, FAM; hsa-miR-126-3p – 002228, VIC; hsa-miR-141-3p – 000463, FAM; hsa-miR-155-5p – 002623, FAM; hsa-miR-200b-3p – 002251, FAM. Droplets were generated on the droplet generator QX200 (Bio-Rad, California, USA) and read on the QX200 Droplet Reader (Bio-Rad, California, USA). The PCR run was set as follows: 95 $^{\circ}$ C 10min, 50 cycles of 94 $^{\circ}$ C 30s and “Annealing Temperature optimized” 1min – ramp rate 2 $^{\circ}$ C/s – and 98 $^{\circ}$ C 10min). The Annealing temperature for ath-miR-159a was set at 56 $^{\circ}$ C and for the other five miRNAs was 55 $^{\circ}$ C.

The limit of blank (LOB) and limit of detection (LOD) was calculated for each target miRNA according with Armsbruster et al. [2]. Additionally, the limit of quantification (LOQ) was assessed by performing a 2-fold dilution series of a RCT sample for the five miRNAs.

5. QUALITY CONTROL STEPS

All plasma samples were visually inspected, and obvious hemolysis was not observed in any samples. Appropriate engineering and manual controls were used to prevent contaminations, including master mix made using a clean hood, clean gloves, PCR reagents and consumables, and reactions performed in separate dedicated labs. RNA was extracted from the cell lines of RCTs (Caki-1, HKC8, 769-P, Caki-2, ACHN, A498, 293 HEK, 786-O) and a pool of them was used as a positive control for the five miRNAs of interest. As reported by Stein and colleagues [3], negative controls as no template control (NTC)

and no enzyme control (NEC) were included in all cDNA synthesis. In ddPCR runs, additionally to these negative controls, NTC for ddPCR reaction was added [3]. All samples were run in a single reaction for each target.

6. STATISTICAL ANALYSIS

Non-parametric tests were performed to compare levels of each miRNA between histologic subtypes, and to evaluate associations with clinicopathological features. Mann-Whitney U test was used for comparisons between two groups, while Kruskal-Wallis test was used for multiple groups, followed by Mann-Whitney U test with Bonferroni's correction for pairwise comparisons. A result was considered statistically significant when $p\text{-value} < 0.05$.

For each miRNA, samples were categorized as positive or negative based on the cut-off values established using Youden's J index [4,5] (value combining highest sensitivity and specificity), through receiver operator characteristic (ROC) curve analysis. Validity estimates (sensitivity, specificity, and accuracy) were determined to assess biomarker performance (Table 4). Panels were constructed to improve performance, considering a positive result whenever at least one miRNA was plotted as positive in individual analysis.

Table 4 – Formulas for biomarker parameters calculation.

Tumor vs Normal			Estimates	
	Tumor	Normal		
miRNA positive	TP	FP	SE (%)	$TP/(TP+FN) \times 100$
miRNA negative	FN	TN	SP (%)	$TN/(TN+FP) \times 100$
			Accuracy (%)	$[(TN+TP)/(Total)] \times 100$
			PPV (%)	$TP/(TP+FP) \times 100$
			NPV (%)	$TN/(TN+FN) \times 100$

Abbreviations: TP – True Positive; FN – False Negative; FP – False Negative; TN – True Negative; SE – Sensitivity; SP – Specificity; PPV – Positive Predictive Value; NPV – Negative Predictive Value

Two-tailed $p\text{-values}$ calculation and ROC curve analysis were performed using SPSS 27.0 for Windows software (IBM-SPSS Inc., Chicago, IL, USA). All graphics were assembled using GraphPad Prism 8.0 for Windows Software (GraphPad Software Inc., LA Jolla, CA, USA).

V.RESULTS

1. PATIENTS COHORTS CHARACTERIZATION

The relevant clinical-pathological features of our optimization and validation cohorts are depicted in Table 5.

Table 5 – Clinicopathological data of Optimization cohort (5 samples) and Validation cohort (compound by 160 Renal Cell Tumors and 78 Healthy donors samples) used in this study.

Optimization Cohort (n=5 samples)	
Cases	Description
Sample #1	66 years, Oncocytoma
Sample #2	53 years, pRCC, Stage I
Sample #3	57 years, ccRCC, Stage I
Sample #4	46 years, chRCC, stage I
Sample #5	45 years, healthy blood donor
Validation Cohort (n= 238 samples)	
Renal cell tumor samples	160
Healthy blood donors	78
Renal cell tumor patients – clinicopathological features	
Age [years (median, interquartile range)]	64 (16.75)
Gender	
Male	115/160 (71.9)
Female	45/160 (28.1)
Size of tumor mass [cm (mean, interquartile range)]	4.55 (4.08)
Histology [n, (%)]	
ccRCC	103/160 (64.4)
pRCC	16/160 (10.0)
chRCC	23/160 (14.4)
Oncocytoma	18/160 (11.3)
Stage [n, (%)]	
I	67/142 (47.2)
II	10/142 (7.0)
III	52/142 (36.6)
IV	13/142 (9.2)
Nuclear grade [n, (%)]	
1	9/104 (8.7)
2	56/104 (53.8)
3	27/104 (26.0)

4	12/104 (11.5)
Vital State	
Alive with disease	7/160 (4.4)
Alive without disease	140/160 (87.5)
Death from the disease	13/160 (8.1)
Healthy Blood Donors – clinicopathological features	
Age [years (median, interquartile range)]	46 (4.25)
Gender	
Male	46/78 (59.0)
Female	32/78 (41.0)

2. OPTIMIZATION PHASE AND COMPARISON OF PIPELINES

2.1. Input and temperature settings

First, the input of ddPCR reactions was optimized to achieve accurate separation of positive and negative droplets for hsa-miR-21-5p, hsa-miR-126-3p, hsa-miR-141-3p, hsa-miR-155-5p and hsa-miR-200b-3p. The optimal input was determined to be 2 μ L for hsa-miR-21-5p and hsa-miR-126-3p, 5 μ L for hsa-miR-155-5p and hsa-miR-200b-3p, and 6 μ L for hsa-miR-141-3p, which rendered an optimal number of positive droplets (Figure 6A-E). Input for ath-miR-159a was validated since it was already optimized in a previous study (Sequeira & Lobo & Constâncio et al. *submitted*) (Figure 6F).

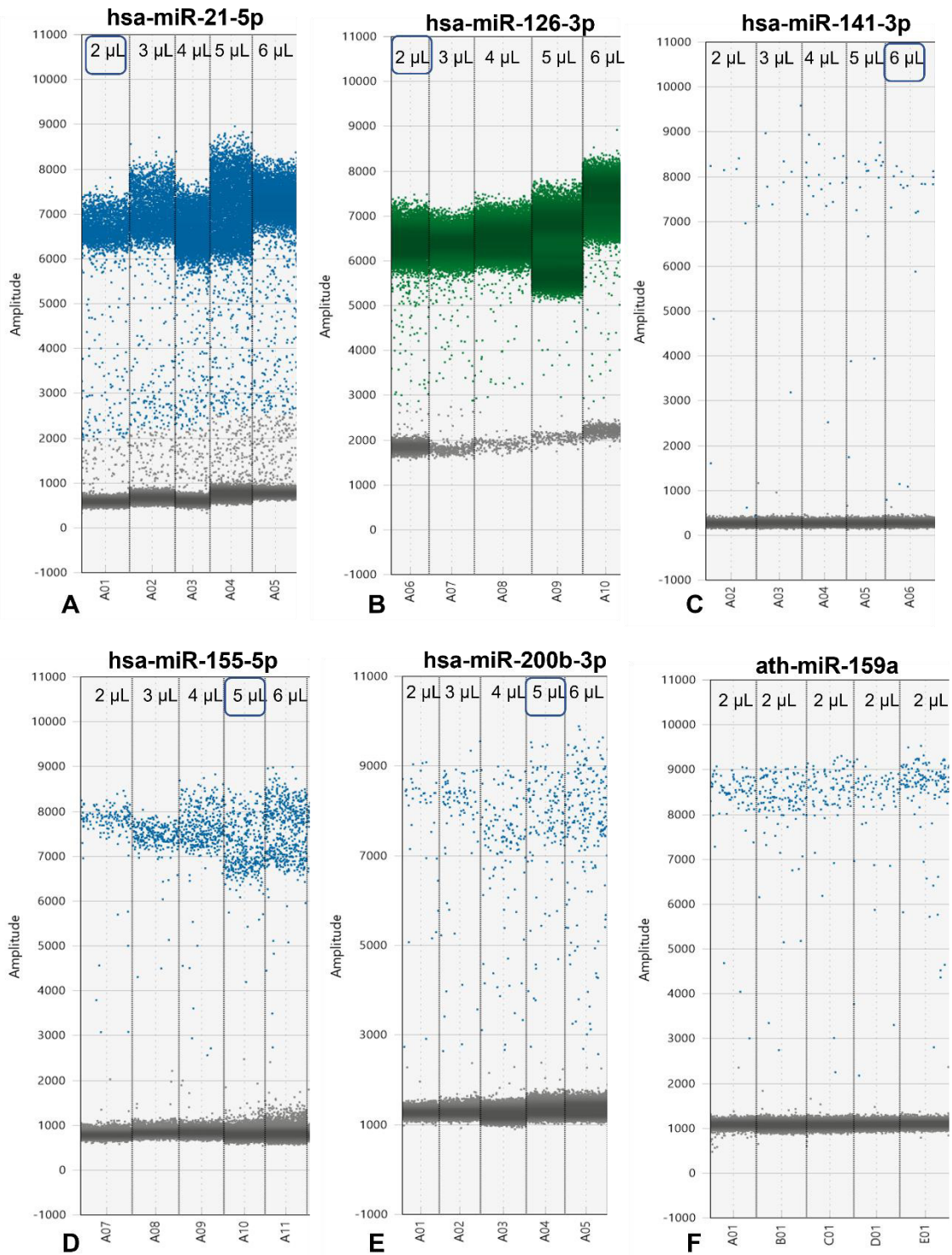


Figure 6 – Optimization of LiKidMiRs pipeline. Hsa-miR-21-5p (A), hsa-miR-126-3p (B), hsa-miR-141-3p (C), hsa-miR-155-5p (D) and hsa-miR-200b-3p (E) input optimization. Validation of ath-miR-159a input (F). Blue squares indicate the optimal input.

A temperature gradient (54-62°C) was run to further optimize droplet separation. A temperature around 55°C (54.7°C) provided the best separation (less rain) and highest amplitude for the target miRNAs (Figure 7A-E) and a temperature around 56°C (55.7 °C) was set for ath-miR-159a (Figure 7F). The optimal amplitude thresholds of 2500 (for hsa-

miR-126-3p, hsa-miR141-3p, hsa-miR-155-5p, hsa-miR-200b-3p and ath-miR-159a) and of 3100 (for hsa-miR-21-5p) were applied to achieve maximal separation for all miRNAs.

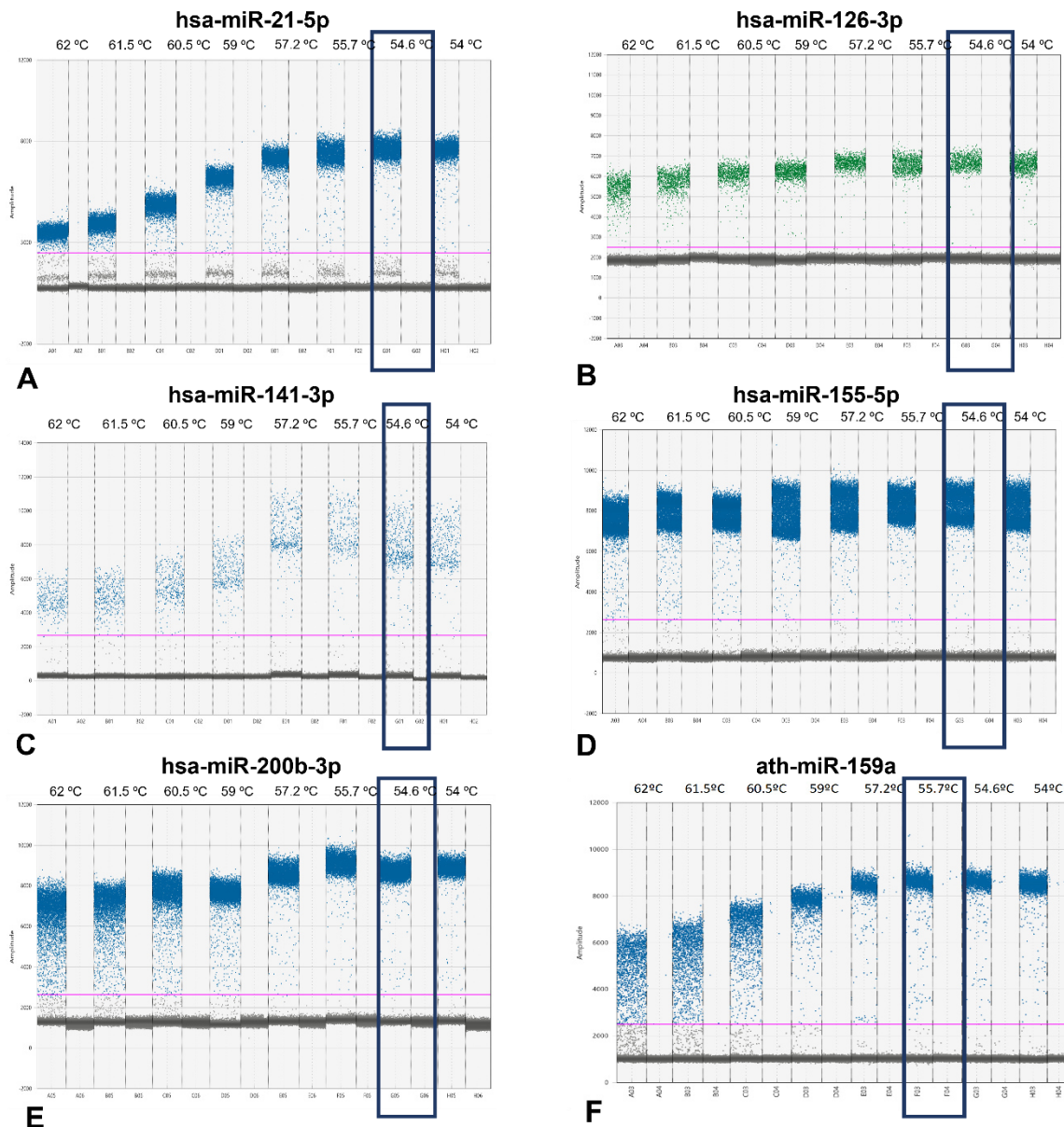


Figure 7 – Temperature gradient for optimization of hsa-miR-21-5p (A), hsa-miR-126-3p (B), hsa-miR-141-3p (C), hsa-miR-155-5p (D) and hsa-miR-200b-3p (E). Validation of temperature optimized for ath-miR-159a (F). The best separation was optimized around 56°C for ath-miR-159a and around 55°C for the other assays. Blue rectangles indicate the optimal temperature.

2.2. Positive Control

To achieve the most accurate separation of positive and negative droplets, serial dilutions of positive control were performed with the best separation set at 1:50 for hsa-miR-21-5p, hsa-miR-126-3p, hsa-miR-155-5p and hsa-miR-200b-3p, and without dilution for hsa-miR-141-3p (Figure 8).

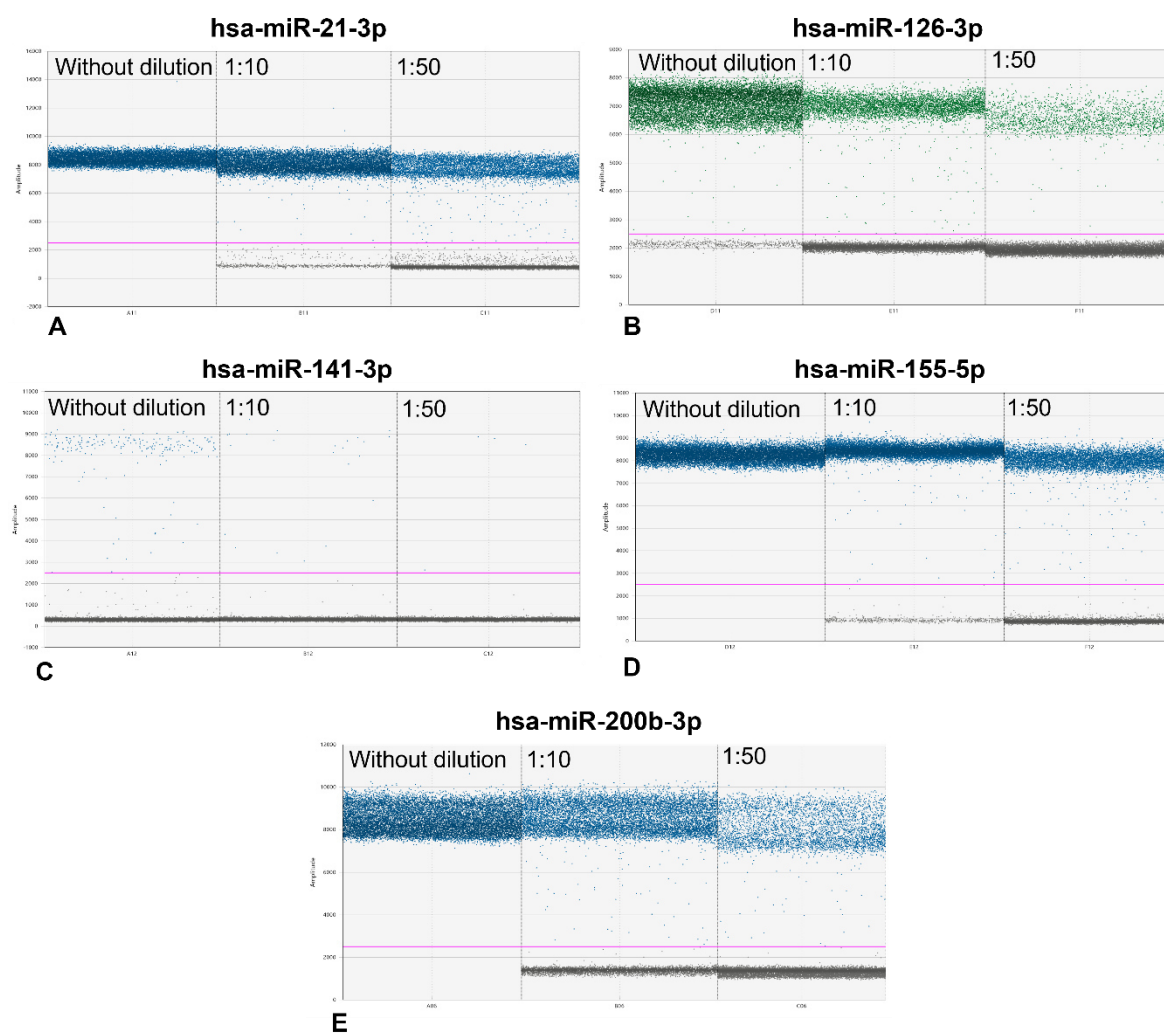


Figure 8 – Optimization of LiKidMiRs pipeline. Best separation of positive and negative droplets in the hsa-miR-141-3p positive control without dilution (C) and 1:50 for the other miRNAs (A,B,D,E). Importantly, for hsa-miR-21-3p, hsa-miR-155-5p and hsa-200b-3p (A,D,E) there is no separation of droplets in the undiluted sample.

2.3. Further optimization of ddPCR protocol

For determining LOB and LOD, 30 NTC samples inserted in the cDNA synthesis step were run for the five miRNAs and analysed according to Armbruster and colleagues [2]. LODs of the assays were set as thresholds of positivity for the corresponding miRNAs in this pipeline (Table 6).

Table 6 – Optimization of LiKidMiRs pipeline. Determination of Limit of Blank (LOB) and Limit of Detection (LOD). LOB and LOD are presented as number of positive droplets.

miRNAs	LOB	LOD
hsa-miR-21-5p	3	8
hsa-miR-126-3p	4	9
hsa-miR-141-3p	2	6
hsa-miR-155-5p	8	14
hsa-miR-200b-3p	2	6

For calculating LOQ (allowing for precise quantification of the absolute number of copies present in the sample), 2-fold dilutions series of a positive case were performed as mentioned above. The determined LOQs were 46.75 copies/ μ L, 33.33 copies/ μ L, 1.54 copies/ μ L, 4.66 copies/ μ L and 0.44 copies/ μ L for hsa-miR-21-5p, hsa-miR-126-3p, hsa-miR-141-3p, hsa-miR-155-5p and hsa-miR-200b-3p, respectively (Figure 9).

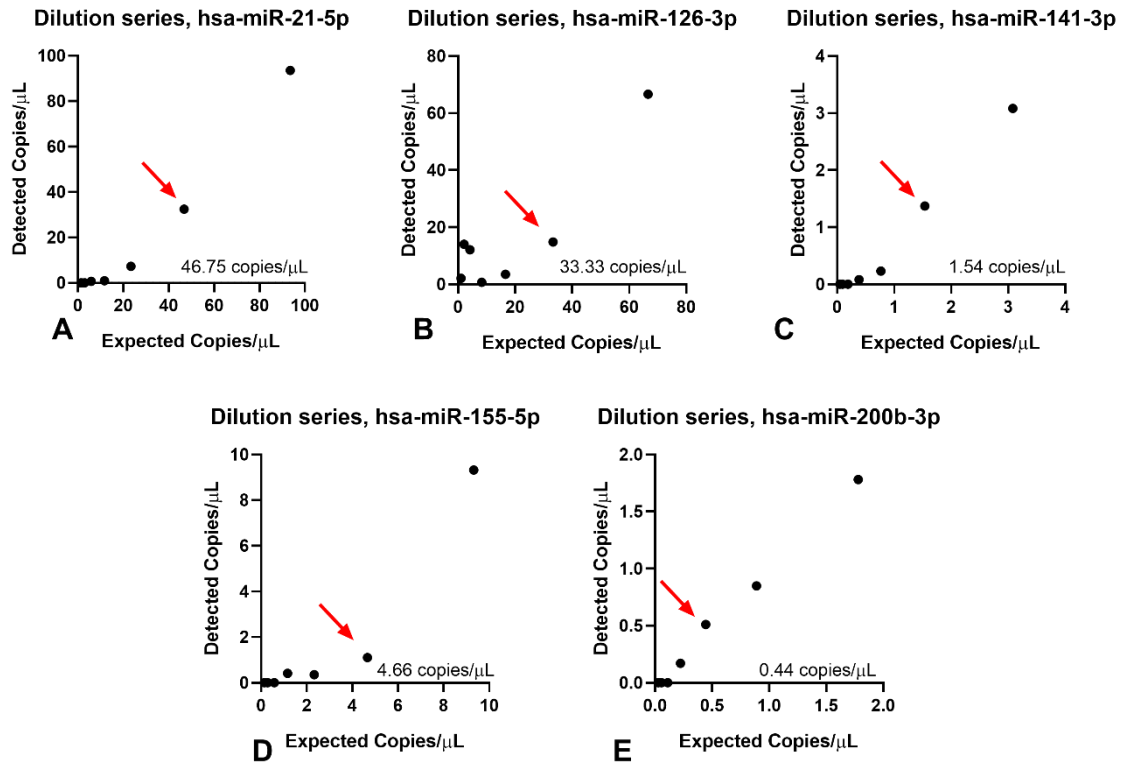


Figure 9 – Limit of quantification of for hsa-miR-21-5p (A), hsa-miR-126-3p (B), hsa-miR-141-3p (C), hsa-miR-155-5p (D) and hsa-miR-200b-3p (E). The red arrow points to the number of copies that the assay can still reliably quantify.

3. EVALUATION OF BIOMARKER DETECTION PERFORMANCE – VALIDATION COHORT

3.1. Distribution of circulating miRNAs levels and biomarkers' performance to detect Malignant Tumors

Initially, target miRNAs levels were compared between oncocytoma (a benign tumor) and healthy donor samples. Importantly, no significant differences between these groups were found for all the tested hsa-miRNAs (Figure 10).

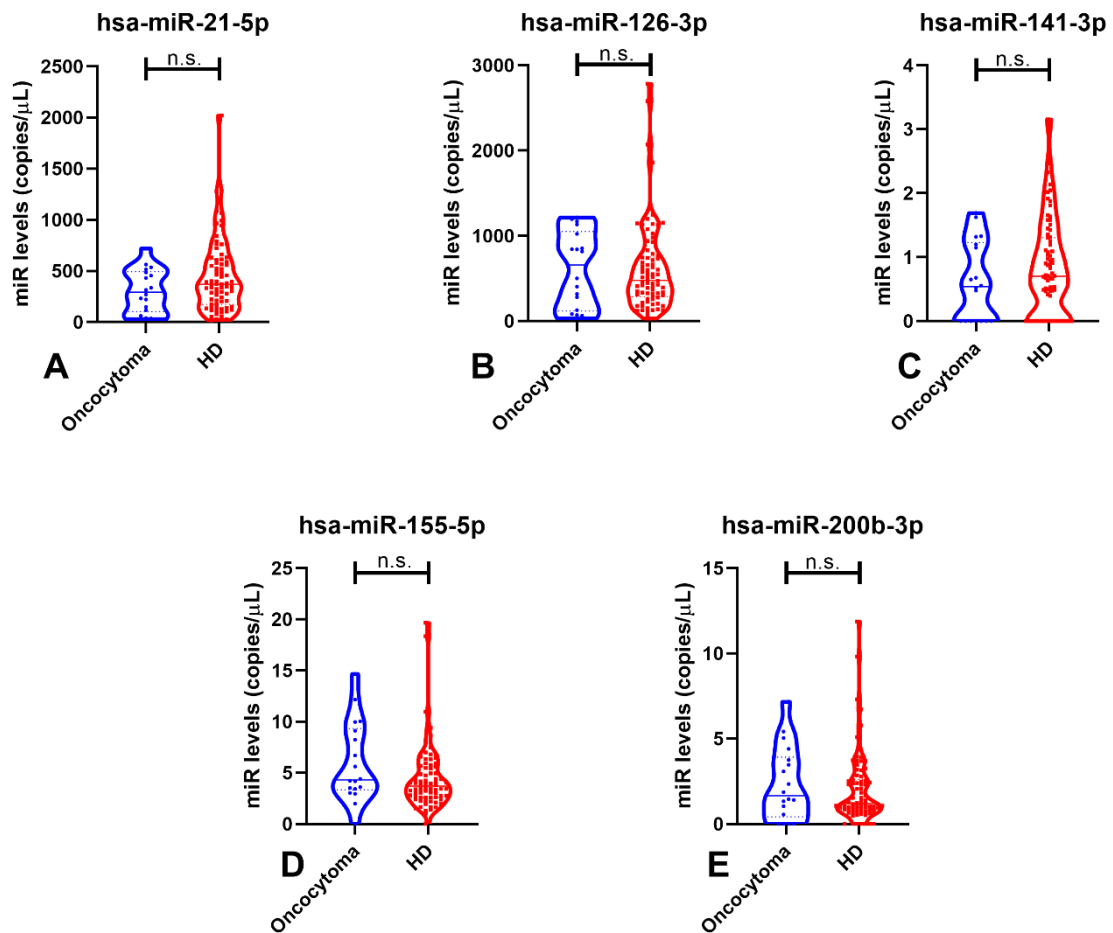


Figure 10 – Violin plots of miRNAs levels in oncocytomas and Healthy Donors (HD) samples of hsa-miR-21-5p (p-value=0.154), hsa-miR-126-3p (p-value=0.851), hsa-miR-141-3p (p-value=0.376), hsa-miR-155-5p (p-value=0.066) and hsa-miR-200b-3p (p-value=0.535). Abbreviations: HD – Healthy Donors, n.s. – not significant.

Due to clinical relevance of discriminating malignant disease (RCC) from benign RCT and healthy individuals, this comparison was subsequently performed. Interestingly, circulating levels of hsa-miR-21-5p, hsa-miR-141-3p and hsa-miR-155-5p significantly differed between these two groups (p -value<0.001, p -value=0.014 and p -value=0.039, respectively) (Figure 11). Circulating levels of hsa-miR-21-5p disclosed the highest accuracy for identifying malignant tumors, although hsa-miR-141-3p depicted the best sensitivity

(65.49%) and hsa-miR-155-5p the highest specificity (88.54%). Remarkably, a panel comprising hsa-miR-21-5p/hsa-miR-155-5p was able to detect 88% of the three major RCC subtypes, with 71.43% accuracy (Table 7). MiRNAs that did not significantly differ between these two groups and other miRNAs panels tested are detailed in Supplementary Figure 1 and Supplementary Table 1.

It is noteworthy that the same three hsa-miRNAs were able to discriminate RCTs from Healthy Donors (Supplementary Figure 2,3 and Supplementary Table 2,3).

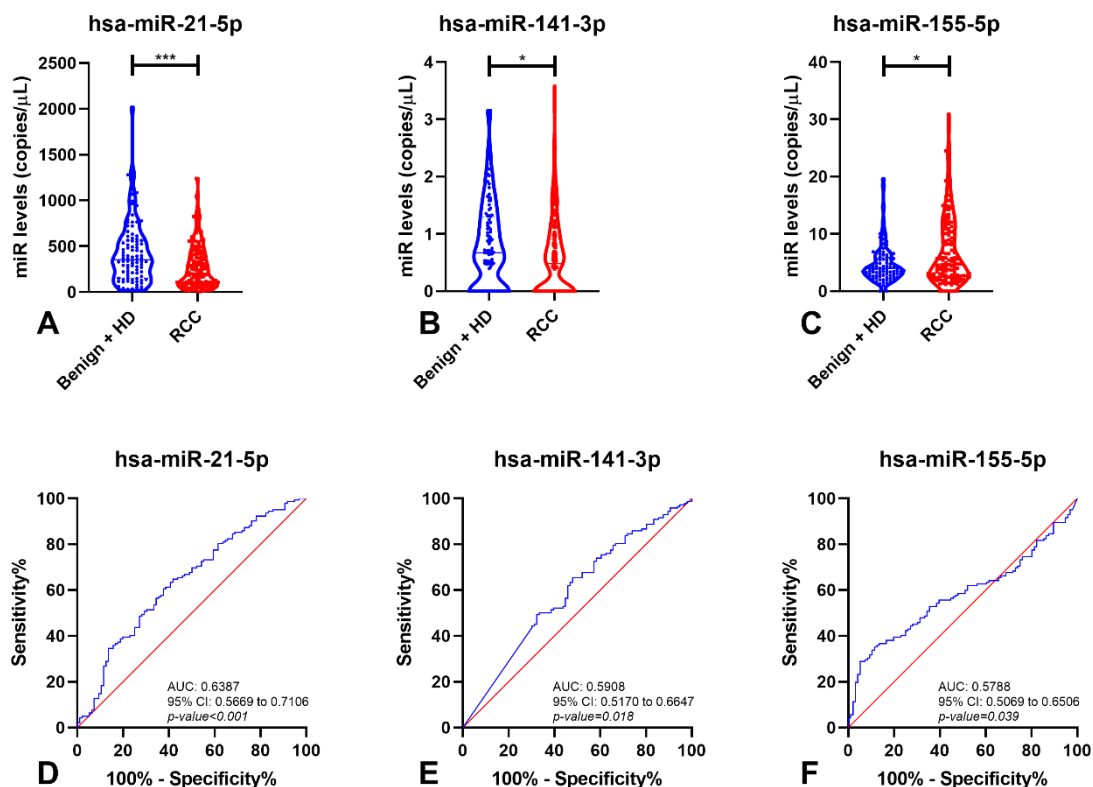


Figure 11 – Violin plots with all points of miRNAs levels in Benign tumors (Oncocytomas) with Healthy Donors (HD) and Renal Cell Carcinomas (RCC) samples of hsa-miR-21-5p (A), hsa-miR141-3p (B) and hsa-miR-155-5p (C) and respective Receiver Operating Characteristic Curve (D-F). Abbreviations: AUC – Area Under the Curve; CI – Confidence Interval, HD – Healthy Donors, RCC – Renal Cell Carcinoma.

Table 7 – Performance of miRNAs as biomarkers for detection of Renal Cell Carcinoma.

miRNAs	SE %	SP %	PPV %	NPV %	Accuracy %
hsa-miR-21-5p	64.08	58.33	69.47	52.34	61.76
hsa-miR-141-3p	65.49	52.08	66.91	50.51	60.08
hsa-miR-155-5p	35.21	88.54	81.97	48.02	56.72
hsa-miR-21-5p/hsa-miR-155-5p	87.32	47.92	71.26	71.88	71.43

Abbreviations: SE – Sensitivity; SP – Specificity; PPV – Positive Predictive Value; NPV – Negative Predictive Value

When the analysis was restricted to early stage disease (patients with organ confined tumor) and healthy donor samples, hsa-miR-21-5p and hsa-miR-155-5p, but not the other miRNAs (Supplementary Figure 4), retained the statistical difference (p -value<0.01 and p -value=0.012) between these two groups (Figure 12 A-B). Thus, these two miRNAs were able to detect small RCC (tumors limited to the kidney, without regional lymph node metastasis) with 96.05% sensitivity and high negative predictive value (NPV) (88.00%) (Table 8).

Remarkably, the AUC for both miRNAs was superior to 60.00% (Figure 12 C-D).

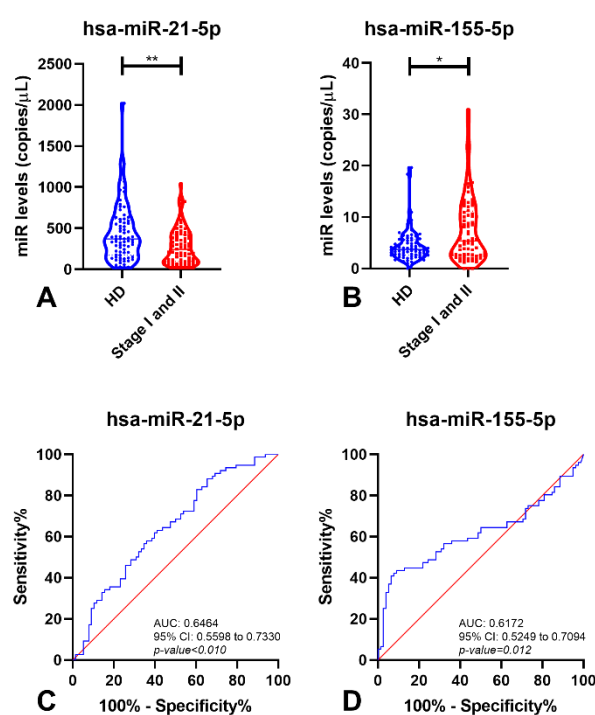


Figure 12 – Violin plots of miRNAs levels in Healthy Donors (HD) and early stages of Renal Cell Carcinomas (Stage I and II) samples of hsa-miR-21-5p (A) and hsa-miR-155-5p (B) and respective Receiver Operating Characteristic Curve (C-D). Abbreviations: AUC – Area Under the Curve; CI – Confidence Interval; HD – Healthy Donors.

Table 8 – Performance of miRNAs as biomarkers for identification of early stages Renal Cell Carcinomas.

miRNAs	SE %	SP %	PPV %	NPV %	Accuracy %
hsa-miR-21-5p	88.16	34.62	56.78	75.00	61.04
hsa-miR-155-5p	43.42	91.03	82.50	62.38	67.53
hsa-miR-21-5p/hsa-miR-155-5p	96.05	28.21	56.59	88.00	61.69

Abbreviations: SE – Sensitivity; SP – Specificity; PPV – Positive Predictive Value; NPV – Negative Predictive Value

4. MIRNAS LEVELS AND CLINICOPATHOLOGICAL FEATURES

Among the malignant RCC subtypes (ccRCC, pRCC and chRCC), significant differences were found for hsa-miR-126-3p, hsa-miR-155-5p and hsa-miR-200b-3p circulating levels (p -value<0.010, p -value=0.018 and p -value=0.013, respectively) (Figure 13).

Furthermore, hsa-miR-126-3p, hsa-miR-155-5p and hsa-miR-200b-3p circulating levels significantly differed between the two major RCC subtypes, ccRCC and pRCC (p -value<0.001 for hsa-miR-126-3p and p -value=0.015 for other miRNAs) (Figure 13B,E,F). However, no statistical differences were found for other miRNAs (Figure 13A, C). Moreover, no statistical differences were found for the tested circulating miRNAs between pRCC and chRCC or between ccRCC and chRCC.

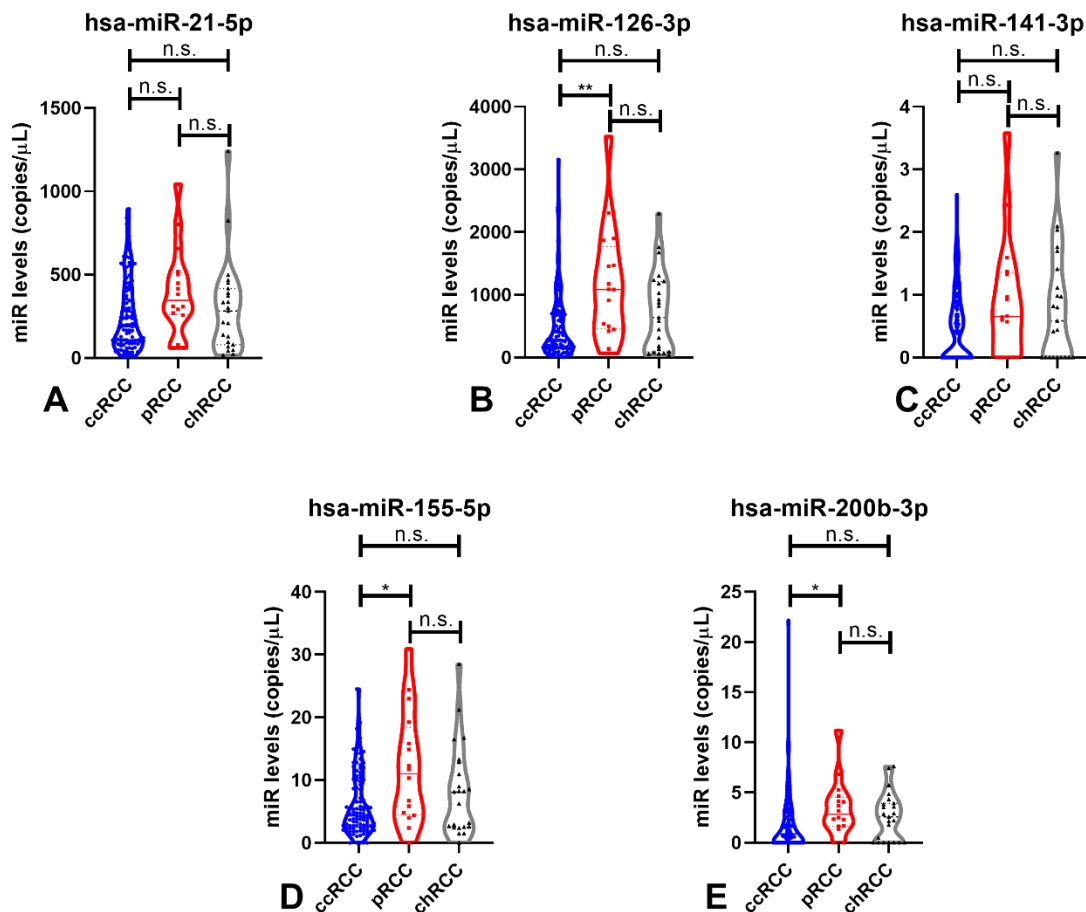


Figure 13 – Violin plots of hsa-miR-21-5p (A), hsa-miR-126-3p (B), hsa-miR-141-3p (C), hsa-miR-155-5p (D) and hsa-miR-200b-3p (E) levels in the malignant subtypes (ccRCC, pRCC and chRCC). Dashed lines indicate the interquartile range and horizontal line the median of miRs levels. Abbreviations: ccRCC – Clear Cell Renal Cell Carcinoma; chRCC – Chromophobe Renal Cell Carcinoma; pRCC – Papillary Renal Cell Carcinoma; n.s. – not significant.

Due to the poorer outcome and higher incidence of ccRCC, comparisons in circulating hsa-miRNAs were performed between this subtype and the other two RCCs subtypes (Figure 14). Interestingly, ccRCC patients displayed significantly lower circulating levels of all hsa-miRs compared to patients diagnosed with the other malignant subtypes (hsa-miR-126-3p, hsa-miR-141-3p, hsa-miR-155-5p and hsa-miR-200b-3p; p -value<0.01, p -value=0.033, p -value=0.018 and p -value<0.01 respectively – Figure 14), except for hsa-miR-21-5p.

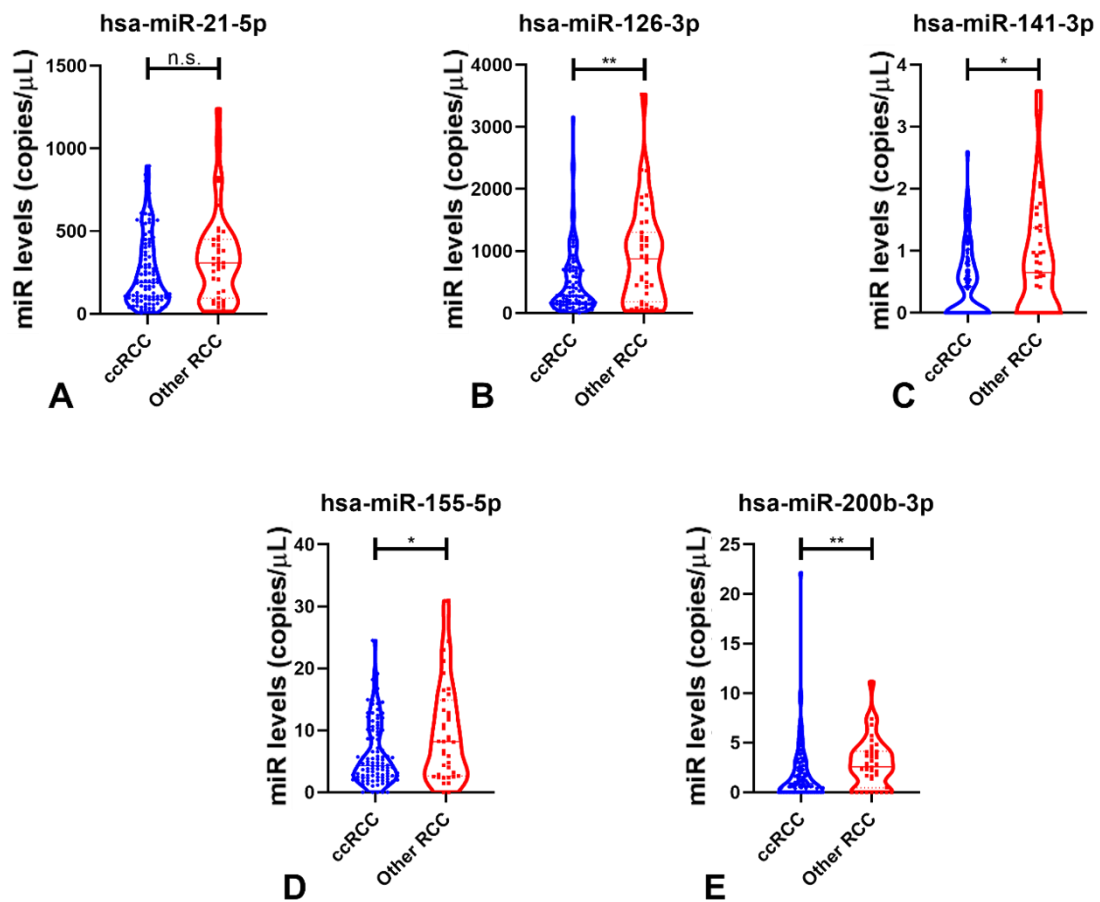


Figure 14 – Violin plots of hsa-miR-21-5p (A), hsa-miR-126-3p (B), hsa-miR-141-3p (C), hsa-miR-155-5p (D) and hsa-miR-200b-3p (E) levels in ccRCC and other RCCs (pRCC and chRCC). Abbreviations: ccRCC – Clear Cell Renal Cell Carcinoma; RCC – Renal Cell Carcinomas; n.s. – not significant.

Moreover, circulating hsa-miR-126-3p and hsa-miR-141-3p levels could discriminate ccRCC from other RCC with 79.61% sensitivity and 81.55% sensitivity (Figure 15 and Table 9). A panel comprising hsa-miR-126-3p and hsa-miR-200b-3p detected ccRCCs with the same sensitivity of hsa-miR-141-3p but with higher specificity (53.85%).

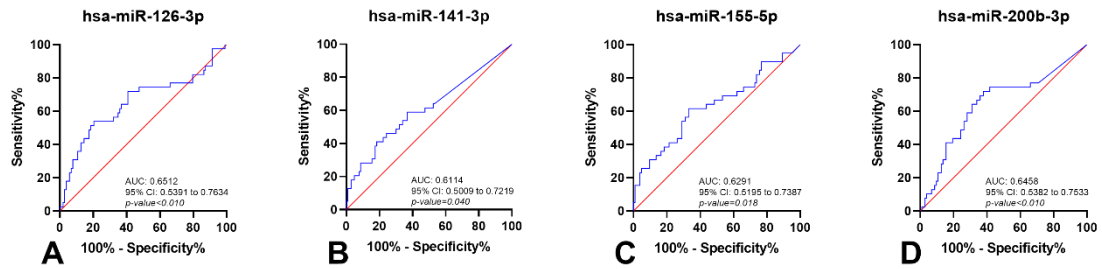


Figure 15 – Receiver Operating Characteristic Curves of hsa-miR-126-3p (A), hsa-miR-141-3p (B), hsa-miR-155-5p (C) and hsa-miR-200b-3p (D) in ccRCC and other RCC (pRCC and chRCC). Abbreviations: AUC – Area Under the Curve; CI – Confidence Interval.

Table 9 – Performance of miRNAs as biomarkers for identification of Clear Cell Renal Cell Carcinoma.

miRNAs	SE %	SP %	PPV %	NPV %	Accuracy %
hsa-miR-126-3p	79.61	53.85	82.00	50.00	72.54
hsa-miR-141-3p	81.55	41.03	78.50	45.71	70.42
hsa-miR-155-5p	66.99	61.54	82.14	41.38	65.49
hsa-miR-200b-3p	62.14	71.79	85.33	41.79	64.79
hsa-miR-126-3p/ hsa-miR-200b-3p	81.55	53.85	82.35	52.50	73.94

Abbreviations: SE – Sensitivity; SP – Specificity; PPV – Positive Predictive Value; NPV – Negative Predictive Value

Interestingly, hsa-miR-141-3p was the only biomarker able to discriminate early stage from advanced stage disease (Supplementary Figure 5). Patients with organ confined tumors (Stage I and II) disclosed significantly higher hsa-miR-141-3p circulating levels compared to those invading beyond the renal capsule (Stage III and IV) (p -value = 0.016; Figure 16). Furthermore, hsa-miR-141-3p displayed 93.85% sensitivity, although with a very modest specificity (15.00%).

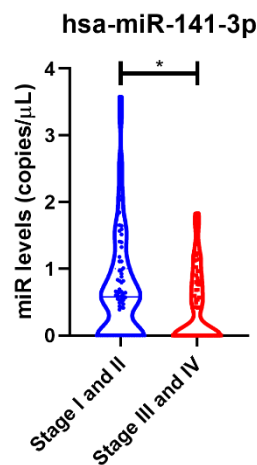


Figure 16 – Violin plot of hsa-miR-141-3p levels in early stages and advanced stages.

VI.DISCUSSION

RCC remains a major cause of cancer-related death worldwide. Alongside with prostate and bladder cancers, RCC is one of the most common urological malignancies [6]. Early detection of RCC (ideally at stage I or II) significantly increases the likelihood of cure through surgical treatment, with a 5-year survival of 98%, avoiding the need for subsequent therapies, which often carry adverse side effects [7]. Nonetheless, 20-30% of patients display metastatic disease at diagnosis [6,8] and following curative-intent nephrectomy, the standard of care treatment for localized RCC, metastases are found in up to 20-40% of patients [8]. Importantly, the response to treatment (mostly targeted therapy or immunotherapy) is rather limited, with a 5-year survival rate lower than 10%. Among RCCs, ccRCC, pRCC and chRCC represent more than 90% of the diagnosis, underlining the importance of accurately detecting these tumor subtypes and discriminate them from benign conditions [8,9].

Currently, circulating miRNAs are suggested as an emergent minimally invasive approach for cancer detection. Thus, these molecules may represent promising RCC biomarkers. Nevertheless, only a small number of studies have tackled this promise in RCC [7,10-21]. Hence, in this dissertation, we assessed the clinical potential of a circulating miRNA-based strategy for RCC detection using ddPCR.

After a first analysis and considering that no significant differences were observed in circulating hsa-miRs between oncocytomas and healthy donors, we showed that three (hsa-miR-21-5p, hsa-miR-141-3p and hsa-miR-155-5p) out of the five candidate miRNAs might be suitable markers for detection of RCC. Despite hsa-miR-21-5p has been described to act as an oncomiR, we observed lower circulating levels in RCC patients [14,22-24]. This might be due to the distinct amounts of miRNAs levels in the different clinical samples. Indeed, higher miRNA levels may be found in tissues comparing with body fluid samples [25]. Importantly, increased hsa-miR-21-5p levels were also found in serum samples of RCC patients, further supporting the fact that, indeed, levels of circulating miRNAs in serum and plasma may be different [14]. In the same line, in breast cancer, hsa-miR-30b-5p levels were lower tissue samples when compared with plasma samples, disclosing the disparities between these two sample sources [26]. Furthermore, Mompéon et al. have shown that these sources exhibit different miRNAs patterns and therefore are not comparable [27]. Of note, plasma has been reported to be the sample of election for translational studies [27-29], as red blood cells lysis during coagulation process increases the discharging of RNA to serum, modifying the circulating miRNAs present in each sample [28]. Also, mistaken normalization and biased results may occur if the used normalizer is not the most suitable. Indeed, U6, which has been used by other research teams [18], is more prone to degradation by serum RNAses. Interestingly, this miRNA was also able to discriminate RCT

patients from healthy donors, and, as previously reported by our research team, hsa-miR-21-5p had significantly lower levels in tissue samples from RCC patients [1].

Concerning hsa-miR-141-3p, it is acknowledged as a tumor suppressor by causing cell cycle arrest, and significant lower levels has been previously reported in RCC samples, in line with our results [1,19,30]. Because the levels of this miRNA decreases during tumor progression, it was able to detect 93.85% of early stage RCC, disclosing higher levels in localized RCC compared to advanced stage RCC. Remarkably, higher levels of circulating hsa-miR-155-5p was found in RCC patients, and a panel comprising hsa-miR-155-5p and hsa-miR-21-5p could identify 87.32% of RCC patients with 71.43% accuracy. Remarkably, hsa-miR-155-5p was shown to have higher levels in tissue [1,30] and in ccRCC serum samples [17], being also associated with cancer development [30]. Moreover, hsa-miR-21-5p/hsa-miR-155-5p panel depicted high sensitivity (96.05%) for identifying organ confined carcinomas, which might allow for reducing false-negative results and increase the likelihood of curative-intent treatment. To the best of our knowledge, this is the first study that evaluated the biomarker performance of plasma circulating hsa-miRs to detect early stage RCC. Previously, Wang and colleagues described a 5-miRNA panel (miR-193a-3p, miR-362, miR-572, miR-378 and miR-28-5p) that was able to identify early stage RCC, although in serum samples [16]. Furthermore, our panel achieved higher NPV than that reported by Wang et al. [16].

We further evaluated whether circulating hsa-miRNAs might also convey relevant information to discriminate ccRCC from the remainder RCC subtypes. Indeed, four out five miRNAs were able to differentiate this major RCC subtype from the remainder. The panel constituted by hsa-miR-126-3p and hsa-miR-200b-3p disclosed the best performance, with 81.55% sensitivity and 53.85% specificity. Considering that ccRCC is an aggressive RCC subtype, early detection is of major importance, and its accurate identification might enable improvement in patients' outcome [14,31].

Despite various studies have reported other strategies for RCC identification (including imaging and epigenetic biomarkers), our results seem to offer the best sensitivity for RCC detection [32,33]. Indeed, the methodology we developed uses lower initial sample volume [7,10,11,13,14,16,21], is more cost-effective and better tolerated by patients. Molecular imaging like ¹⁸F-fluorodeoxyglucose (FDG) positron emission tomography/computed tomography (PET/CT) was reported to detect localized RCC, but it discloses lower sensitivity (only 22%) [32,34]. Despite the superior specificity (85.9%) of ¹²⁴I-cG250 PET for RCC detection, when compared to our hsa-miR-21-5p/hsa-miR-155-5p panel (47.92%), this monoclonal antibody has a half-life of several days, constituting a significant disadvantage in relation to the protocol reported by us [35]. Moreover, diffusion magnetic resonance imaging was reported to be able to characterize malignant lesions with similar sensitivity

(86%) to our panel but with higher specificity (78%) [36]. Nevertheless, it should be noted that despite better performance, these imaging biomarkers are more costly and less well tolerated by the patient, compared to liquid biopsies [32].

The intense exploration of circulating epigenetic markers such as DNA methylation, miRNAs and lncRNAs is well illustrated by the number (over 60) articles published in this field since 2003 [33]. So far, 10 DNA methylation-based studies (e.g., using *VHL*, *RASSF1A*, *P16*, *P14*, *RARB*, *TIMP3*, *GSTP1*, *APC*) for RCC detection were published [37-46] and only 33.33% of these had a RCC cohort with more than 50 patients [39,42,43]. Compared with those studies, our results provide higher sensitivity (6-83%). However, DNA methylation-based markers displayed high specificity (53-100%). This was also observed in three lncRNAs studies (e.g., *GIHCG*, *LINC00887*) [47-49], in which the diagnostic performance was generally lower than in our study (67.1-87.0%), but the specificity reached >80% for all biomarkers. Although our biomarker panels disclosed high sensitivity, their specificity is limited. Thus, in an envisaged routine setting, they would ideally be used in first line screening, requiring complementary use of more specific biomarkers in cases deemed as positive. In liquid biopsies, DNA methylation-based markers such as *VHL*, *RASSF1A*, *TIMP3*, *SFRP1*, *SFRP2*, *SFRP4*, *SFRP5*, *PCDH17* and *TCF21* have been shown to be highly specific (100%) [37,38,40,41,44-46], and, thus, constitute good candidates as second-line tests, in this setting.

As previously reported by us, most circulating miRNA studies are based on blood-based liquid biopsies [50]. When compared with our protocol, only few studies included more than 100 RCC patients, which might, at the least partially, explain the differences in results [33]. Additionally, the discrepant results might also be explained, as described above, by the biased normalization (e.g., spike-in as normalizer miRNA, U6, RNU48) [12,14,18-20]. Nevertheless, the sensitivity reported for the most widely studied serum miRNAs (miR-210, miR-1233 and miR-378) was generally lower than our plasma panel [13,18,21]. Indeed, using this less time-consuming and more cost effective approach, we were able to detect RCC using a minimally invasive technique, with lower initial quantity of plasma than serum-based studies (although detecting other miRNAs), and obtained similar or even better results, obviating the need for normalization and the associated bias (due to ddPCR absolute quantification) [7,10,11,13,14,16,21]. Hence, our results clearly demonstrate a potential clinical application of this technology for identification of RCC, being the first study to quantify circulating miRNAs in these patients using ddPCR (Figure 17).

These results require validation in larger multicenter prospective studies. Overall, and notwithstanding our promising results for RCC detection, it should be acknowledged that the lack of long-term follow-up constitutes a major limitation. Also, further studies using

liquid biopsies should also be considered to further subtype RCC, namely, to distinguish oncocytomas from chRCCs avoiding unnecessary treatment.

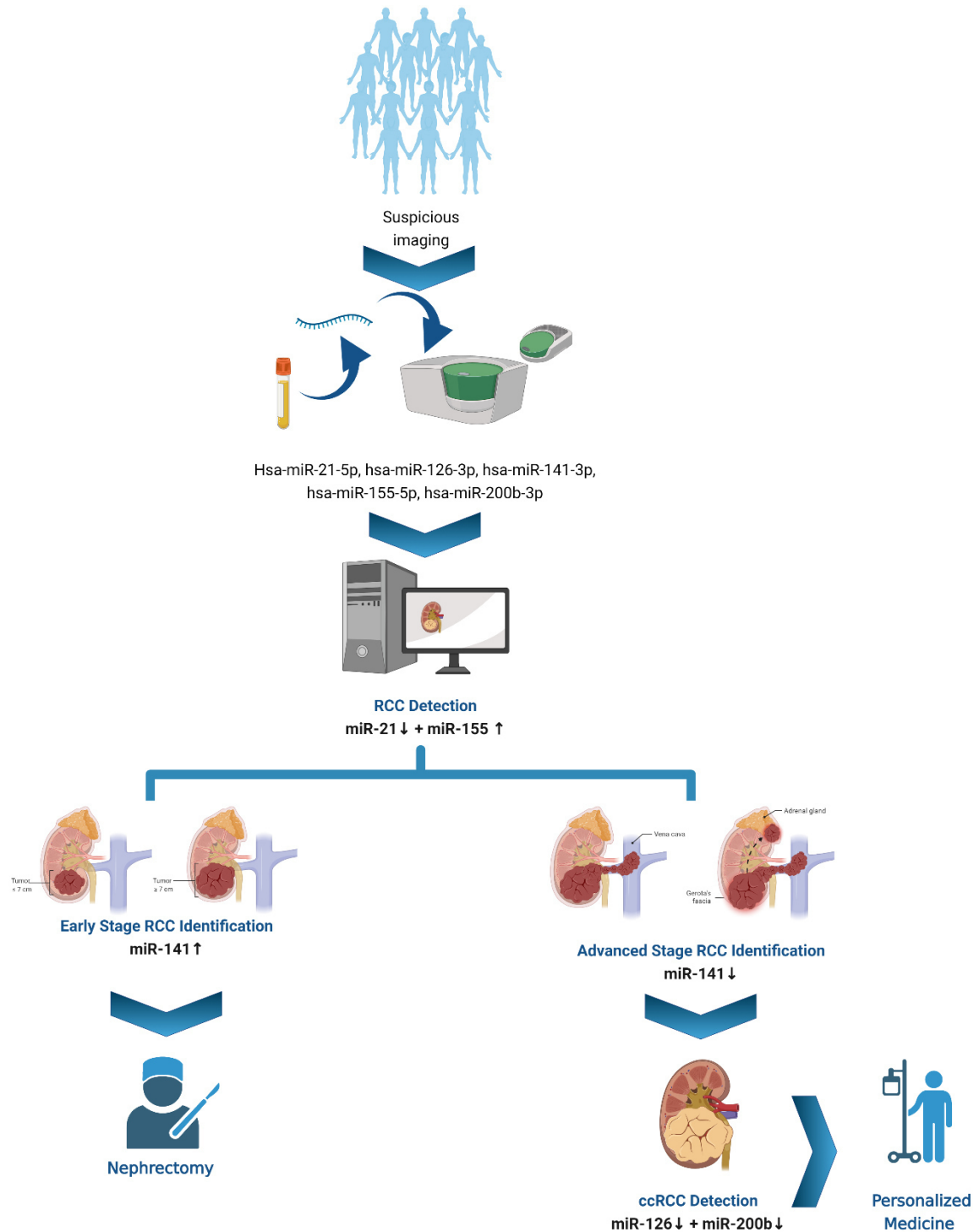


Figure 17 – Algorithm for LiKidMiRs' clinical application. Created with BioRender.com.

VII.CONCLUSIONS AND FUTURE PERSPECTIVES

In conclusion, our findings support the research question that a minimally invasive test can be developed to detect RCC, improving RCC patients' survival through increased diagnosis at earlier stages. This might help reduce the morbidity associated with advanced disease, as well the lack of curative treatment at those stages. Furthermore, and to the best of our knowledge, this work is the first to report a novel tool to quantify circulating miRNAs using ddPCR in RCC patients.

Considering our findings, we intend to:

- Test novel miRNAs for RCC subtyping;
- Explore miRNAs as discriminators between chRCC and oncocytomas;
- Develop a miRNAs multiplex ddPCR-based test with selected miRNAs;
- Explore whether exosomal miRNAs might improve the sensitivity of the selected miRNAs;
- Establish the most sensitive and specific miRNA analysis technique (circulating miRNAs or exosomal miRNAs) for RCC detection;
- Validate the results in a larger multicenter prospective cohort of RCC patients, including those with advanced stage disease.

VIII.REFERENCES

1. Silva-Santos, R.M.; Costa-Pinheiro, P.; Luis, A.; Antunes, L.; Lobo, F.; Oliveira, J.; Henrique, R.; Jeronimo, C. MicroRNA profile: a promising ancillary tool for accurate renal cell tumour diagnosis. *British journal of cancer* **2013**, *109*, 2646-2653, doi:10.1038/bjc.2013.552.
2. Armbruster, D.A.; Pry, T. Limit of blank, limit of detection and limit of quantitation. *Clin Biochem Rev* **2008**, *29 Suppl 1*, S49-S52.
3. Stein, E.V.; Duewer, D.L.; Farkas, N.; Romsos, E.L.; Wang, L.; Cole, K.D. Steps to achieve quantitative measurements of microRNA using two step droplet digital PCR. *PLoS One* **2017**, *12*, e0188085, doi:10.1371/journal.pone.0188085.
4. Schisterman, E.F.; Perkins, N.J.; Liu, A.; Bondell, H. Optimal cut-point and its corresponding Youden Index to discriminate individuals using pooled blood samples. *Epidemiology (Cambridge, Mass.)* **2005**, *16*, 73-81.
5. Youden, W.J. Index for rating diagnostic tests. *Cancer* **1950**, *3*, 32-35.
6. Fan, B.; Jin, Y.; Zhang, H.; Zhao, R.; Sun, M.; Sun, M.; Yuan, X.; Wang, W.; Wang, X.; Chen, Z.; et al. MicroRNA-21 contributes to renal cell carcinoma cell invasiveness and angiogenesis via the PDCD4/c-Jun (AP-1) signalling pathway. *International journal of oncology* **2020**, *56*, 178-192, doi:10.3892/ijo.2019.4928.
7. Iwamoto, H.; Kanda, Y.; Sejima, T.; Osaki, M.; Okada, F.; Takenaka, A. Serum miR-210 as a potential biomarker of early clear cell renal cell carcinoma. *Int J Oncol* **2014**, *44*, 53-58, doi:10.3892/ijo.2013.2169.
8. Carlsson, J.; Christiansen, J.; Davidsson, S.; Giunchi, F.; Fiorentino, M.; Sundqvist, P. The potential role of miR-126, miR-21 and miR-10b as prognostic biomarkers in renal cell carcinoma. *Oncol Lett* **2019**, *17*, 4566-4574, doi:10.3892/ol.2019.10142.
9. Lopez-Beltran, A.; Carrasco, J.C.; Cheng, L.; Scarpelli, M.; Kirkali, Z.; Montironi, R. 2009 update on the classification of renal epithelial tumors in adults. *Int J Urol* **2009**, *16*, 432-443, doi:10.1111/j.1442-2042.2009.02302.x.
10. Fedorko, M.; Juracek, J.; Stanik, M.; Svoboda, M.; Poprach, A.; Buchler, T.; Pacik, D.; Dolezel, J.; Slaby, O. Detection of let-7 miRNAs in urine supernatant as potential diagnostic approach in non-metastatic clear-cell renal cell carcinoma. *Biochem Med (Zagreb)* **2017**, *27*, 411-417, doi:10.11613/BM.2017.043.
11. Fedorko, M.; Stanik, M.; Iliev, R.; Redova-Lojova, M.; Machackova, T.; Svoboda, M.; Pacik, D.; Dolezel, J.; Slaby, O. Combination of MiR-378 and MiR-210 Serum Levels Enables Sensitive Detection of Renal Cell Carcinoma. *Int J Mol Sci* **2015**, *16*, 23382-23389, doi:10.3390/ijms161023382.
12. Mytsyk, Y.; Dosenko, V.; Borys, Y.; Kucher, A.; Gazdikova, K.; Busselberg, D.; Caprnda, M.; Kruzliak, P.; Farooqi, A.A.; Lubov, M. MicroRNA-15a expression

- measured in urine samples as a potential biomarker of renal cell carcinoma. *Int Urol Nephrol* **2018**, *50*, 851-859, doi:10.1007/s11255-018-1841-x.
13. Redova, M.; Poprach, A.; Nekvindova, J.; Iliev, R.; Radova, L.; Lakomy, R.; Svoboda, M.; Vyzula, R.; Slaby, O. Circulating miR-378 and miR-451 in serum are potential biomarkers for renal cell carcinoma. *J Transl Med* **2012**, *10*, 55, doi:10.1186/1479-5876-10-55.
 14. Tusong, H.; Maolakuerban, N.; Guan, J.; Rexiati, M.; Wang, W.G.; Azhati, B.; Nuerrula, Y.; Wang, Y.J. Functional analysis of serum microRNAs miR-21 and miR-106a in renal cell carcinoma. *Cancer Biomark* **2017**, *18*, 79-85, doi:10.3233/cbm-160676.
 15. von Brandenstein, M.; Pandarakalam, J.J.; Kroon, L.; Loeser, H.; Herden, J.; Braun, G.; Wendland, K.; Dienes, H.P.; Engelmann, U.; Fries, J.W. MicroRNA 15a, inversely correlated to PKC α , is a potential marker to differentiate between benign and malignant renal tumors in biopsy and urine samples. *Am J Pathol* **2012**, *180*, 1787-1797, doi:10.1016/j.ajpath.2012.01.014.
 16. Wang, C.; Hu, J.; Lu, M.; Gu, H.; Zhou, X.; Chen, X.; Zen, K.; Zhang, C.-Y.; Zhang, T.; Ge, J.; et al. A panel of five serum miRNAs as a potential diagnostic tool for early-stage renal cell carcinoma. *Scientific Reports* **2015**, *5*, 7610, doi:10.1038/srep07610.
 17. Wang, X.; Wang, T.; Chen, C.; Wu, Z.; Bai, P.; Li, S.; Chen, B.; Liu, R.; Zhang, K.; Li, W.; et al. Serum exosomal miR-210 as a potential biomarker for clear cell renal cell carcinoma. *J Cell Biochem* **2018**, doi:10.1002/jcb.27347.
 18. Wulfken, L.M.; Moritz, R.; Ohlmann, C.; Holdenrieder, S.; Jung, V.; Becker, F.; Herrmann, E.; Walgenbach-Brünagel, G.; von Ruecker, A.; Müller, S.C.; et al. MicroRNAs in Renal Cell Carcinoma: Diagnostic Implications of Serum miR-1233 Levels. *PLOS ONE* **2011**, *6*, e25787, doi:10.1371/journal.pone.0025787.
 19. Yadav, S.; Khandelwal, M.; Seth, A.; Saini, A.K.; Dogra, P.N.; Sharma, A. Serum microRNA Expression Profiling: Potential Diagnostic Implications of a Panel of Serum microRNAs for Clear Cell Renal Cell Cancer. *Urology* **2017**, *104*, 64-69, doi:10.1016/j.urology.2017.03.013.
 20. Zhai, Q.; Zhou, L.; Zhao, C.; Wan, J.; Yu, Z.; Guo, X.; Qin, J.; Chen, J.; Lu, R. Identification of miR-508-3p and miR-509-3p that are associated with cell invasion and migration and involved in the apoptosis of renal cell carcinoma. *Biochem Biophys Res Commun* **2012**, *419*, 621-626, doi:10.1016/j.bbrc.2012.02.060.
 21. Zhao, A.; Li, G.; Péoc'h, M.; Genin, C.; Gigante, M. Serum miR-210 as a novel biomarker for molecular diagnosis of clear cell renal cell carcinoma. *Experimental*

and Molecular Pathology **2013**, *94*, 115-120,
doi:<https://doi.org/10.1016/j.yexmp.2012.10.005>.

22. Chen, J.; Gu, Y.; Shen, W. MicroRNA-21 functions as an oncogene and promotes cell proliferation and invasion via TIMP3 in renal cancer. *Eur Rev Med Pharmacol Sci* **2017**, *21*, 4566-4576.
23. Jung, M.; Mollenkopf, H.J.; Grimm, C.; Wagner, I.; Albrecht, M.; Waller, T.; Pilarsky, C.; Johannsen, M.; Stephan, C.; Lehrach, H.; et al. MicroRNA profiling of clear cell renal cell cancer identifies a robust signature to define renal malignancy. *Journal of cellular and molecular medicine* **2009**, *13*, 3918-3928, doi:10.1111/j.1582-4934.2009.00705.x.
24. Lokeshwar, S.D.; Talukder, A.; Yates, T.J.; Hennig, M.J.P.; Garcia-Roig, M.; Lahorewala, S.S.; Mullani, N.N.; Klaassen, Z.; Kava, B.R.; Manoharan, M.; et al. Molecular Characterization of Renal Cell Carcinoma: A Potential Three-MicroRNA Prognostic Signature. *Cancer Epidemiol Biomarkers Prev* **2018**, *27*, 464-472, doi:10.1158/1055-9965.Epi-17-0700.
25. Nagy, Z.B.; Barták, B.K.; Kalmár, A.; Galamb, O.; Wichmann, B.; Dank, M.; Igaz, P.; Tulassay, Z.; Molnár, B. Comparison of Circulating miRNAs Expression Alterations in Matched Tissue and Plasma Samples During Colorectal Cancer Progression. *Pathol Oncol Res* **2019**, *25*, 97-105, doi:10.1007/s12253-017-0308-1.
26. Adam-Artigues, A.; Garrido-Cano, I.; Simón, S.; Ortega, B.; Moragón, S.; Lameirinhas, A.; Constâncio, V.; Salta, S.; Burgués, O.; Bermejo, B.; et al. Circulating miR-30b-5p levels in plasma as a novel potential biomarker for early detection of breast cancer. *ESMO open* **2021**, *6*, 100039, doi:10.1016/j.esmoop.2020.100039.
27. Mompeón, A.; Ortega-Paz, L.; Vidal-Gómez, X.; Costa, T.J.; Pérez-Cremades, D.; Garcia-Blas, S.; Brugaletta, S.; Sanchis, J.; Sabate, M.; Novella, S.; et al. Disparate miRNA expression in serum and plasma of patients with acute myocardial infarction: a systematic and paired comparative analysis. *Scientific Reports* **2020**, *10*, 5373, doi:10.1038/s41598-020-61507-z.
28. Wang, K.; Yuan, Y.; Cho, J.-H.; McClarty, S.; Baxter, D.; Galas, D.J. Comparing the MicroRNA spectrum between serum and plasma. *PloS one* **2012**, *7*, e41561-e41561, doi:10.1371/journal.pone.0041561.
29. Dufourd, T.; Robil, N.; Mallet, D.; Carcenac, C.; Boulet, S.; Brishoual, S.; Rabois, E.; Houeto, J.-L.; de la Grange, P.; Carnicella, S. Plasma or serum? A qualitative study on rodents and humans using high-throughput microRNA sequencing for circulating biomarkers. *Biology Methods and Protocols* **2019**, *4*, doi:10.1093/biomethods/bpz006.

30. Ji, H.; Tian, D.; Zhang, B.; Zhang, Y.; Yan, D.; Wu, S. Overexpression of miR-155 in clear-cell renal cell carcinoma and its oncogenic effect through targeting FOXO3a. *Exp Ther Med* **2017**, *13*, 2286-2292, doi:10.3892/etm.2017.4263.
31. Cheng, T.; Wang, L.; Li, Y.; Huang, C.; Zeng, L.; Yang, J. Differential microRNA expression in renal cell carcinoma. *Oncol Lett* **2013**, *6*, 769-776.
32. Farber, N.J.; Kim, C.J.; Modi, P.K.; Hon, J.D.; Sadimin, E.T.; Singer, E.A. Renal cell carcinoma: the search for a reliable biomarker. *Transl Cancer Res* **2017**, *6*, 620-632, doi:10.21037/tcr.2017.05.19.
33. Kubiliute, R.; Jarmalaite, S. Epigenetic Biomarkers of Renal Cell Carcinoma for Liquid Biopsy Tests. *Int J Mol Sci* **2021**, *22*, 8846, doi:10.3390/ijms22168846.
34. Gofrit, O.N.; Orevi, M. Diagnostic Challenges of Kidney Cancer: A Systematic Review of the Role of Positron Emission Tomography-Computerized Tomography. *J Urol* **2016**, *196*, 648-657, doi:10.1016/j.juro.2016.02.2992.
35. Divgi, C.R.; Uzzo, R.G.; Gatsonis, C.; Bartz, R.; Treutner, S.; Yu, J.Q.; Chen, D.; Carrasquillo, J.A.; Larson, S.; Bevan, P.; et al. Positron emission tomography/computed tomography identification of clear cell renal cell carcinoma: results from the REDECT trial. *J Clin Oncol* **2013**, *31*, 187-194, doi:10.1200/jco.2011.41.2445.
36. Kang, S.K.; Zhang, A.; Pandharipande, P.V.; Chandarana, H.; Braithwaite, R.S.; Littenberg, B. DWI for Renal Mass Characterization: Systematic Review and Meta-Analysis of Diagnostic Test Performance. *AJR Am J Roentgenol* **2015**, *205*, 317-324, doi:10.2214/ajr.14.13930.
37. Battagli, C.; Uzzo, R.G.; Dulaimi, E.; Ibanez de Caceres, I.; Krassenstein, R.; Al-Saleem, T.; Greenberg, R.E.; Cairns, P. Promoter hypermethylation of tumor suppressor genes in urine from kidney cancer patients. *Cancer Res* **2003**, *63*, 8695-8699.
38. Costa, V.L.; Henrique, R.; Danielsen, S.A.; Eknaes, M.; Patrício, P.; Morais, A.; Oliveira, J.; Lothe, R.A.; Teixeira, M.R.; Lind, G.E.; et al. TCF21 and PCDH17 methylation: An innovative panel of biomarkers for a simultaneous detection of urological cancers. *Epigenetics* **2011**, *6*, 1120-1130, doi:10.4161/epi.6.9.16376.
39. de Martino, M.; Klatte, T.; Haitel, A.; Marberger, M. Serum cell-free DNA in renal cell carcinoma: a diagnostic and prognostic marker. *Cancer* **2012**, *118*, 82-90, doi:10.1002/cncr.26254.
40. Hauser, S.; Zahalka, T.; Fechner, G.; Müller, S.C.; Ellinger, J. Serum DNA hypermethylation in patients with kidney cancer: results of a prospective study. *Anticancer Res* **2013**, *33*, 4651-4656.

41. Hoque, M.O.; Begum, S.; Topaloglu, O.; Jeronimo, C.; Mambo, E.; Westra, W.H.; Califano, J.A.; Sidransky, D. Quantitative detection of promoter hypermethylation of multiple genes in the tumor, urine, and serum DNA of patients with renal cancer. *Cancer Res* **2004**, *64*, 5511-5517, doi:10.1158/0008-5472.Can-04-0799.
42. Nuzzo, P.V.; Berchuck, J.E.; Korthauer, K.; Spisak, S.; Nassar, A.H.; Abou Alaiwi, S.; Chakravarthy, A.; Shen, S.Y.; Bakouny, Z.; Boccardo, F.; et al. Detection of renal cell carcinoma using plasma and urine cell-free DNA methylomes. *Nat Med* **2020**, *26*, 1041-1043, doi:10.1038/s41591-020-0933-1.
43. Outeiro-Pinho, G.; Barros-Silva, D.; Aznar, E.; Sousa, A.I.; Vieira-Coimbra, M.; Oliveira, J.; Gonçalves, C.S.; Costa, B.M.; Junker, K.; Henrique, R.; et al. MicroRNA-30a-5p(me): a novel diagnostic and prognostic biomarker for clear cell renal cell carcinoma in tissue and urine samples. *J Exp Clin Cancer Res* **2020**, *39*, 98, doi:10.1186/s13046-020-01600-3.
44. Skrypckina, I.; Tsyba, L.; Onyshchenko, K.; Morderer, D.; Kashparova, O.; Nikolaienko, O.; Panasenko, G.; Vozianov, S.; Romanenko, A.; Rynditch, A. Concentration and Methylation of Cell-Free DNA from Blood Plasma as Diagnostic Markers of Renal Cancer. *Dis Markers* **2016**, *2016*, 3693096, doi:10.1155/2016/3693096.
45. Urakami, S.; Shiina, H.; Enokida, H.; Hirata, H.; Kawamoto, K.; Kawakami, T.; Kikuno, N.; Tanaka, Y.; Majid, S.; Nakagawa, M.; et al. Wnt antagonist family genes as biomarkers for diagnosis, staging, and prognosis of renal cell carcinoma using tumor and serum DNA. *Clin Cancer Res* **2006**, *12*, 6989-6997, doi:10.1158/1078-0432.Ccr-06-1194.
46. Xin, J.; Xu, R.; Lin, S.; Xin, M.; Cai, W.; Zhou, J.; Fu, C.; Zhen, G.; Lai, J.; Li, Y.; et al. Clinical potential of TCF21 methylation in the diagnosis of renal cell carcinoma. *Oncol Lett* **2016**, *12*, 1265-1270, doi:10.3892/ol.2016.4748.
47. He, Z.H.; Qin, X.H.; Zhang, X.L.; Yi, J.W.; Han, J.Y. Long noncoding RNA GIHCG is a potential diagnostic and prognostic biomarker and therapeutic target for renal cell carcinoma. *Eur Rev Med Pharmacol Sci* **2018**, *22*, 46-54, doi:10.26355/eurrev_201801_14099.
48. Wu, Y.; Wang, Y.Q.; Weng, W.W.; Zhang, Q.Y.; Yang, X.Q.; Gan, H.L.; Yang, Y.S.; Zhang, P.P.; Sun, M.H.; Xu, M.D.; et al. A serum-circulating long noncoding RNA signature can discriminate between patients with clear cell renal cell carcinoma and healthy controls. *Oncogenesis* **2016**, *5*, e192, doi:10.1038/oncsis.2015.48.
49. Xie, J.; Zhong, Y.; Chen, R.; Li, G.; Luo, Y.; Yang, J.; Sun, Z.; Liu, Y.; Liu, P.; Wang, N.; et al. Serum long non-coding RNA LINC00887 as a potential biomarker for

diagnosis of renal cell carcinoma. *FEBS Open Bio* **2020**, *10*, 1802-1809, doi:10.1002/2211-5463.12930.

50. Sequeira, J.P.; Constâncio, V.; Lobo, J.; Henrique, R.; Jerónimo, C. Unveiling the World of Circulating and Exosomal microRNAs in Renal Cell Carcinoma. *Cancers (Basel)* **2021**, *13*, 5252.

IX.APPENDIX

I. ARTICLE I – UNDER REVISION

DigiMir test: establishing a novel pipeline for miR-371a quantification using droplet digital PCR in liquid biopsies from testicular germ cell tumor patients

José Pedro Sequeira^{a,*}, João Lobo^{a,c,d*}, Vera Constâncio^{a,e*}, Tiago Brito-Rocha^{a,b}, Carina Carvalho-Maia^a, Isaac Braga^f, Joaquina Maurício^g, Rui Henrique^{a,c,d,§,#}, Carmen Jerónimo^{a,d,§,#}

^aCancer Biology and Epigenetics Group, Research Center of IPO Porto (CI-IPOP) / RISE@CI-IPOP (Health Research Network), Portuguese Oncology Institute of Porto (IPO Porto) / Porto Comprehensive Cancer Center (Porto.CCC), R. Dr. António Bernardino de Almeida, 4200-072, Porto, Portugal

^bMaster in Oncology, School of Medicine & Biomedical Sciences, University of Porto (ICBAS-UP), Rua Jorge Viterbo Ferreira 228, 4050-513, Porto, Portugal

^cDepartment of Pathology, Portuguese Oncology Institute of Porto (IPOP), R. Dr. António Bernardino de Almeida, 4200-072, Porto, Portugal

^dDepartment of Pathology and Molecular Immunology, Institute of Biomedical Sciences Abel Salazar, University of Porto (ICBAS-UP), Rua Jorge Viterbo Ferreira 228, 4050-513, Porto, Portugal

^eDoctoral Programme in Biomedical Sciences, School of Medicine & Biomedical Sciences, University of Porto (ICBAS-UP), Rua Jorge Viterbo Ferreira 228, 4050-513, Porto, Portugal

^fDepartment of Urology & Urology Clinics, Portuguese Oncology Institute of Porto (IPOP), R. Dr. António Bernardino de Almeida, 4200-072, Porto, Portugal

^gDepartment of Medical Oncology & Urology Clinics, Portuguese Oncology Institute of Porto (IPOP), R. Dr. António Bernardino de Almeida, 4200-072, Porto, Portugal

*shared first authorship

§joint senior authors

Corresponding authors: Rui Henrique, MD, PhD & Carmen Jerónimo, PhD

Full mailing address: Portuguese Oncology Institute of Porto (IPOP), R. Dr. António Bernardino de Almeida, 4200-072, Porto, Portugal. *Tel:* +351 22 225084000; *Fax:* +351 225084199.

E-mail address: henrique@ipoporto.min-saude.pt; carmenjeronimo@ipoporto.min-saude.pt

ORCID ID:

José Pedro Sequeira: 0000-0002-4687-3347

João Lobo: 0000-0001-6829-1391

Vera Constâncio: 0000-0002-3151-0367

Tiago Brito-Rocha: 0000-0001-5852-4585

Isaac Braga: 0000-0001-9265-4324

Rui Henrique: 0000-0003-3171-4666

Carmen Jerónimo: 0000-0003-4186-5345

Abstract

Testicular germ cell tumors (TGCTs) are the most common cancers in young-adult males aged between 15-39 years. Hsa-miR-371a-3p is currently the most reliable biomarker for diagnosis and monitoring of these patients non-invasively in liquid biopsies, and it is destined to be introduced in the clinic due to improved performance compared to the classical serum tumor markers available. Current studies have focused on real-time quantitative PCR (RT-qPCR) protocols for its determination; still, some challenges remain, since these protocols often require preamplification steps (costly and time-consuming), and report relative levels normalized to a housekeeping microRNA, not always performed the same way. Droplet digital PCR (ddPCR) shows the promise to overcome these challenges, skipping normalization and preamplifications, but has hardly been explored in the field of TGCTs.

In this work, we provide a report of a ddPCR-based pipeline for quantification of hsa-miR-371a-3p (the DigiMir pipeline) and compare it with two RT-qPCR protocols. A total of 107 plasma samples were investigated in the validation setting. The DigiMir pipeline detected TGCTs in a manner representative of tumor burden, with a sensitivity and specificity of 94% and 100%, respectively, outperforming the combined sensitivity of all three classical serum tumor markers (61,5%). Therefore, in this proof-of-concept investigation, we have showed that DigiMir pipeline constitutes a new promising methodology for accurately reporting hsa-miR-371a-3p in the clinical setting.

Keywords

Testicular germ cell tumors; ddPCR; hsa-miR-371a-3p; RT-qPCR; liquid biopsies; diagnosis.

Introduction

MicroRNAs are small non-coding RNAs that are becoming more and more popular as biomarkers of disease, including cancer. They are interesting for clinical use in part due to their stability in bodily fluids, making them attractive non-invasive liquid biopsy biomarker candidates, but also due to ease of detection with relatively low-cost methodologies widely available, such as PCR-based ones ¹. These microRNAs are also dynamic and versatile, reflecting the status of disease and often being useful both for diagnostic, prognostic, and follow-up purposes. However, still, few of these promising microRNAs actually make it to full integration in the clinic, in part due to technological challenges related to detection and reporting ².

Testicular germ cell tumors (TGCTs) are among the most common solid neoplasms arising in young-adult Caucasian men ³. For these tumors, a set of microRNAs which regulate embryonic development have proved their value as accurate liquid biopsy biomarkers of the disease ⁴⁻⁶. Among them, the hsa-miR-371a-3p has shown the best clinical results, outperforming the classical serum tumor markers nowadays available in the routine [alpha fetoprotein (AFP), human chorionic gonadotropin (HCG) and lactate dehydrogenase (LDH)], which show important limitations ⁷⁻¹¹. Since the study of Voorhoeve et al in 2006 ¹², an overwhelming amount of evidence has built in the last decade, demonstrating the accuracy of hsa-miR-371a-3p, determined by real-time quantitative PCR (RT-qPCR), for the diagnosis and follow-up of TGCT patients (except for pure teratoma ¹³), with sensitivities and specificities mostly >90% ¹⁴⁻¹⁷. This microRNA has a short half-life, correlates with tumor burden, can reliably be detected in several bodily fluids, and is able to predict recurrences and viable tumor in post-chemotherapy masses ¹⁸⁻²⁷. The confirmation of these findings in large, prospective, multicentric studies increased even more the interest in this biomarker ^{28,29}, leading to organization of clinical trials (NCT03067181; NCT04435756) and proposals for introduction of a quantitative test in the clinic ^{30,31}.

However, there is still some room for attempting to improve such a test. An increased technical sensitivity is desirable for stage I patients with low tumor burden, sometimes missed by the hsa-miR-371a-3p test, not only for diagnosis but especially for early discrimination of patients at risk of relapsing, allowing for timely adjusting the therapeutic strategy (surveillance versus adjuvant chemotherapy), sparing young patients from unnecessary cytotoxic treatments ^{32,33}. Moreover, most protocols for determination of hsa-miR-371a-3p levels rely on preamplification steps, which may be argued to produce some variability related to increased cycling (besides being costly, time-consuming, and facilitating events of contamination and unspecific amplifications). Also, the commonly used

protocols rely on normalization to housekeeping microRNAs (variable from study to study), giving a relative quantification (as opposed to the absolute number of copies of the marker), and the method of normalizing and reporting RT-qPCR data differs among studies, raising the need for a consensus procedure and pipeline ^{31,34}.

In recent years, droplet digital PCR (ddPCR) has emerged as a new methodology for accurately quantifying liquid biopsy biomarkers and for detection of minimal residual disease ^{35,36}. DdPCR provides absolute quantification, obviating the need for normalization to housekeeping microRNAs and facilitating setting of cutoffs of positivity, and is less influenced by inhibitory substances, due to the partitioning process. However, its application for microRNA quantification is still largely unexplored [with few studies available ³⁷⁻⁴⁴], and only one very recent study attempted to apply such protocol to hsa-miR-371a-3p determination in TGCTs ⁴⁵.

In this work we describe a pipeline for quantification and reporting of hsa-miR-371a-3p in plasma samples of TGCT patients using ddPCR (*DigiMir test*) and provide a direct comparison with two other available RT-qPCR methods for quantification of this biomarker. We perform several technical optimizations of the ddPCR pipeline, which obviated the preamplification step, and finally validate our findings in a larger cohort of plasma samples.

Methods

Samples

A total of five plasma samples were included in the proof-of-concept phase of the study, where the three pipelines were compared and optimization of technique was performed: two stage I seminomas, one stage II embryonal carcinoma, one stage III embryonal carcinoma, and a young-adult male healthy blood donor.

After optimization of the ddPCR pipeline, a validation set of 107 plasma samples was investigated, comprising: 56 samples from TGCT patients (31 drawn right before orchiectomy; 25 in the context of routine follow-up); three samples from patients with non-TGCT testicular masses (two Leydig cell tumors and one Mullerian type tumor of the testis); 47 male healthy blood donors; and additionally one patient with an AFP-secreting hepatocarcinoma (representing the context of non TGCT-related AFP elevation). Of the 31 TGCT patients included in the study, all 31 had a pre-orchiectomy sample, six had one follow-up sample, eight had two follow-up samples and one patient had an additional intermediate sample, totalizing three follow-up samples. The median time from orchiectomy to the first follow-up samples was 6 months (interquartile range [IQR] = 8 months); the median time from orchiectomy to the second follow-up samples was 15 months (IQR = 7

months). Also, all blood samples coincided with routine determinations of classical serum markers AFP, HCG and LDH, which were available and compared to hsa-miR-371a-3p measurements.

All patients were diagnosed and treated at IPO Porto by the same multidisciplinary team. Patients with suspicion of other malignancies were excluded. After collection of peripheral blood into EDTA-containing tubes, plasma was separated centrifuging at 2,500 rpm for 30 min at 4°C, and subsequently stored at -80°C in the institutional tumor bank. All blood samples were processed within 4h maximum from collection. All clinical and histopathological data of the patients was reviewed by a TGCT-dedicated pathologist and according to most recent WHO 2016 classification and AJCC 8th edition staging manual ⁴⁶.

Complete description of the optimization and validation cohorts is provided on Table 1.

RNA Extraction

Total RNA was extracted from 100µL plasma and eluted in 50µL of elution buffer, using the MagMAX miRvana Total RNA Isolation kit (Thermo Fisher, A27828), according to manufacturer's protocol. As a technical control, the non-human synthetic spike-in ath-miR-159a (0.2µL per sample of a stock solution at 0.2nM) was added to the lysis buffer (with 5'-Phosphate modification for TaqMan Advanced microRNA protocol, see below).

Table 1 – Clinicopathological description of the optimization and validation cohorts.

Optimization cohort (n=5 samples)	
Cases	Description
Sample #1	37 years, Seminoma, Stage I
Sample #2	28 years, Seminoma, Stage I
Sample #3	37 years, Embryonal carcinoma, Stage II
Sample #4	34 years, Embryonal carcinoma, stage III
Sample #5	44 years, healthy blood donor
Validation cohort summary (n= 107 samples)	
TGCT samples	56
Pre-orchietomy	31
First follow-up timing	15
Second follow-up timing	9
Third follow-up timing	1
Non-TGCT testicular mass samples	3
Male healthy blood donors	47
Non-testicular tumor with elevated AFP (hepatocarcinoma)	1
TGCT patients – clinicopathological features	
Age (years [median, interquartile range])	33 (8.5)
Size of tumor mass (cm [mean, interquartile range])	5.7 (3.95)
Histology (n, %)	
Seminoma	19/31 (61.3)
Embryonal carcinoma	2/31 (6.5)

Mixed tumor	9/31 (29.0)
Postpubertal-type yolk sac tumor	1/31 (3.2)
Stage (n, %)	
I	19/31 (61.3)
II	6/31 (19.4)
III	6/31 (19.4)
AFP positive (n, %)	9/31 (29.0)
HCG positive (n, %)	12/31 (38.7)
LDH positive (n, %)	14/31 (45.2)
Either AFP or HCG or LDH positive (n, %)	20/31 (64.5)

Abbreviations: AFP – alpha fetoprotein; HCG – human chorionic gonadotropin; LDH – lactate dehydrogenase.

TaqMan Advanced (global) microRNA pipeline

Two microliters of isolated RNA were reverse transcribed and preamplified (14 cycles) using the Taqman Advanced hsa-miRNA cDNA synthesis (Thermo Fisher, A28007) in a Veriti™ 96-Well Thermal Cycler (Applied Biosystems™), following the manufacturer's protocol. Then, 2.5 µL of the diluted preamplification product were plated on 96-well plates and run on a QuantStudio 12K Flex platform using the following conditions: 5µL TaqMan Fast Advanced Master Mix (2x), 0.5µL of TaqMan Advanced hsa-miRNA Assay (20x) and 2µL RNase-free water; assays: ath-miR-159a – 478411_mir, FAM; hsa-miR-371a-3p – 478070_mir, FAM; hsa-miR-30b-5p – 478007_mir, VIC; run conditions: 95°C 20s followed by 40 cycles at 95°C 1s and 60°C 20s).

TaqMan (target-specific) microRNA pipeline

Five microliters of isolated RNA were reverse transcribed for the following pool of microRNAs (ath-miR-159a, hsa-miR-371a-3p and hsa-miR-30b-5p) using the TaqMan microRNA Reverse Transcription kit (Thermo Fisher, 4366596) in the same Veriti™ thermocycler, according to the protocol reported in ¹⁸. Next, 5µL of cDNA were preamplified (12 cycles) using the TaqMan Preamp Master Mix (Thermo Fisher, 4391128), and then eluted in 75µL bidistilled water. One microliter of the diluted preamplification product was plated on the same QuantStudio 12K Flex platform using the following conditions: 5µL 2x TaqMan Universal Master Mix no UNG, 0.5µL of TaqMan hsa-miRNA Assay (20x) and 3.5µL RNase-free water; assays: ath-miR-159a – 000338, FAM; hsa-miR-371a-3p – 002124, FAM; hsa-miR-30b-5p – 000602, VIC; run conditions: 50°C 2min, 95°C 10min, followed by 40 cycles at 95°C 15s and 60°C 1min).

Droplet Digital PCR (ddPCR): DigiMir pipeline

Five microliters of isolated RNA were reverse transcribed for the following pool of microRNAs (ath-miR-159a, hsa-miR-371a-3p) using the TaqMan microRNA Reverse Transcription kit (Thermo Fisher, 4366596) in the same Veriti™ thermocycler, according to the protocol reported in ¹⁸. DdPCR reactions were prepared as follows: 2µL (ath-miR-159a)

or 4 μ L (hsa-miR-371a-3p) of cDNA, 11 μ L ddPCR Supermix for probes (Bio-Rad, California, USA, #1863010), 1 μ L TaqMan hsa-miRNA Assay (20x) and 8 μ L (ath-miR-159a) or 6 μ L (hsa-miR-371a-3p) of bidistilled water; assays: ath-miR-159a – 000338, FAM and hsa-miR-371a-3p – 002124, FAM. Droplets were generated on the automated droplet generator QX200 AutoDG (Bio-Rad, California, USA) and read on the QX200 Droplet Reader (Bio-Rad, California, USA). The PCR run was set as follows: 95 $^{\circ}$ C 10min, 50 cycles of 94 $^{\circ}$ C 30s and 56 $^{\circ}$ C 1min – ramp rate 2 $^{\circ}$ C/s – and 98 $^{\circ}$ C 10min).

The limit of blank (LOB) and limit of detection (LOD) of the assays were calculated as indicated in ⁴⁷. The limit of quantification (LOQ) was assessed by performing a 2-fold dilution series of a TGCT sample for both miRNAs.

Quality control steps and statistics

Plasma samples were visually inspected, and no samples had obvious signs of hemolysis. Appropriate engineering and manual controls were used to prevent contaminations, including master mix made using a clean and UV-irradiated hood prior to adding any template, clean gloves, PCR reagents and consumables, and reactions performed in separate dedicated Labs. RNA was extracted from the seminoma-like cell line TCam-2 and used as a positive control for hsa-miR-371a-3p in all pipelines. No template control (NTC) and no enzyme control (NEC) were included in all cDNA synthesis and PCR stages, as negative controls. For ddPCR pipeline optimization, further negative controls (“no cDNA control”, “no Supermix control” and “no assay control”) were included, as recommended ⁴⁴. All RT-qPCR reactions were performed in triplicates, and those in ddPCR in duplicates. Results were plotted in GraphPad Prism 9. The thresholds of positivity of the hsa-miR-371a-3p and ath-miR-159a assays were defined based on LOD calculation, as determined below. Correlations were computed using the non-parametric Spearman correlation coefficient. Diagnostic performance of the DigiMir pipeline was assessed by calculating sensitivity, specificity, negative predictive value (NPV) and positive predictive value (PPV) for diagnosis of TGCT.

A diagram of the study protocol is provided in Figure 1.

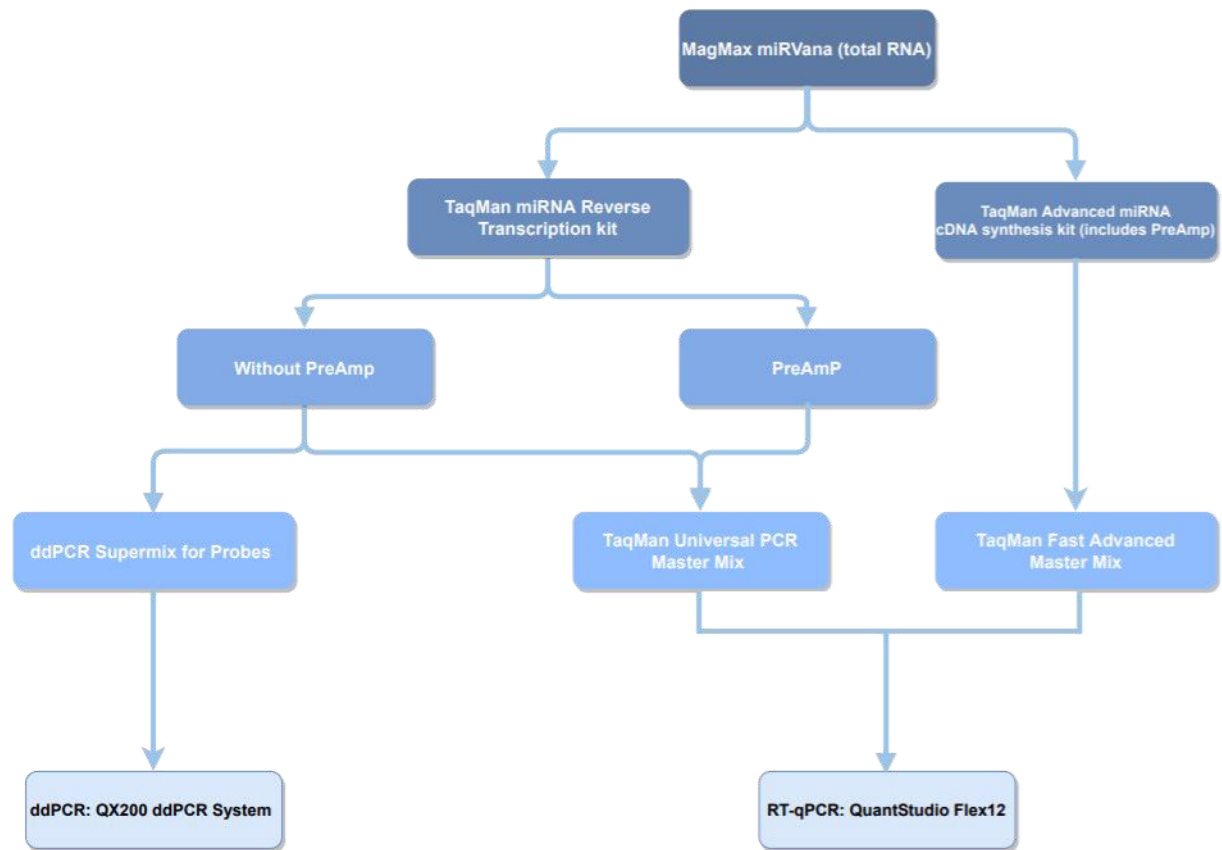


Figure 1 – Diagram of the study protocol, including RT-qPCR and ddPCR pipelines. Abbreviations: ddPCR – droplet digital PCR; preamp – preamplification; RT-qPCR – real-time quantitative PCR

Results

Optimization phase and comparison of pipelines

Input and temperature settings

We first optimized the input of the PCR reactions, specifically in the TaqMan (target-specific) microRNA protocol. We found no remarkable differences in Ct values obtained for synthetic ath-miR-159a when using either 1 μ L or 2 μ L of cDNA as input (Cts 13.940-14.285 and 13.873-14.130).

For the DigiMir pipeline, and to achieve accurate separation of positive and negative droplets for the ath-miR-159a, the optimal input was determined to be 2 μ L, which rendered an optimal number of positive droplets - Figure 2A). The optimal input for hsa-miR-371a-3p was determined to be 4 μ L, which rendered more positive droplets when compared to 2 μ L and 3 μ L and, approximately, the same positive droplets when compared to 5 μ L and 6 μ L.

These optimized input conditions were used for the following tasks.

A temperature gradient (56-62°C) was then run to further optimize the droplet separation of the protocol. We verified that a temperature around 56°C (55.7 °C) provided the best separation (less rain) and highest amplitude for both ath-miR-159a and hsa-miR-371a-3p, and this was set for the validation study (Figure 2B, respectively). The optimal amplitude thresholds of 2500 were applied to achieve maximal separation for both ath-miR-159a and hsa-miR-371a-3p.

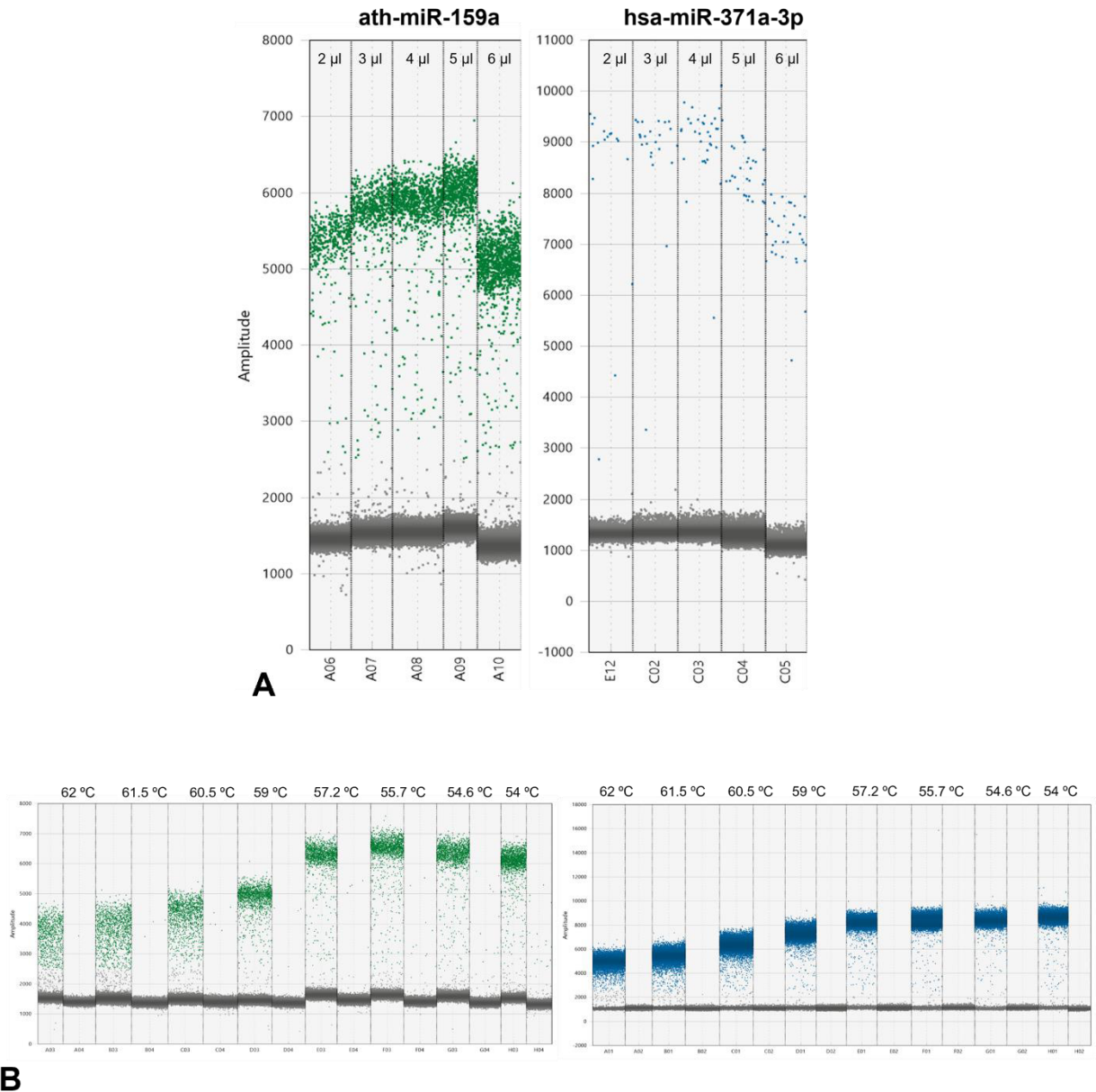


Figure 2 – A - Optimization of DigiMir pipeline. Ath-miR-159a and hsa-miR-371a-3p input optimization. B - Temperature gradient for further optimization of ath-miR-159a (green) and hsa-miR-371a-3p (blue) assays on the DigiMir pipeline. Notice that the best separation is achieved around 56°C for both assays.

Controls, sensitivity, and specificity

Related to non-specific amplifications with both RT-qPCR-based protocols, we found the TaqMan Advanced (global) microRNA pipeline to result in “undetermined” Ct for the healthy blood donor (and in the TCam-2 sample, which was not spiked-in with the synthetic oligo), but to produce sporadic late amplifications for ath-miR-159a in the NTC inserted on cDNA synthesis (Ct 33.3) and for hsa-miR-30b-5p in the NEC (Ct 37.5).

For the TaqMan (target-specific) microRNA protocol, in the runs performed for optimization, we could detect non-specific late amplification for the hsa-miR-371a-3p in the male healthy blood donor (Ct 30.5) and in the NTC inserted on cDNA synthesis (Ct 38). Also, non-specific amplifications were detected for both hsa-miR-30b-5p and ath-miR-159a in the NTC inserted in cDNA synthesis (Ct 32 and Ct 29.5, respectively) and in the NEC (Ct 34 for both). The ath-miR-159a also rendered a non-specific late amplification in the non-spiked-in TCam-2 sample (Ct 38).

For the DigiMir protocol and using the thresholds of positivity defined below for both hsa-miR-371a-3p and ath-miR-159a, the healthy male blood donor sample was negative for the hsa-miR-371a-3p. The remaining negative controls (NTCs, NECs, and additionally “no cDNA control”, “no Supermix control” and “no assay control”) were consistently negative for hsa-miR-371a-3p and for ath-miR-159a considering the calculated LOB.

As for the TCam-2 positive control, the TaqMan Advanced (global) microRNA pipeline detected hsa-miR-371a-3p at Ct 14.5, while an earlier Ct of 8 was produced with the TaqMan (target-specific) microRNA protocol. For the DigiMir pipeline, and to achieve accurate separation of positive and negative droplets, TCam-2 serial dilutions were performed, with the best separation being set at 1:50 (Figure 3).

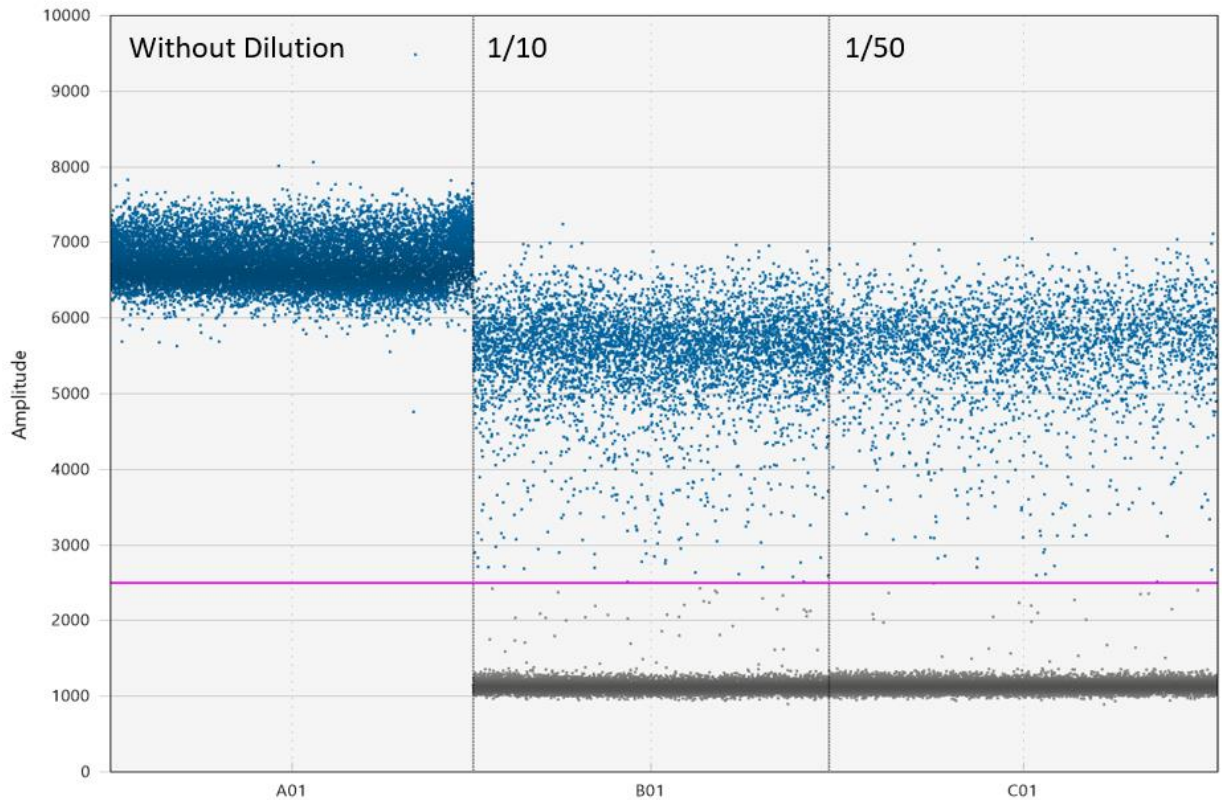


Figure 3 – Optimization of DigiMir pipeline. Best separation of positive and negative droplets in the hsa-miR-371a-3p TCam-2 positive control with 1:50 dilution. Notice that there is no separation of droplets in the undiluted sample.

Related to ability of detection of small burden stage I disease, we verified that with the TaqMan Advanced (global) microRNA pipeline we could only detect hsa-miR-371a-3p in one of the two stage I seminoma samples (Figure 4A). There was a positive correlation with tumor burden, with higher relative levels being detected in stage III compared to stage II and stage I disease.

However, both stage I samples could be detected with TaqMan (target-specific) microRNA protocol and with ddPCR pipeline (Figure 4B-D). A positive correlation with tumor burden was also shown by both protocols, with higher levels in stage III compared to stage II and I (Figure 4D for the ddPCR pipeline and Figure 4E for RT-qPCR).

We also performed the TaqMan (target-specific) microRNA protocol omitting the preamplification step, with 2 μ L input in the PCR run. The stage III sample was detected (Ct 30.0), but both the stage I and II samples gave only late amplifications (Ct >34), evidencing the reduced sensitivity for detecting low burden disease without preamplification in the RT-qPCR method (Figure 4F).

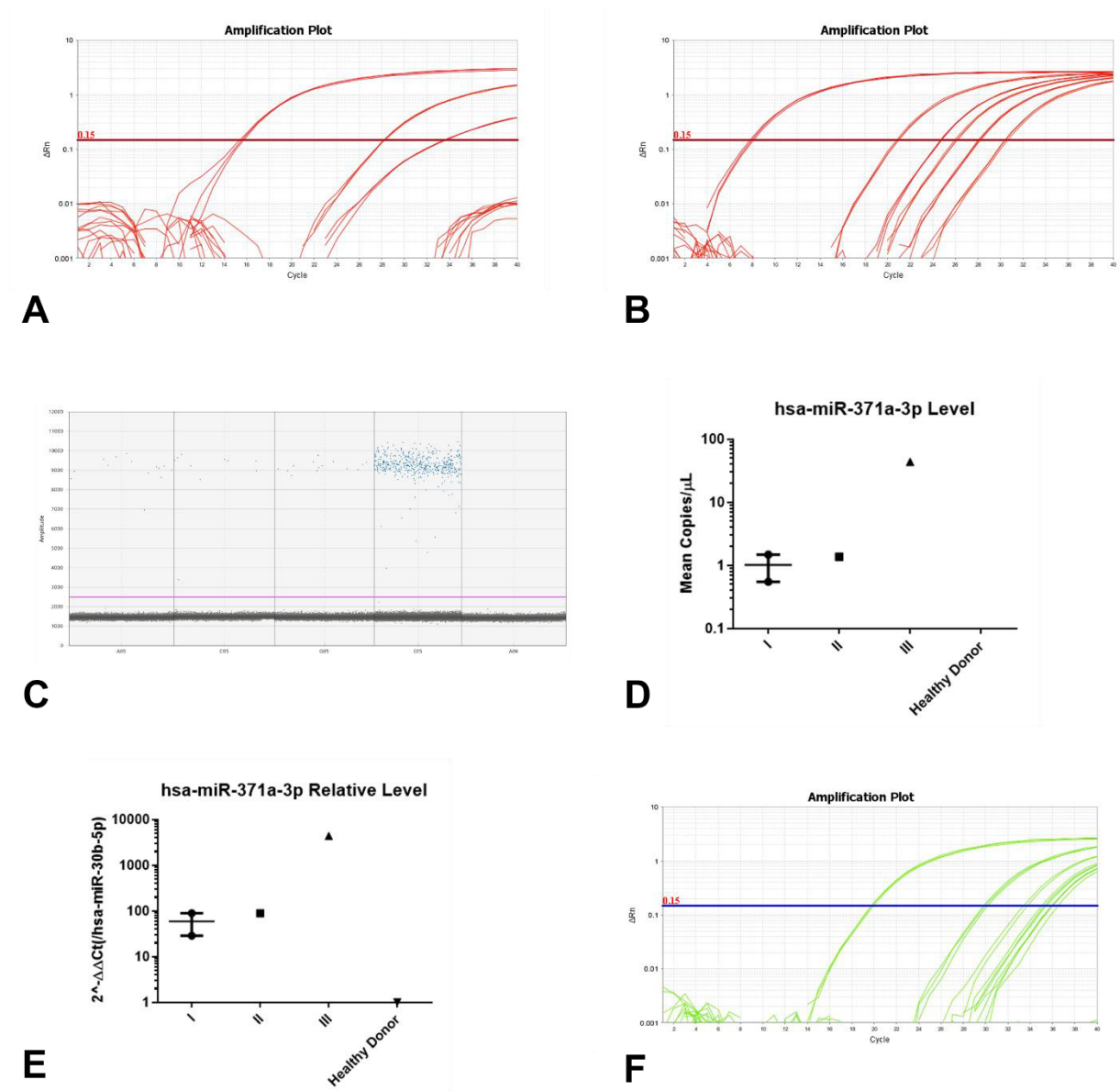


Figure 4. Detection of patient samples by PCR methodologies. A – Detection of samples of the optimization phase using the TaqMan Advanced (global) microRNA pipeline. Notice amplification of positive control TCam-2, followed by the stage III patient and one of the stage I patients. The remaining two patients (and the healthy blood donor) do not amplify; B – Detection of the same samples using the TaqMan (target-specific) microRNA pipeline. Notice the overall earlier amplification of all samples. The positive control TCam-2 is detected, followed by all patient samples (stage III, stage I, stage II and stage I from left to right). However, the healthy blood donor also shows amplification (curve most to the right); C – Detection of the same samples using the ddPCR pipeline. Notice the overall amplification of all samples. All patient samples (stage I, stage I, stage II, stage III and healthy donor from left to right) amplified; D – Absolute levels of hsa-miR-371a-3p using the ddPCR pipeline; E – Relative levels of hsa-miR-371a-3p, normalized to hsa-miR-30b-5p levels, using the TaqMan (target-specific) microRNA pipeline; F – Same samples and protocol used in B, but omitting the preamplification step. Notice that all samples amplify later, and only the TCam-2 and the stage III patient (curves most to the left, respectively) are detected with a Ct value lower than 34.

Variability and Precision

For assessing variability of the three pipelines, we defined four experimental settings: “Setting #1”, with cases being extracted in two distinct timings; “Setting #2”, where the same extraction was always used but cases were submitted to two different cDNA syntheses; “Setting #3”, with samples deriving from the same extraction and cDNA synthesis, but with two different operators plating the PCR reaction; and “Setting #4”, same as Setting #3 but with the same operator plating the PCR reaction twice, on two distinct occasions (Figure 5)

The TaqMan Advanced (global) microRNA pipeline showed the highest variability between the various experimental settings, as observed in Figure 5A-C. This included the assessment of the non-human spike-in ath-miR-159a, which had poorer recovery (later Ct range) when compared to the TaqMan (target-specific) microRNA protocol and resulted in higher variability in spike-in detection among samples. The overall higher reproducibility of the TaqMan (target-specific) microRNA protocol is evidenced in Figure 5D-F.

For the DigiMir pipeline, ath-miR-159a was well recovered in all samples (Figure 5G) and hsa-miR-371a-3p was detected in all experimental instances, illustrating tumor burden (with higher detection in the stage III sample) and being negative (below the threshold of positivity) for the healthy blood donor (Figure 5H).

When comparing the results for hsa-miR-371a-3p quantification between the various experimental settings, a strong positive correlation was found for all instances (Figure 6A-L). Additionally, when comparing the quantification of hsa-miR-371a-3p using the TaqMan (target-specific) microRNA protocol with the one obtained with the DigiMir pipeline, a strong positive correlation between hsa-miR-371a-3p relative levels (normalized to hsa-miR-30b-5p) and absolute copies/ μ L was obtained (Figure 6M).

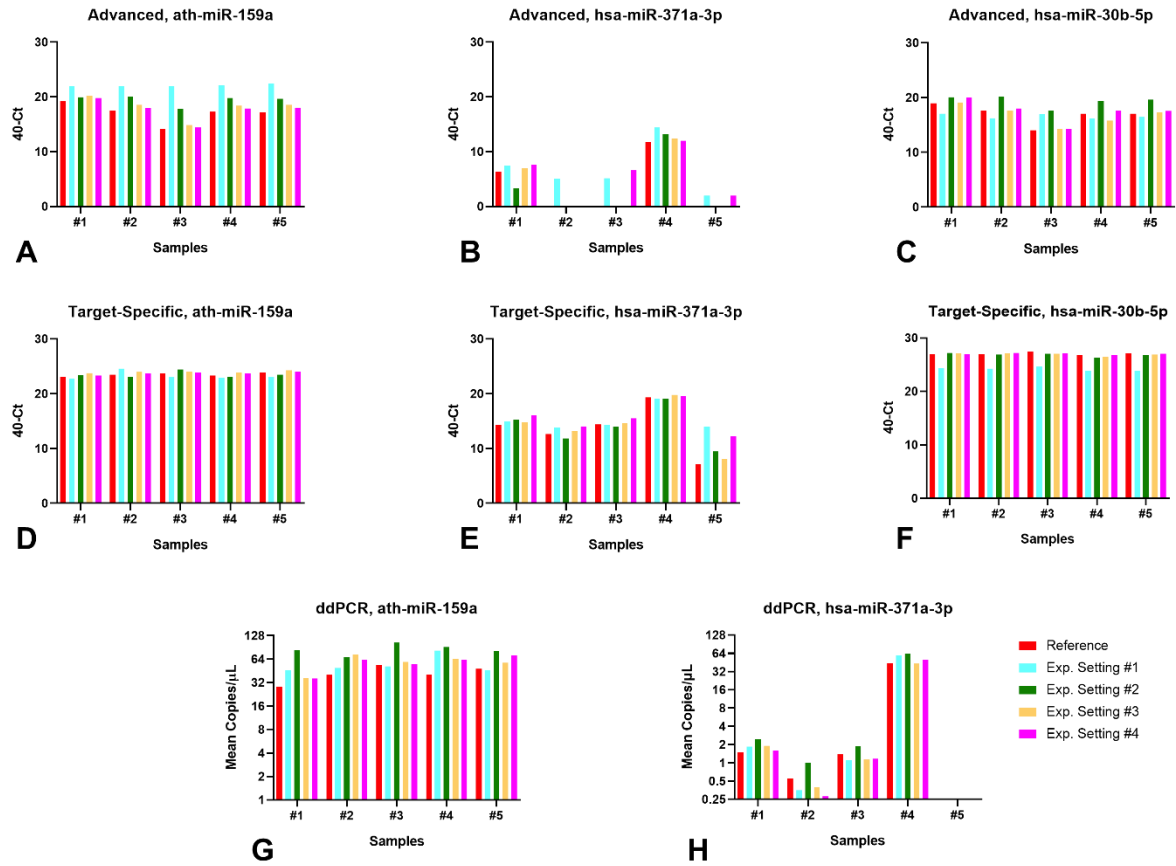


Figure 5 – Comparison of pipelines. A-C: TaqMan Advanced (global) microRNA pipeline; D-F: TaqMan (target-specific) microRNA pipeline; G-H: DigiMir pipeline. The x-axis represents the samples used for the optimization phase: #1 and #2 – stage I seminomas; #3 – stage II embryonal carcinoma; #4 – stage III embryonal carcinoma; #5 – age-matched healthy blood donor. The color code refers to experimental settings: setting #1 – different extraction; setting #2 – different cDNA synthesis; setting #3 – different operator; setting #4 – same operator; and reference for comparison.

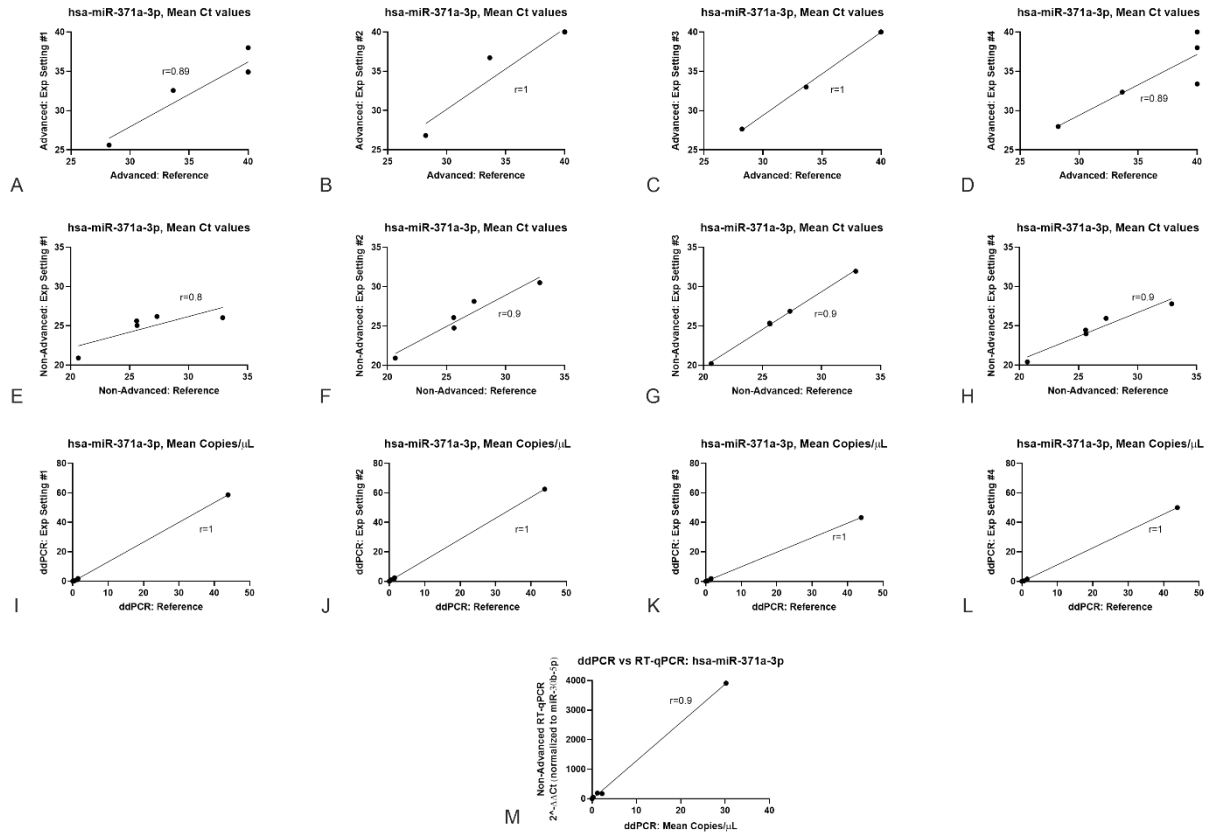


Figure 6 – Correlation between hsa-miR-371a-3p quantifications. A-D: TaqMan Advanced (global) microRNA pipeline; E-H: TaqMan (target-specific) microRNA pipeline; I-L: DigiMir pipeline; M – correlation between the DigiMir pipeline and the TaqMan (target-specific) microRNA pipeline quantifications (the latter normalized to hsa-miR-30b-5p and using the $2^{-\Delta\Delta C_t}$ method).

Further optimization of ddPCR protocol

For determining the LOB and LOD, 30 NTC samples inserted in the cDNA synthesis step were run for both hsa-miR-371a-3p and ath-miR-159a. The LOB of the hsa-miR-371a-3p was then determined to be 3 droplets, meaning a LOD of 5 droplets. The LOB of ath-miR-159a was determined to be 14 droplets, meaning a LOD of 21 droplets. The LODs of the assays were set as thresholds of positivity for the corresponding assays in this pipeline.

For calculating the actual LOQ (allowing for precise quantification of the absolute number of copies present in the sample), 2-fold dilutions series of a positive case were performed as indicated above. The LOQ was determined to be 18.4 copies/ μ L for ath-miR-159a and 1.17 copies/ μ L for hsa-miR-371a-3p (Figure 7).

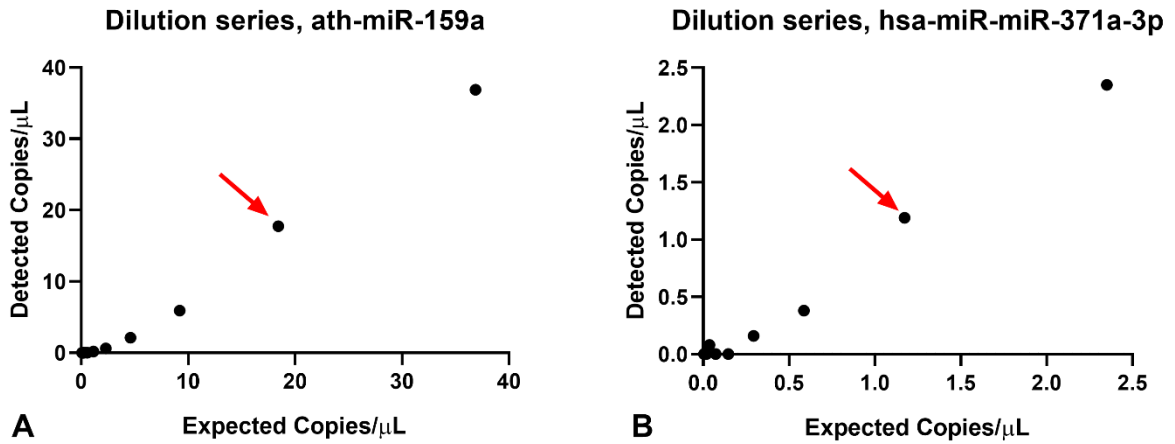


Figure 7 – Limit of quantification of ath-miR-159a (A) and hsa-miR-371a-3p (B) assays. The red arrow points to the number of copies that the assay can still reliably quantify.

A summary of the comparison among the three protocols is provided in Table 2.

Clinical validation of the DigiMir pipeline

There were 19 seminoma and 12 non-seminoma samples. The median age of the TGCT patient cohort was 33 years, and the one of the male healthy blood donors was 46 years. Most patients were stage I TGCTs (61.3%). AFP, HCG and LDH were elevated at time of diagnosis (pre-orchietomy) in 29%, 38.7% and 45.2% of patients. Elevation of any of the classical serum tumor markers was found in 64.5% of TGCT patients (Table 1).

Using the DigiMir pipeline, hsa-miR-371a-3p outperformed the classical serum tumor markers, achieving sensitivity of 93.6%, specificity of 100%, NPV of 96%, PPV of 100% and accuracy of 97.5% for identifying TGCT patients in the pre-orchietomy setting. No healthy blood donors showed detectable hsa-miR-371a-3p above the defined cutoff, and only two TGCT patients were negative for hsa-miR-371a-3p, corresponding to two seminomas (also negative for all three classical serum tumor markers). Additionally, the three non-TGCT testicular masses were negative for hsa-miR-371a-3p, as was the hepatocarcinoma patient with elevated AFP. Hsa-miR-371a-3p levels were significantly positively correlated with levels of HCG, LDH and tumor size ($r=0.57$, $p<0.001$; $r=0.544$, $p=0.002$; and $r=0.475$, $p=0.007$, respectively).

Regarding the follow-up samples of TGCT patients, they were all negative in patients with no signs of disease after the orchietomy, with normalization of classical serum tumor markers and negative imaging scans. Of notice, the single patient with stage III and S1 disease after orchietomy (with persistent HCG elevation) also showed elevation of hsa-miR-371a-3p 10 days after the orchietomy. The patient was treated with 4xBEP but

showed only partial response and is now with disease progression (elevation of AFP, HCG, and *de novo* supraclavicular lymphadenopathies). One patient with a seminoma but with slight AFP elevation pre- and post-orchietomy (interpreted clinically as a constitutional elevation of this marker) was decided to put on surveillance; remarkably, the hsa-miR-371a-3p was negative in the post-orchietomy follow-up samples of this patient.

Table 2 – Summary of the three different pipelines for comparing hsa-miR-371a-3p

Variables	MagMax miRvana extraction, spike in ath-miR-159a, 100µL plasma		
	Thermo Fisher, Advanced (global)	Thermo Fisher, non-Advanced (targeted)	DigiMir, BioRad (targeted)
Preamp: <i>Room for bias / variability</i> <i>Extra step – time consuming</i> €€	Mandatory (part of the protocol)	Detection of hsa-miR-371a-3p with preamp; low detection without preamp	Accurate detection of hsa-miR-371a-3p <u>without</u> preamp with 4µL cDNA
Volumes of reactions	No difference in Cts between using 1µL or 2µL (ath-miR-159a: Cts 13.423-14.379 and 13.453-13.774) Need for triplicates	No difference in Cts between using 1µL or 2µL (ath-miR-159a: Cts 13.940-14.285 and 13.873-14.130) Need for triplicates	More sensitivity with 4µL Duplicates suffice
Spike-in recovery	Higher variability, poorer recovery (higher Cts) 0.2µL of 1nM	Lower variability, better recovery (lower Cts) 0.2µL of 1nM	Good recovery 0.2µL of 0.2nM
Normalization to housekeeping (miR-30b-5p)	Needed Relative quantification (delta delta Ct method or standard curve)	Needed Relative quantification (delta delta Ct method or standard curve)	Not needed Precise absolute number of copies/µL
Healthy blood donor (related to clinical specificity)	Hsa-miR-371a-3p: Undetermined	Hsa-miR-371a-3p: Sporadic amplification	Hsa-miR-371a-3p: Negative
Detection of stage I SE (related to clinical sensitivity)	+/- (1/2)	+ (2/2)	+ (2/2)
Representation of tumor burden	Yes (stage III >>> stage I)	Yes (stage III >>> stage I)	Yes (stage III >>> stage I)
Variability: <i>Intra-operator</i> <i>Inter-operator</i> <i>Inter-synthesis</i> <i>Inter-extractions</i>	Overall poorer	Adequate	Adequate

NTC inserted on cDNA synthesis	Hsa-miR-371a-3p: Undetermined ath-miR-159a: sporadic amplification (Ct +-33.3)	Hsa-miR-371a-3p: sporadic late amplification (Ct 38) ath-miR-159a: late amplification (Ct +-29.5)	Hsa-miR-371a-3p: Negative ath-miR-159a: Negative
NEC inserted on cDNA synthesis	Hsa-miR-371a-3p: Undetermined ath-miR-159a: Undetermined	Hsa-miR-371a-3p: Undetermined ath-miR-159a: sporadic amplification (Ct +-34.0)	Hsa-miR-371a-3p: Negative (“no cDNA control”, “no Supermix control” and “no assay control” Negative)
NTC inserted on PCR step (plate)	Hsa-miR-371a-3p: Undetermined Hsa-miR-30b-5p: Undetermined ath-miR-159a: Undetermined	Hsa-miR-371a-3p: Undetermined Hsa-miR-30b-5p: Undetermined ath-miR-159a: Undetermined	Hsa-miR-371a-3p: Negative ath-miR-159a: Negative
Positive control (TCam-2)	Adequate Hsa-miR-371a-3p: Cts +-14.5	Adequate Hsa-miR-371a-3p: Cts +-8	Adequate Hsa-miR-371a-3p: optimal dilution for separation is 1:50

A summary of the several steps undertaken for optimization of the DigiMir pipeline are illustrated in Figure 8.

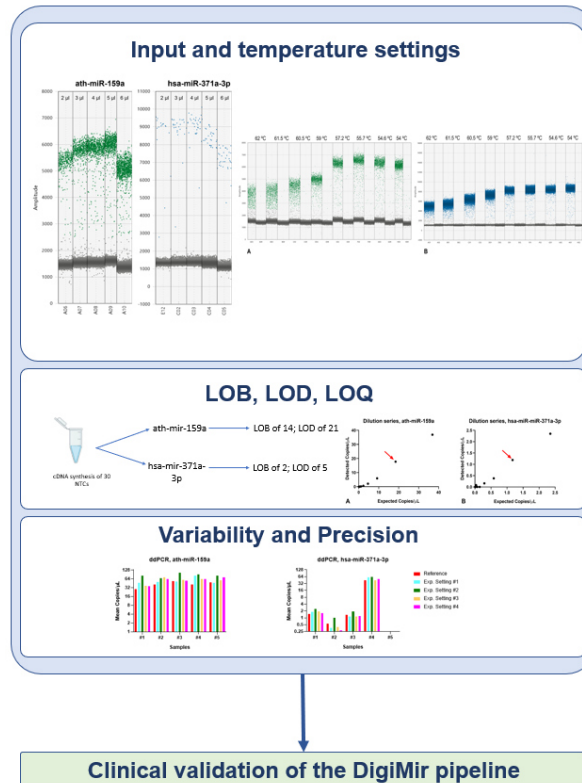


Figure 8 – DigiMir pipeline optimization steps.

Discussion

In this work we describe a pipeline for quantifying the most remarkable liquid biopsy biomarker in the field of TGCTs based on ddPCR, being approximately 3 times cheaper than RT-qPCR-based techniques. In fact, and despite an increase interest on ddPCR for accurately determining biomarkers in samples with low burden and low input (like in circulating markers such as microRNAs and cell-free DNA in plasma), few studies have procured to invest on microRNA detection using this technology ⁴², perhaps because the more conventional RT-qPCR-based techniques have been performing well in this task, at low cost and with more disseminated know-how. DdPCR has emerged as a very robust way to determine mutation status in circulation ⁴⁸, and also as a way to study DNA methylation patterns in circulating cell-free DNA ⁴⁹. Studies on microRNAs are very recent, and report different protocols for achieving distinct needs. Tavano et al reported a protocol for determining hsa-miR-1290 for diagnosis of pancreatic cancer in plasma using ddPCR ³⁷, with this method being superior to routine CA19-9 determination, while Zhao and collaborators investigated ddPCR for determining a panel of microRNAs diagnostic of gastric cancer ⁴⁰. Campomenosi and co-workers compared RT-qPCR with ddPCR for assessment of several microRNAs in serum of lung cancer patients and demonstrated a strong positive correlation between the two techniques, with equal or smaller variation in the ddPCR approach ³⁸. This high concordance between the two methods reported by the authors led us to seek a similar methodological approach for our study. Indeed, we have performed back-to-back comparison of three independent pipelines for quantifying hsa-miR-371a-3p. Two of the protocols were RT-qPCR-based (the TaqMan Advanced method, where a global microRNA synthesis with preamplification is performed, and the TaqMan non-Advanced method, with targeted microRNA synthesis for the desired microRNAs and preamplification). While both pipelines produced similar results, the TaqMan Advanced methodology (less reported in literature specifically in the field of TGCTs ²³) produced more variability in recovery of non-human spike-in ath-miR-159a and resulted in lower sensitivity of detection of low burden stage I cases. We hypothesize this could be explained by the global preamplification (instead of targeted reaction), interfering with sensitivity of detection ⁵⁰. For these reasons, the targeted approach for cDNA synthesis was considered more reliable and was chosen to translate into ddPCR quantification. Nevertheless, both RT-qPCR protocols detected hsa-miR-371a-3p in a manner consistent with disease burden, with the stage III patient rendering higher levels of hsa-miR-371a-3p.

In this work we attempted to omit the preamplification stage by stepping-up to the ddPCR methodology. Preamplification may theoretically introduce bias by increased cycling and is cumbersome and frequently the most expensive section of the experimental protocols, but is highly adopted in most recent works in the field (as summarized in ³¹), only not performed

in older works⁹, because of increasing sensitivity of detection of low amounts of circulating microRNA, such as in stage I small tumors. However, it can also elicit sporadic detection of trace amounts of hsa-miR-371a-3p in teratoma-only cases or even in healthy subjects, which are undesirable and create discomfort with reporting the results – also evidenced in this work. In this study, we have optimized the DigiMir pipeline (after fulfilling ddPCR technical requirements and precision assessment, such as assuring the greatest separation of positive and negative droplets, temperature gradient, LOB and LOD calculation, dilution series, as required and reported^{39,41,44}) and were able to quantify hsa-miR-371a-3p absolute copy number in a manner consistent with tumor burden (higher in stage III), with all negative controls and the healthy blood donor being below the threshold of positivity, hence being considered negative.

We designed experimental settings to illustrate variability in quantification of microRNAs with the three distinct pipelines, again with the TaqMan Advanced RT-qPCR protocol demonstrating to be poorer, with higher variability in results upon the various repetitions of the run under different conditions. Shifting to ddPCR, recovery of spike-in was homogeneous among samples (within the range reported in³⁹) and variability of detection of hsa-miR-371a-3p was acceptable, with a strong positive correlation found between the amounts determined at varied moments (like reported also in³⁹). Most importantly, like Campomenosi³⁸, we too found the quantification results by RT-qPCR (normalized to housekeeping hsa-miR-30b-5p) and those of ddPCR (with the advantage of obviating normalization) to be strongly positively correlated.

Then, in an early attempt to provide clinical validation, we have applied the defined DigiMir pipeline to a set of 107 plasma samples, including those from TGCT patients, non-TGCT testicular masses, healthy male blood donors and one patient with AFP secretion due to a hepatocarcinoma. Remarkably, hsa-miR-371a-3p identified all but two TGCT patients (which were also negative for AFP, HCG and LDH), and correctly discriminated all 47 healthy blood donor male individuals as negative. The resultant specificity of 100% and a sensitivity of 94% is similar or even superior to the one reported in previous RT-qPCR-based studies⁵¹ (summarized in³⁴), outperforming the combined sensitivity of the three classical serum tumor markers (61.5%). Indeed, there were 11 TGCTs negative for all three classical serum tumor markers available in routine, that were however detected by our assay, representing an important clinical benefit in diagnosis. Furthermore, as additional negative controls from a clinical standpoint, the three non-TGCT testicular masses were negative for hsa-miR-371a-3p, a point in favor of the specificity of our assay. Non-TGCT masses are not infrequent and constitute an important differential diagnosis of TGCTs, that can however only be confirmed after orchiectomy is performed⁵². Importantly, for small

benign tumors, partial orchiectomy may be an option, allowing to spare fertility and function of the testis ⁵³. A large study already reported that such masses are negative for hsa-miR-371a-3p by RT-qPCR ⁵⁴, and we show the same by ddPCR approach. Additionally, our assay has proved useful in clarifying elevations of AFP due to other causes rather than TGCTs, as has been recently reported for RT-qPCR ⁵⁵. The patient with important elevation of AFP due to a hepatocarcinoma was negative (with 0 copies) for hsa-miR-371a-3p. Also, of interest, a seminoma patient showed elevation of AFP pre-operatively, which he maintained post-orchiectomy and during follow-up. The elevation was interpreted clinically as constitutional since no further disease could be identified, but caused discomfort in clinical decisions, especially for the decision to put the patient on surveillance only. In this setting, our hsa-miR-371a-3p assay would have been useful to the clinic, since it was positive at pre-orchiectomy (due to the presence of the seminoma), but completely negative (0 copies) after orchiectomy despite the persistence of AFP, confirming that the elevation was constitutional or derived from other cause.

Finally, we also tested an additional setting of relevance which is the one of follow-up of these patients ⁵⁶. Follow-up routinely involves repeat measurements of classical serum tumor markers (which show important limitations in detecting relapses) and continuing imaging (both costly, with limited sensitivity for very small metastatic deposits and exposing young patients to radiation if computed tomography is performed ^{30,57,58}). In this sense, hsa-miR-371a-3p measurements are attractive for adequate monitoring and for guiding treatment decisions ³⁴. In our study, all follow-up samples from patients showing disease resolution and no signs of disease recurrence (negative imaging and classical serum tumor markers) were negative for hsa-miR-371a-3p, while the follow-up sample of a patient with stage III S1 disease was positive.

The data we present is overall corroborated by the very recent study of Myklebust et al ⁴⁵, who also describe a ddPCR pipeline for determining hsa-miR-371a-3p. However, there are important differences in methodology between the two studies: (1) whereas they used serum, we tested plasma samples, which may have an impact in microRNAs determination, namely on the levels of the housekeeping microRNA miR-30b-5p ¹⁸; (2) the RNA extraction kits and methodologies differed; and (3) Myklebust and co-workers did not include a spike-in (technical control) in their experimental setting, whereas, in our pipeline, spike-in recovery was demonstrated in all experiments as quality control (ath-miR-159a). Nevertheless, the main results of both studies completely concur in that ddPCR is a promising new methodology for reporting hsa-miR-371a-3p, with high sensitivity (89% for the authors and 94% in our study) and specificity (100% in both works) and associating with tumor burden. Additionally, both investigations report a good correlation and technical performance in

comparison with RT-qPCR, having the advantage of obviating the preamplification step and allowing to report absolute copy numbers (without need of a standard curve) in a clinical setting. In our view, this further supports the relevance of our findings and suggests that the DigiMir pipeline will be also useful in the follow-up setting. Validation in larger cohorts of TGCT patients on surveillance, like performed in other studies³³, are warranted and would definitely contribute to clarify the clinical utility of our assay.

To conclude, in this proof-of-concept investigation we describe a methodology to quantify the most relevant liquid biopsy biomarker of TGCTs in plasma samples, disclosing adjustments to the protocol and technologies that can make the quantification less variable and more precise, achieving an accuracy of 97.5% in a validation cohort of 107 samples. Further investigations and validation of the protocol are warranted in different clinical contexts, like follow-up of stage I patients on active surveillance or determination of viable germ cell malignancy in the post-chemotherapy metastatic context, to better personalize treatment and monitoring of TGCT patients⁵⁹.

Declarations

Ethics approval and consent to participate: This study was approved by the Ethics Committee (CES-IPO-12-018) of Portuguese Oncology Institute of Porto, Portugal. All procedures performed in tasks involving human participants were in accordance with the ethical standards of the institutional and/or national research committee and with the 1964 Helsinki declaration and its later amendments or comparable ethical standards.

Author contributions: JPS, JL and VC performed molecular analyses and wrote the manuscript. JL collected the clinical data. TB-R assisted in specific tasks related to molecular analyses. JPS, JL and VC analyzed the data. CC-M processed clinical samples. JM provided clinical information about the patients. RH and CJ supervised the work and revised the manuscript. All authors read and approved the manuscript.

Consent for publication: Not applicable.

Availability of data and materials: All data generated or analyzed during this study are included in this article.

Competing interests: The authors declare that they have no competing interests.

Funding: The authors would like to acknowledge the support of the Programa Operacional Competitividade e Internacionalização (POCI), in the component FEDER, and by national funds (OE) through FCT/MCTES, in the scope of the project EpiMarkGermCell (PTDC/MEC-URO/ 29043/2017). The authors would also like to acknowledge the support of MSD (“Prémio de Investigação em Saúde”), Banco Carregosa / Secção Regional do

Norte da Ordem dos Médicos (SRNOM) and Fundação Rui Osório de Castro / Millennium bcp. JL is recipient of a fellowship from FCT - Fundação para a Ciência e Tecnologia— (SFRH/BD/132751/2017). VC received the support of a fellowship from “la Caixa” Foundation (ID 100010434). The fellowship code is LCF/BQ/DR20/11790013.

Acknowledgements: We thank to ThermoFisher Scientific/Alfagene for the useful technical support.

References

- 1 Condrat, C. E. *et al.* miRNAs as Biomarkers in Disease: Latest Findings Regarding Their Role in Diagnosis and Prognosis. *Cells* **9**, doi:10.3390/cells9020276 (2020).
- 2 Cacheux, J., Bancaud, A., Leichle, T. & Cordelier, P. Technological Challenges and Future Issues for the Detection of Circulating MicroRNAs in Patients With Cancer. *Front Chem* **7**, 815, doi:10.3389/fchem.2019.00815 (2019).
- 3 Cheng, L. *et al.* Testicular cancer. *Nat Rev Dis Primers* **4**, 29, doi:10.1038/s41572-018-0029-0 (2018).
- 4 Lobo, J., Gillis, A. J. M., Jeronimo, C., Henrique, R. & Looijenga, L. H. J. Human Germ Cell Tumors are Developmental Cancers: Impact of Epigenetics on Pathobiology and Clinic. *Int J Mol Sci* **20**, doi:10.3390/ijms20020258 (2019).
- 5 Murray, M. J. *et al.* Identification of microRNAs From the miR-371~373 and miR-302 clusters as potential serum biomarkers of malignant germ cell tumors. *Am J Clin Pathol* **135**, 119-125, doi:10.1309/AJCPOE11KEYZCJHT (2011).
- 6 Palmer, R. D. *et al.* Malignant germ cell tumors display common microRNA profiles resulting in global changes in expression of messenger RNA targets. *Cancer Res* **70**, 2911-2923, doi:10.1158/0008-5472.CAN-09-3301 (2010).
- 7 Dieckmann, K. P. *et al.* MicroRNAs miR-371-3 in serum as diagnostic tools in the management of testicular germ cell tumours. *Br J Cancer* **107**, 1754-1760, doi:10.1038/bjc.2012.469 (2012).
- 8 Belge, G., Dieckmann, K. P., Spiekermann, M., Balks, T. & Bullerdiek, J. Serum levels of microRNAs miR-371-3: a novel class of serum biomarkers for testicular germ cell tumors? *Eur Urol* **61**, 1068-1069, doi:10.1016/j.eururo.2012.02.037 (2012).
- 9 Gillis, A. J. *et al.* Targeted serum miRNA (TSmiR) test for diagnosis and follow-up of (testicular) germ cell cancer patients: a proof of principle. *Mol Oncol* **7**, 1083-1092, doi:10.1016/j.molonc.2013.08.002 (2013).
- 10 Syring, I. *et al.* Circulating serum miRNA (miR-367-3p, miR-371a-3p, miR-372-3p and miR-373-3p) as biomarkers in patients with testicular germ cell cancer. *J Urol* **193**, 331-337, doi:10.1016/j.juro.2014.07.010 (2015).

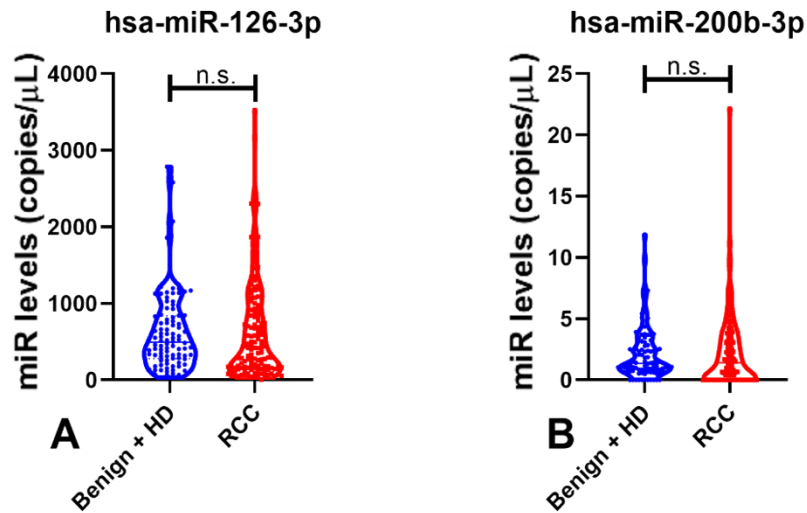
- 11 van Agthoven, T. & Looijenga, L. H. J. Accurate primary germ cell cancer diagnosis using serum based microRNA detection (ampTSmiR test). *Oncotarget* **8**, 58037-58049, doi:10.18632/oncotarget.10867 (2017).
- 12 Voorhoeve, P. M. *et al.* A genetic screen implicates miRNA-372 and miRNA-373 as oncogenes in testicular germ cell tumors. *Cell* **124**, 1169-1181, doi:10.1016/j.cell.2006.02.037 (2006).
- 13 Christiansen, A., Lobo, J. & Fankhauser, C. D. Re: Lucia Nappi, Marisa Thi, Nabil Adra, *et al.* Integrated Expression of Circulating miR375 and miR371 to Identify Teratoma and Active Germ Cell Malignancy Components in Malignant Germ Cell Tumors. *Eur Urol* 2021;79:16-9. *Eur Urol* **80**, e35-e36, doi:10.1016/j.eururo.2021.03.032 (2021).
- 14 Dieckmann, K. P. *et al.* Serum Levels of MicroRNA miR-371a-3p: A Sensitive and Specific New Biomarker for Germ Cell Tumours. *Eur Urol* **71**, 213-220, doi:10.1016/j.eururo.2016.07.029 (2017).
- 15 Anheuser, P. *et al.* Serum Levels of MicroRNA371a-3p: A Highly Sensitive Tool for Diagnosing and Staging Testicular Germ Cell Tumours: A Clinical Case Series. *Urol Int* **99**, 98-103, doi:10.1159/000477446 (2017).
- 16 Spiekermann, M. *et al.* MicroRNA miR-371a-3p in serum of patients with germ cell tumours: evaluations for establishing a serum biomarker. *Andrology* **3**, 78-84, doi:10.1111/j.2047-2927.2014.00269.x (2015).
- 17 van Agthoven, T., Eijkenboom, W. M. H. & Looijenga, L. H. J. microRNA-371a-3p as informative biomarker for the follow-up of testicular germ cell cancer patients. *Cell Oncol (Dordr)* **40**, 379-388, doi:10.1007/s13402-017-0333-9 (2017).
- 18 Lobo, J. *et al.* Identification and Validation Model for Informative Liquid Biopsy-Based microRNA Biomarkers: Insights from Germ Cell Tumor In Vitro, In Vivo and Patient-Derived Data. *Cells* **8**, doi:10.3390/cells8121637 (2019).
- 19 Radtke, A. *et al.* The Novel Biomarker of Germ Cell Tumours, Micro-RNA-371a-3p, Has a Very Rapid Decay in Patients with Clinical Stage 1. *Urol Int* **100**, 470-475, doi:10.1159/000488771 (2018).
- 20 Mego, M. *et al.* Clinical utility of plasma miR-371a-3p in germ cell tumors. *J Cell Mol Med* **23**, 1128-1136, doi:10.1111/jcmm.14013 (2019).
- 21 Terbuch, A. *et al.* MiR-371a-3p Serum Levels Are Increased in Recurrence of Testicular Germ Cell Tumor Patients. *Int J Mol Sci* **19**, doi:10.3390/ijms19103130 (2018).
- 22 Lafin, J. T. *et al.* Serum MicroRNA-371a-3p Levels Predict Viable Germ Cell Tumor in Chemotherapy-naive Patients Undergoing Retroperitoneal Lymph Node Dissection. *Eur Urol* **77**, 290-292, doi:10.1016/j.eururo.2019.10.005 (2020).

- 23 Morup, N., Rajpert-De Meyts, E., Juul, A., Daugaard, G. & Almstrup, K. Evaluation of Circulating miRNA Biomarkers of Testicular Germ Cell Tumors during Therapy and Follow-up-A Copenhagen Experience. *Cancers (Basel)* **12**, doi:10.3390/cancers12030759 (2020).
- 24 Rosas Plaza, X. *et al.* miR-371a-3p, miR-373-3p and miR-367-3p as Serum Biomarkers in Metastatic Testicular Germ Cell Cancers Before, During and After Chemotherapy. *Cells* **8**, doi:10.3390/cells8101221 (2019).
- 25 Leao, R. *et al.* Serum miRNA Predicts Viable Disease after Chemotherapy in Patients with Testicular Nonseminoma Germ Cell Tumor. *J Urol* **200**, 126-135, doi:10.1016/j.juro.2018.02.068 (2018).
- 26 Belge, G. *et al.* Serum levels of microRNA-371a-3p are not elevated in testicular tumours of non-germ cell origin. *J Cancer Res Clin Oncol*, doi:10.1007/s00432-020-03429-x (2020).
- 27 Dieckmann, K. P. *et al.* High Expression of microRNA-371a-3p in Cystic Fluid of Post-Chemotherapy Teratoma with Concurrent Normal Serum Levels in Patients with Non-Seminomatous Testicular Germ Cell Tumours. *Urol Int*, 1-6, doi:10.1159/000510760 (2020).
- 28 Dieckmann, K. P. *et al.* Serum Levels of MicroRNA-371a-3p (M371 Test) as a New Biomarker of Testicular Germ Cell Tumors: Results of a Prospective Multicentric Study. *J Clin Oncol* **37**, 1412-1423, doi:10.1200/JCO.18.01480 (2019).
- 29 Nappi, L. *et al.* Developing a Highly Specific Biomarker for Germ Cell Malignancies: Plasma miR371 Expression Across the Germ Cell Malignancy Spectrum. *J Clin Oncol* **37**, 3090-3098, doi:10.1200/JCO.18.02057 (2019).
- 30 Charytonowicz, D. *et al.* Cost Analysis of Noninvasive Blood-Based MicroRNA Testing Versus CT Scans for Follow-up in Patients With Testicular Germ-Cell Tumors. *Clin Genitourin Cancer* **17**, e733-e744, doi:10.1016/j.clgc.2019.03.015 (2019).
- 31 Nappi, L. & Nichols, C. MicroRNAs as Biomarkers for Germ Cell Tumors. *Urol Clin North Am* **46**, 449-457, doi:10.1016/j.ucl.2019.04.011 (2019).
- 32 Singla, N., Lafin, J. T. & Bagrodia, A. MicroRNAs: Turning the Tide in Testicular Cancer. *Eur Urol* **76**, 541-542, doi:10.1016/j.eururo.2019.06.010 (2019).
- 33 Lobo, J. *et al.* Utility of Serum miR-371a-3p in Predicting Relapse on Surveillance in Patients with Clinical Stage I Testicular Germ Cell Cancer. *Eur Urol Oncol*, doi:10.1016/j.euo.2020.11.004 (2020).
- 34 Almstrup, K. *et al.* Application of miRNAs in the diagnosis and monitoring of testicular germ cell tumours. *Nat Rev Urol* **17**, 201-213, doi:10.1038/s41585-020-0296-x (2020).

- 35 Olmedillas-Lopez, S., Garcia-Arranz, M. & Garcia-Olmo, D. Current and Emerging Applications of Droplet Digital PCR in Oncology. *Mol Diagn Ther* **21**, 493-510, doi:10.1007/s40291-017-0278-8 (2017).
- 36 Drandi, D., Ferrero, S. & Ladetto, M. Droplet Digital PCR for Minimal Residual Disease Detection in Mature Lymphoproliferative Disorders. *Methods Mol Biol* **1768**, 229-256, doi:10.1007/978-1-4939-7778-9_14 (2018).
- 37 Tavano, F. *et al.* Droplet digital PCR quantification of miR-1290 as a circulating biomarker for pancreatic cancer. *Sci Rep* **8**, 16389, doi:10.1038/s41598-018-34597-z (2018).
- 38 Campomenosi, P. *et al.* A comparison between quantitative PCR and droplet digital PCR technologies for circulating microRNA quantification in human lung cancer. *BMC Biotechnol* **16**, 60, doi:10.1186/s12896-016-0292-7 (2016).
- 39 Cirillo, P. D. R., Margiotti, K., Mesoraca, A. & Giorlandino, C. Quantification of circulating microRNAs by droplet digital PCR for cancer detection. *BMC Res Notes* **13**, 351, doi:10.1186/s13104-020-05190-3 (2020).
- 40 Zhao, G. *et al.* Droplet digital PCR-based circulating microRNA detection serve as a promising diagnostic method for gastric cancer. *BMC Cancer* **18**, 676, doi:10.1186/s12885-018-4601-5 (2018).
- 41 Miotto, E. *et al.* Quantification of circulating miRNAs by droplet digital PCR: comparison of EvaGreen- and TaqMan-based chemistries. *Cancer Epidemiol Biomarkers Prev* **23**, 2638-2642, doi:10.1158/1055-9965.EPI-14-0503 (2014).
- 42 Ferracin, M. *et al.* Absolute quantification of cell-free microRNAs in cancer patients. *Oncotarget* **6**, 14545-14555, doi:10.18632/oncotarget.3859 (2015).
- 43 Hindson, C. M. *et al.* Absolute quantification by droplet digital PCR versus analog real-time PCR. *Nat Methods* **10**, 1003-1005, doi:10.1038/nmeth.2633 (2013).
- 44 Stein, E. V. *et al.* Steps to achieve quantitative measurements of microRNA using two step droplet digital PCR. *PLoS One* **12**, e0188085, doi:10.1371/journal.pone.0188085 (2017).
- 45 Myklebust, M. P. *et al.* Serum miR371 in testicular germ cell cancer before and after orchiectomy, assessed by digital-droplet PCR in a prospective study. *Scientific Reports* **11**, 15582, doi:10.1038/s41598-021-94812-2 (2021).
- 46 Lobo, J. *et al.* Testicular germ cell tumors: revisiting a series in light of the new WHO classification and AJCC staging systems, focusing on challenges for pathologists. *Hum Pathol* **82**, 113-124, doi:10.1016/j.humpath.2018.07.016 (2018).
- 47 Armbruster, D. A. & Pry, T. Limit of blank, limit of detection and limit of quantitation. *Clin Biochem Rev* **29 Suppl 1**, S49-52 (2008).

- 48 Rowlands, V. *et al.* Optimisation of robust singleplex and multiplex droplet digital PCR assays for high confidence mutation detection in circulating tumour DNA. *Sci Rep* **9**, 12620, doi:10.1038/s41598-019-49043-x (2019).
- 49 Shemer, R., Magenheim, J. & Dor, Y. Digital Droplet PCR for Monitoring Tissue-Specific Cell Death Using DNA Methylation Patterns of Circulating Cell-Free DNA. *Curr Protoc Mol Biol* **127**, e90, doi:10.1002/cpmb.90 (2019).
- 50 Kroneis, T., Jonasson, E., Andersson, D., Dolatabadi, S. & Stahlberg, A. Global preamplification simplifies targeted mRNA quantification. *Sci Rep* **7**, 45219, doi:10.1038/srep45219 (2017).
- 51 Badia, R. R. *et al.* Real-World Application of Pre-Orchiectomy miR-371a-3p Test in Testicular Germ Cell Tumor Management. *J Urol* **205**, 137-144, doi:10.1097/JU.0000000000001337 (2021).
- 52 Lobo, J., Leao, R., Jeronimo, C. & Henrique, R. Liquid Biopsies in the Clinical Management of Germ Cell Tumor Patients: State-of-the-Art and Future Directions. *Int J Mol Sci* **22**, doi:10.3390/ijms22052654 (2021).
- 53 Zuniga, A., Lawrentschuk, N. & Jewett, M. A. Organ-sparing approaches for testicular masses. *Nat Rev Urol* **7**, 454-464, doi:10.1038/nrurol.2010.100 (2010).
- 54 Belge, G. *et al.* Serum levels of microRNA-371a-3p are not elevated in testicular tumours of non-germ cell origin. *J Cancer Res Clin Oncol* **147**, 435-443, doi:10.1007/s00432-020-03429-x (2021).
- 55 Lembeck, A. L. *et al.* MicroRNAs as appropriate discriminators in non-specific Alpha-Fetoprotein (AFP) elevation in testicular germ cell tumor patients. *Non-coding RNA* **6**, 2 (2020).
- 56 Heidenreich, A. Personalized Follow-up in Clinical Stage I Testicular Germ Cell Tumors: The Future is Beginning. *Eur Urol Oncol* **4**, 492-493, doi:10.1016/j.euo.2020.11.012 (2021).
- 57 Leao, R. *et al.* Circulating MicroRNAs, the Next-Generation Serum Biomarkers in Testicular Germ Cell Tumours: A Systematic Review. *Eur Urol*, doi:10.1016/j.eururo.2021.06.006 (2021).
- 58 Bagrodia, A. *et al.* Impact of circulating microRNA test (miRNA-371a-3p) on appropriateness of treatment and cost outcomes in patients with Stage I non-seminomatous germ cell tumours. *BJU Int* **128**, 57-64, doi:10.1111/bju.15288 (2021).
- 59 Lafin, J. T. *et al.* The Road Ahead for Circulating microRNAs in Diagnosis and Management of Testicular Germ Cell Tumors. *Mol Diagn Ther* **25**, 269-271, doi:10.1007/s40291-021-00526-6 (2021)

II. DETECTION OF RENAL CELL CARCINOMA



Supplementary Figure 1 – Violin plots of miRNAs levels in Benign tumors (Oncocytomas) with Healthy Donors (HD) and Renal Cell Carcinomas (RCC) samples of hsa-miR-126-3p (p -value=0.279) and hsa-miR-200b-3p (p -value=0.280). Abbreviations: HD – Healthy Donors; RCC – Renal Cell Carcinomas; n.s. – not significant.

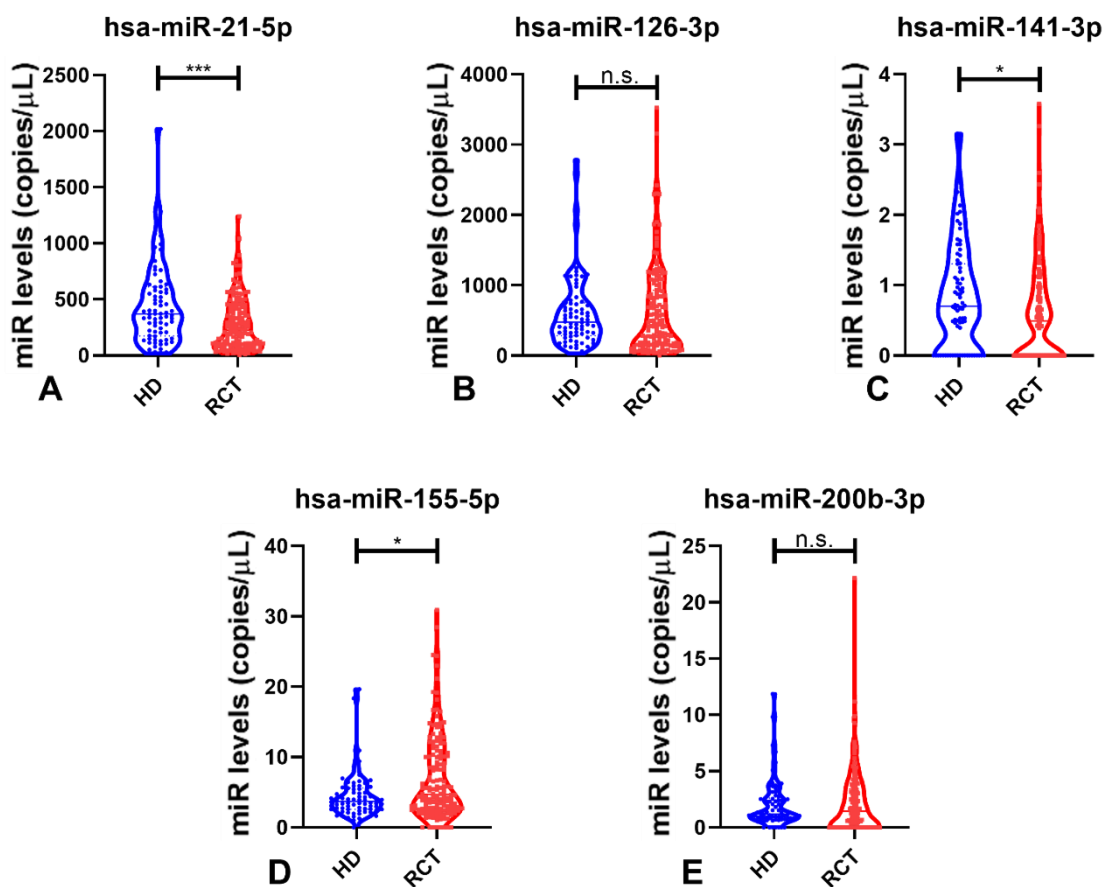
Supplementary Table 1 – Performance of miRNAs panels as biomarkers for detection of Renal Cell Carcinomas.

miRNAs	SE %	SP %	PPV %	NPV %	Accuracy %
hsa-miR-21-5p/hsa-miR-141-3p	72.54	42.71	65.19	51.25	60.50
hsa-miR-141-3p/hsa-miR-155-5p	91.55	41.67	69.89	76.92	71.43
hsa-miR-21-5p/hsa-miR-141-3p/hsa-miR-155-5p	95.07	32.29	67.50	81.58	69.75

Abbreviations: SE – Sensitivity; SP – Specificity; PPV – Positive Predictive Value; NPV – Negative Predictive Value

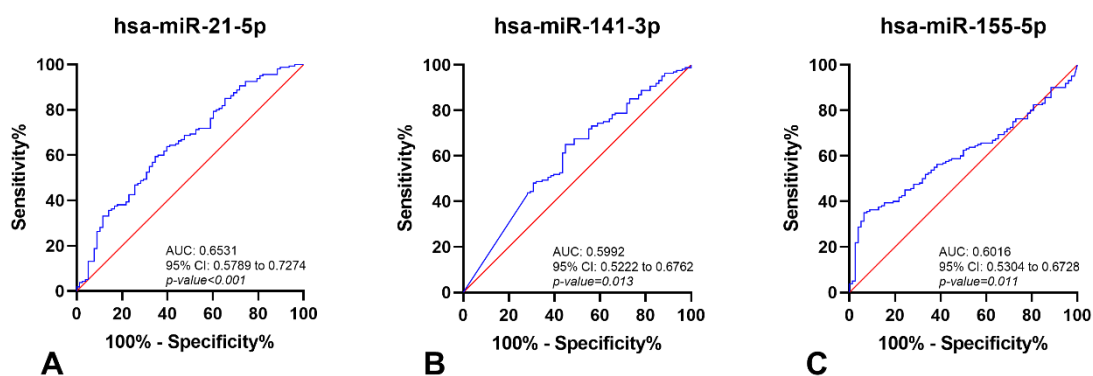
III. DISTRIBUTION OF CIRCULATING MIRNAS LEVELS IN RENAL CELL TUMORS AND BIOMARKERS PERFORMANCE

Initially, target miRNAs levels were compared between RCT and healthy donor samples. Hsa-miR-21-5p and hsa-miR-141-3p had lower levels in RCT (p -value<0.001 and p -value=0.011, respectively), while hsa-miR-155-5p had higher levels in RCT (p -value=0.011). Conversely, no significant differences were found for hsa-miR-126-3p and hsa-miR-200b-3p, (p -value=0.334 and p -value=0.474, respectively) (Supplementary Figure 2).



Supplementary Figure 2 – Violin plots with all points of miRNAs levels in Healthy Donors (HD) and Renal Cell Tumors (RCT) samples of hsa-miR-21-5p (A), hsa-miR-126-3p (B), hsa-miR-141-3p (C), hsa-miR-155-5p (D) and hsa-miR-200b-3p (E). Abbreviations: HD – Healthy Donors; RCT – Renal Cell Tumors; n.s. – not significant.

ROC curves (Supplementary Figure 3) were constructed, and empirical cut-off value was determined for each miRNA that showed significant differences between RCT and healthy donor samples.



Supplementary Figure 3 – Receiver Operating Characteristic Curve of hsa-miR-21-5p (A), hsa-miR-141-3p (B) and hsa-miR-155-5p (C). Abbreviations: AUC – Area Under the Curve; CI – Confidence Interval.

The empirical cut-off from ROC curve for each miRNA (Supplementary Figure 3) allowed for the calculation of performance for each miRNA individually (Supplementary Table 2). Hsa-miR-21-5p detected RCT with 59.38% sensitivity, 65.38% specificity and 61.34% accuracy, whereas hsa-miR-141-3p showed higher sensitivity (65.00%), although presenting 55.13% specificity and similar accuracy. Despite the modest sensitivity, hsa-miR-155-5p showed 93.59 % specificity for detecting the presence of kidney tumors, with the highest Positive Predictive Value, 91.80%.

Supplementary Table 2 – Performance of miRNAs as biomarkers for detection of Renal Cell tumors.

miRNAs	SE %	SP %	PPV %	NPV %	Accuracy %
hsa-miR-21-5p	59.38	65.38	77.87	43.97	61.34
hsa-miR-141-3p	65.00	55.13	74.82	43.43	61.76
hsa-miR-155-5p	35.00	93.59	91.80	41.24	54.20
hsa-miR-21-5p/ hsa-miR-155-5p	85.00	58.97	80.95	65.71	76.47

Abbreviations: SE-Sensitivity; SP-Specificity PPV – Positive Predictive Value; NPV – Negative Predictive Value

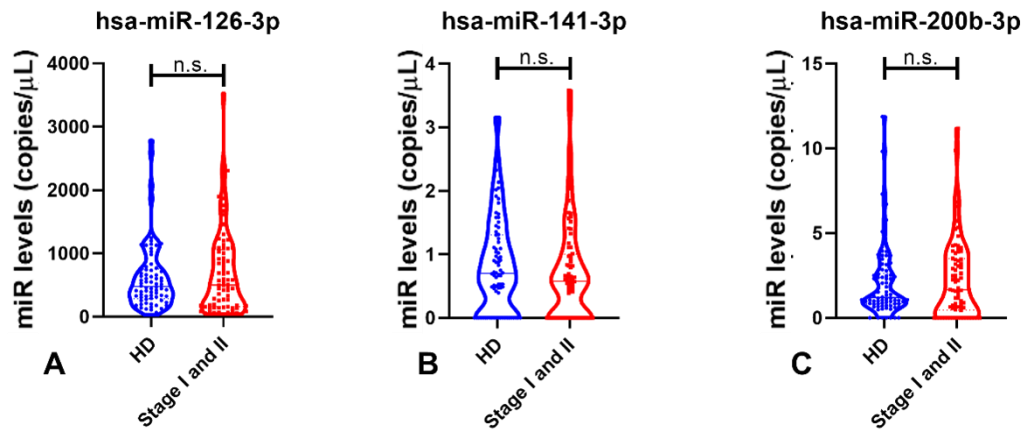
The combination of multiple circulating miRNAs was tested to improve the biomarker performance (Supplementary Table 3). The best performance was achieved by the panel comprising hsa-miR-21-5p and hsa-miR-155-5p which showed an accuracy of 76.47%. Moreover, this panel detected RCT with 85.00% sensitivity, 58.97% specificity and a high PPV (Supplementary Table 2).

Supplementary Table 3 – Performance of miRNAs panels as biomarkers for detection of Renal Cell Tumors.

miRNAs	SE %	SP %	PPV %	NPV %	Accuracy %
hsa-miR-21-5p/hsa-miR-141-3p	70.00	47.44	73.20	43.53	62.61
hsa-miR-141-3p/hsa-miR-155-5p	91.88	48.72	78.61	74.51	77.73
hsa-miR-21-5p/hsa-miR-141-3p/hsa-miR-155-5p	94.38	41.03	76.65	78.05	76.89

Abbreviations: SE-Sensitivity; SP-Specificity PPV – Positive Predictive Value; NPV – Negative Predictive Value

IV. DETECTION OF EARLY STAGES RENAL CELL CARCINOMAS



Supplementary Figure 4 – Violin plots (A, B and C) of miRNAs levels without significant differences between Healthy Donors (HD) and early stages of Renal Cell Carcinomas (Stage I and II) samples of hsa-miR-126-3p (p -value=0.931), hsa-miR-141-3p (p -value=0.226) and hsa-miR-200b-3p (p -value=0.896). Abbreviations: HD – Healthy Donors; n.s. – not significant.

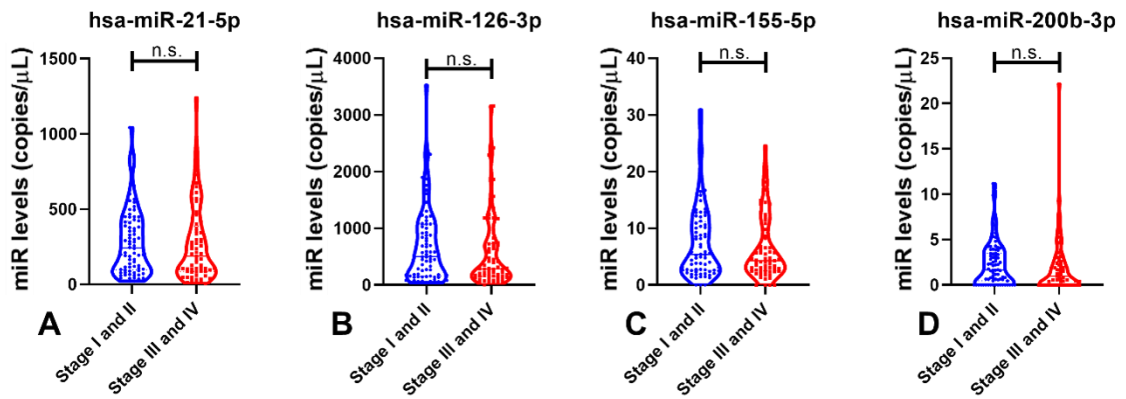
V. DETECTION OF CLEAR CELL RENAL CELL CARCINOMAS

Supplementary Table 4 – Performance of miRNAs panels as biomarkers for detection of Clear Cell Renal Cell Carcinoma.

miRNAs	SE %	SP %	PPV %	NPV %	Accuracy %
hsa-miR-126-3p/hsa-miR-141-3p	89.32	38.46	79.31	57.69	75.35
hsa-miR-141-3p/hsa-miR-155-5p	85.44	41.03	79.28	51.61	73.24
hsa-miR-141-3p/hsa-miR-200b-3p	83.50	41.03	78.90	48.48	71.83
hsa-miR-126-3p/hsa-miR-155-5p	80.58	53.85	82.18	51.22	73.24
hsa-miR-155-3p/hsa-miR-200b-3p	70.87	61.54	82.95	44.44	68.31
hsa-miR-126-3p/hsa-miR-141-3p/hsa-miR-155-5p	89.32	38.46	79.31	57.69	75.35
hsa-miR-126-3p/hsa-miR-141-3p/hsa-miR-200b-3p	89.32	38.46	79.31	57.69	75.35
hsa-miR-126-3p/hsa-miR-155-5p/hsa-miR-200b-3p	81.55	53.85	82.35	52.50	73.94
hsa-miR-141-3p/hsa-miR-155-5p/hsa-miR-200b-3p	86.41	41.03	79.46	53.33	73.94
hsa-miR-126-3p/hsa-miR-141-3p/hsa-miR-155-5p/hsa-miR-200b-3p	89.32	38.46	79.31	57.69	75.35

Abbreviations: SE-Sensitivity; SP-Specificity PPV – Positive Predictive Value; NPV – Negative Predictive Value

VI. COMPARISON BETWEEN EARLY STAGES RCC AND ADVANCED STAGES RCC



Supplementary Figure 5 – Violin plots of miRNAs levels without significant differences between Early stages (I and II) and Advanced Stages (III and IV) Renal Cell Carcinomas samples of hsa-miR-21-5p (p -value=0.361), hsa-miR-126-3p (p -value=0.162), hsa-miR-155-5p (p -value=0.372) and hsa-miR-200b-3p (p -value=0.108). Abbreviations: n.s. – not significant.